

# International Journal of Applied Sciences and Smart Technologies

**Volume 05, Issue 01, June 2023**

**Forensic Investigation In SQL Server Database Using Temporal Tables & Extended Events**  
Shadi K. A. Zakarneh

**Rfid Application For Designing Lowcost Learning Device For Play And Learning To  
Read Early Braille For Blind Children**  
Bertha Bintari W

**Smart Technology In Construction Industry: Opportunity During COVID-19 Pandemic**  
Putri Fatimah, Ahyahudin Sodri, Udi Syahnoedi Hamzah

**Performance Of Low Power Electric Energy Clothes Dryers For Households**  
Doddy Purwadianto, Budi Sugiharto

**Application Of Augmented Reality-Based Solar System Recognition  
Using Metaverse Studio**  
Izza Wildan Ridhoni, Muhammad Sholeh

**Laser Based Vibration Sensor Through Mobile**  
Rashmita K. Mahapatra, Shalini J. Yadav, Rajan Yadav

**Smoothing Module For Optimization Cranium Segmentation Using 3D Slicer**  
Gilang Argya Dyaksa, Nur Arfian, Herianto, Lina Choridah, Yosef Agung Cahyanta

**Educational Media Introduction To Human Internal And External Organs For High School  
Students Based On Augmented Reality By Using The Assemblr Application**  
I Dewa Ayu Sri Murdhani, Yunika Putri Oktavia, Muhammad Sholeh

**A Brief On Optical-Based Investigation Towards The Interfacial Behaviors During High  
Viscous Liquid/Gas Countercurrent Two-Phase Flow In A Complex Conduit  
Representing 1/30 Down-Scaled Of PWR Hot Leg Geometry**  
Achilleus Hermawan Astyanto, Indarto, Deendarlianto

**Input Power Measurement System For Driving Motor In Testing Low-Speed Generator**  
Ignasius Eko Yuliyanto, Tjendro, Bernadeta Wuri Harini, Martanto

**Classification Of Lung And Colon Cancer Histopathological Images Using  
Convolutional Neural Network (CNN) Method On A Pre-Trained Models**  
Brilly Lutfan Qasthari, Erma Susanti, Muhammad Sholeh

**p-ISSN 2655-8564 & e-ISSN 2685-9432**

**CONTENTS**

<b>CONTENTS</b>	i
<b>EDITORIAL BOARD</b>	iii
<b>PREFACE</b>	iv
<b>Forensic Investigation in SQL Server Database Using Temporal Tables &amp; Extended Events Artifacts</b> Shadi K. A. Zakarneh	1–16
<b>Rfid Application For Designing Lowcost Learning Device For Play And Learning To Read Early Braille For Blind Children</b> Bertha Bintari W	17–26
<b>Smart Technology in Construction Industry: Opportunity during COVID-19 Pandemic</b> Putri Fatimah, Ahyahudin Sodri, Udi Syahnoedi Hamzah	27–38
<b>Performance of Low Power Electric Energy Clothes Dryers for Households</b> Doddy Purwadianto, Budi Sugiharto	39–54
<b>Application of Augmented Reality-Based Solar System Recognition Using Metaverse Studio</b> Izza Wildan Ridhoni, Muhammad Sholeh	55–66
<b>Laser Based Vibration Sensor Through Mobile</b> Rashmita. K. Mahapatra, Shalini J. Yadav and Rajan Yadav	67–74
<b>Smoothing Module for Optimization Cranium Segmentation Using 3D Slicer</b> Gilang Argya Dyaksa, Nur Arfian, Herianto, Lina Choridah, Yosef Agung Cahyanta	75–88
<b>Educational Media Introduction To Human Internal And External Organs For High School Students Based On Augmented Reality By Using The Assemblr Application</b> I Dewa Ayu Sri Murdhani, Yunika Putri Oktavia and Muhammad Sholeh	89–100
<b>A Brief on Optical-based Investigation towards The Interfacial Behaviors during High Viscous Liquid / Gas Countercurrent Two-Phase Flow in a Complex Conduit Representing 1/30 Down-Scaled of PWR Hot Leg Geometry</b> Achilleus Hermawan Astyanto, Indarto, Deendarlianto	101-112
<b>Input Power Measurement System For Driving Motor In Testing Low-Speed Generator</b> Ignasius Eko Yuliyanto, Tjendro, Bernadeta Wuri Harini, Martanto	113-132

<b>Classification Of Lung and Colon Cancer Histopathological Images Using Convolutional Neural Network (CNN) Method An A Pre-Trained Models</b> Brilly Lutfan Qasthari, Erma Susanti, Muhammad Sholeh	133-142
--	---------

<b>AUTHOR GUIDELINES</b>	143-144
--------------------------	---------

**EDITORIAL BOARD**

**Editor in Chief**

Dr. I Made Wicaksana Ekaputra (Sanata Dharma University, Yogyakarta, Indonesia)  
Email: made@usd.ac.id

**Associate Editor**

Dr. Pham Nhu Viet Ha (Vietnam Atomic Energy Institute, Hanoi, Vietnam)  
Dr. Hendra Gunawan Harno (Gyeongsang National University, Jinju, The Republic of Korea)  
Dr. Mukesh Jewariya (National Physical Laboratory, New Delhi, India)  
Dr. Mongkolserj Lin (Institute of Technology of Cambodia, Phnom Penh, Cambodia)  
Dr. Yohanes Baptista Lukiyanto (Sanata Dharma University, Yogyakarta, Indonesia)  
Dr. Apichate Maneewong (Thailand Institute of Nuclear Technology, Bangkok, Thailand)  
Prof. Dr. Sudi Mungkasi (Sanata Dharma University, Yogyakarta, Indonesia)  
Dr. Pranowo (Universitas Atma Jaya Yogyakarta, Yogyakarta, Indonesia)  
Dr. Monica Cahyaning Ratri (Sanata Dharma University, Yogyakarta, Indonesia)  
Dr. Mahardhika Pratama (Nanyang Technological University, Singapore)  
Prof. Dr. Leo Hari Wiryanto (Bandung Institute of Technology, Bandung, Indonesia)  
Dr. Ranggo Tungga Dewa (Universitas Pertahanan, Bogor, Indonesia)

**Editorial Assistant**

Rosalia Arum Kumalasanti, M.T. (Sanata Dharma University, Yogyakarta, Indonesia)  
Vittalis Ayu, M.Cs. (Sanata Dharma University, Yogyakarta, Indonesia)

**Contact us**

International Journal of Applied Sciences and Smart Technologies  
Faculty of Science and Technology  
Sanata Dharma University  
Kampus III Paingan, Maguwoharjo, Depok, Sleman  
Yogyakarta, 55282  
Phone : +62 274883037 ext. 523110, 52320  
Fax : +62 272886529  
Email : [editorial.ijasst@usd.ac.id](mailto:editorial.ijasst@usd.ac.id)  
Website : <http://e-journal.usd.ac.id/index.php/IJASST>

**IJASST** is an open-access peer-reviewed journal that mediates the dissemination of research and studies conducted by academicians, researchers, and practitioners in science, engineering, and technology.

## **PREFACE**

Dear readers, we are delighted to serve you Volume 5, Issue 1 of International Journal of Applied Sciences and Smart Technologies (IJASST), which is managed and published by the Faculty of Science and Technology, Sanata Dharma University. IJASST is an open-access peer-reviewed journal that mediates the dissemination of research and studies conducted by academicians, researchers, and practitioners in science, engineering, and technology. Its scope also includes basic sciences which relate to technology, such as applied mathematics, physics, and chemistry.

In this edition, we have thirteen papers authored by researchers from Indonesia, India, and Palestine. Submitted papers are reviewed fairly using the open journal system (OJS) of IJASST. After the review process, accepted papers of the journal are publicly available for free at the website of IJASST.

For future issues, we are looking forward to your contributions to IJASST.

Dr. I Made Wicaksana Ekaputra  
Editor in Chief  
IJASST

This page intentionally left blank

# Forensic Investigation in SQL Server Database Using Temporal Tables & Extended Events Artifacts

Shadi K. A. Zakarneh<sup>1,\*</sup>

<sup>1</sup>M.Sc. Student, Palestine Technical University- Kadoorei, Tulkarem, Palestine,

\*Corresponding Author: [zakarnehshadi@gmail.com](mailto:zakarnehshadi@gmail.com)

(Received 21-09-2022; Revised 26-09-2022; Accepted 22-11-2022)

## Abstract

Different Database management systems (DBMS) were developed and introduced to store and manipulate data. Microsoft SQL (MSSQL) Server one of the most popular relational DBMS used for large databases. With the increasing use of databases, intentional and unintentional accidents on databases are increasing dramatically. Therefore, there is a great need to develop database forensic investigation (DBFI) tools and models. The temporal table is a new feature introduced with MSSQL server 2012 for track changes, database audit, data loss protection, and data recovery. In addition, the extended events another new feature introduced with MSSQL server 2008 for database performance troubleshooting. This study focused on DBFI in the MSSQL server using temporal tables and extended events artifacts. The experiment is conducted and the results have presented the use of the temporal tables and extended events artifacts in analyzing and determining the internal unauthorized modification on the database.

**Keywords:** SQL Server, database forensic, forensic investigation, database management system.

## 1 Introduction

MSSQL Server is a relational DBMS. Microsoft in 1998 developed the first version of the MSSQL server, which is version 7.0. Microsoft continues in developing newer versions in the MSSQL server until the last version today which is the MSSQL server 2019 [1].

In the MSSQL server, there are two main types of databases, system databases that are used for SQL server operations. The second type is the user's databases, which are



created by the users for their needs and business [1]. Each database in MSSQL Server mainly consists of two types of files. A transaction log file that stores information about the transactions executed on the database. Each time the data is modified, the transaction log information is used to undo or redo the changes, so the transaction log is also used in the database recovery after the failure occurred [2]. The other file is the data file, which is used to store the data [2].

MSSQL Server consists of several services, which are database engine, agent, MSSQL server browser, and MSSQL server full-text search. Also, the MSSQL server provides other services called business intelligence services which are used for database analysis, these services are MSSQL server integration service, MSSQL server reporting service, and MSSQL server analysis service [3].

Since the stable and reliable MSSQL server 2019 is an improved version of the previous versions, the new version includes all the previous version's features in addition to a set of new features related to performance, security, availability, and big data [4]. The MSSQL server 2019 new features include intelligent query processing, which improves the query optimizer behavior, as a result, the performance will improve [4]. Accelerated database recovery (ADR) is another new feature, by adding this feature; the time required for the database recovery process has been greatly reduced [1]. AlwaysEncrypted with secure enclaves feature, by this feature, administrators are not allowed to access the decryption keys, while the transparent column encryption is allowed [1]. This feature enables MSSQL Server to encrypt part of the memory to perform computations on encrypted fields without exposing the unencrypted values to the rest of the operations [1]. To achieve this goal, secure enclave technology is used [5]. The other feature is memory-optimized tempdb metadata, in this feature; improvements have been made to the tempdb code by improving access to RAM so that metadata can rely completely on memory. Thus, the so-called bottleneck problem that large data is exposed to when using a large amount of tempdb is bypassed [5].

In recent decades, the use of databases has increased dramatically. The computerization of businesses and services and the use of applications in the daily lives of individuals have greatly increased the need for databases [6]. With this expansion in the use of databases, the need to improve security and privacy protection means increases



dramatically, especially with the increase in security problems and security incidents that affect data confidentiality and users' privacy [6]. Because of the increase in security incidents on databases, there has become a great need for DBFI to identify digital evidence and perpetrators and improve information security [6].

MSSQL server one of the top ten relational DBMS due to the database engines ranking due to the popularity in 2020 as shown in Fig. 1 [7].

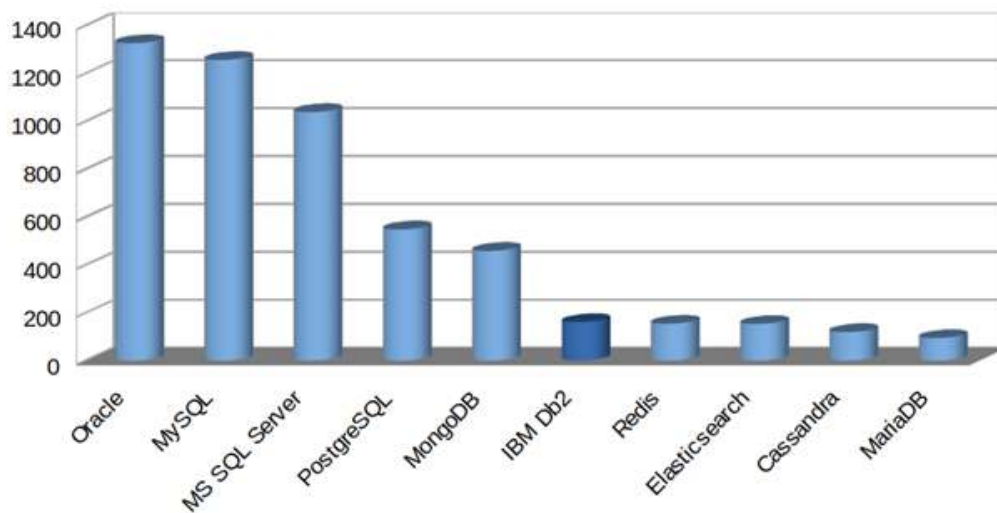


**Figure 1.** Database Ranking Score in Dec 2020 [7]

A new feature introduced in the MSSQL server named a temporal table. This feature was introduced with ANSI SQL 2011 [8]. Temporal Table started as a new feature with the MSSQL server 2016. Temporal tables are introduced for track changes, audit purposes, data loss protection, and data recovery in case of intentional or unintentional changes [9]. Another new feature that was developed in the MSSQL Server to help database developers troubleshoot performance issues during and after the development of the databases is the Extended events feature. This feature was first launched with MSSQL Server 2008 and then it was improved in MSSQL Server 2012 [10].

With the high popularity and wide use of the MSSQL server. Therefore, DBFI in the MSSQL server is highly important to determine the artifacts that can be extracted from the MSSQL server's new versions with its new features, especially in security features.

This study will focus on the DBFI in MSSQL server 2019 to determine the new artifacts according to the temporal table and extended events features.

## 2 Literature review

Database forensics is one of the branches of digital forensics [11]. DBFI is based on examining and retrieving the contents of databases and analyzing metadata to identify digital evidence related to incidents that the databases are exposed to [12]. Because of the wide use and spread of digital data and the heavy reliance on databases, DBFI has become necessary to investigate accidents affecting databases [11]. As well as in other cybercrimes, where the digital forensic investigation in many cases includes extracting digital evidence from the databases of systems and applications related to the committed cybercrime [11].

To perform DBFI, many tools are used to extract databases and their metadata for analysis and investigation [13]. Some of the features of these tools are the ability to clone a hard drive, compare files, and encrypt them. These tools also work to recover deleted or damaged data [14]. In addition to the ability to recover lost or deleted database components such as tables, views, keys, and stored procedures [13].

While the DBFI includes the identification, collection, preservation, reconstruction, analysis, and reporting of the investigation results and findings. However, the multiplicity and diversity of DBMS such as Oracle, MSSQL Server, and PostgreSQL, etc. made it difficult to have a specific model for DBFI. Several DBFI models were designed based on specific accidents that some types of databases were exposed to [11].

Where the DBFI aims to find the digital evidence in the database, different forensic investigation models were conducted [15]. Some of these models analyzed transactions and journal logs. While other models worked to recover deleted data, among these, the models that rely on transaction logs to recover data. While other models depend on the analysis of the database engine to bypass the problem of deleting records for the antiforensic, overwriting, or changing them every period [15].

The engine-based method for data recovery is based on raw-level data analysis. This method is often used in small DBMS such as SQLite, where the internal structure of

the databases must be understood for the investigator to use this method [15]. Thus, to use the forensic investigation method based on database engine analysis on large DBMS such as MSSQL server, it is necessary to understand the internal structure of the database engine and its storage [15].

In MSSQL server DBFI different artifacts can be collected and analyzed such as transaction logs files, Data files, SQL server logs, database schemas [15]. While the log file can be deleted or modified, so the investigator may need to analyze the data file. To Analyze the data file, the investigator needs to understand how is the MSSQL Server storage engine stores the raw data and the internal structure of the data file [11].

The data file in MSSQL Server consists of a set of pages. A page consists of a header, a data row, and a row offset array as shown in Fig. 2. The page size is 8192 bytes, of which 96 bytes are reserved for the header. The page metadata is stored in the first 64 bytes of the header and the rest of the header space is filled with 0x00. While record data in the tables stored in the data row, if the record size more than 8060 bytes the SQL server stores the record in multiple pages. The record location in the page is stored in the row offset array [15].

While DBMS record data changes in transaction logs and record information about transactions in audit logs such as what changed, when the changes were made, and who made the change. However, this data may not be sufficient for some systems such as financial systems that sometimes need to access a snapshot of the data at a certain time [2]. To solve this problem, temporal tables are defined by ANSI SQL 2011 to meet these requirements. Temporal tables are designed to keep a complete record of data changes and are easy to analyze on time. There are two types of temporal tables. The first type is system-versioned temporal tables, these tables keep a history of data changes based on the time changes occurred in the system [3]. Thus, system-versioned temporal tables provide a snapshot of the data that was on the system at a specific time. The second type is application-versioned temporal tables that provide data that is valid from a business point of view [3].

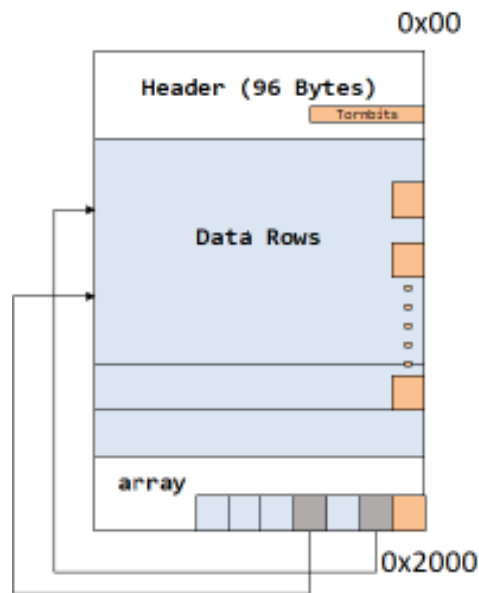


**Figure 2.** Page Structure [15]

Extended events feature was launched in MSSQL Server to collect as much data as needed to help database administrators or developers troubleshoot and identify database performance problems [16]. This feature was released with MSSQL Server 2008 and later versions. In MSSQL Server 2008 this feature was introduced without a GUI, so developers had to write large and complex queries to get the required data [5]. This feature has been further developed in MSSQL server 2012 and later to enable the user to set it up through the GUI and to give greater choices of data that can be collected to identify performance problems and to be used for troubleshooting by developers [5]. The extended events performance monitoring system is lightweight so it uses minimal performance resources. Extended events sessions can be created or modified, and the collected data is displayed and analyzed through the GUI provided by the MSSQL server management studio. The developer can choose the data he wants to collect and thus display it on the live monitoring screen, as well as store it in files or a table in a database for follow-up and analysis at any time [16].

Many previous studies were researched in the DBFI field. A study entitled: Development and validation of a Database Forensic Metamodel, this study aimed to present a model for DBFI called database forensic metamodel [17]. where the study

analyzed a set of models used in DBFI to reach this model, which consists of four phases as identification, artifacts collection, artifacts analysis, and documentation and presentation [17]. Another study entitled: Detecting Database File Tampering through Page Carving, The study focused on presenting a component that detects modifications in the database file, this component relies on forensic investigation to identify discrepancies between indexes and tables in the database [14]. A study entitled: Dual Security-Detection of Database Modification Attack and Restore Facility from Unauthorized Access, this study proposed a model for dual security to identify and prevent attacks on the database by monitoring web and database requests [18]. In the proposed model the modified data can be restored using the MD5 algorithm [18].

While the previous studies focused on reviewing DBFI models and presenting a proposed model. Other studies focused on data recovery using DBFI techniques and tools by collecting and analyzing the log files. While other studies focused on analyzing the data files to recover the deleted or tampered data. This study aims to analyze and detect internal unauthorized modifications on the MSSQL server Database using temporal tables and extended events artifacts. In addition, the modified data will be recovered using the temporal table. The study used a DBFI model consist of four phases (identification, artifacts collection, artifacts analysis, and documentation and presentation).

### 3 Research methodology

Two basic steps to complete this study. The first step is to collect data and information from literature studies, as a literature study is a method of collecting data through reading books, thesis, journals, and other related resources. The second step is to design a scenario to implement the DBFI in the MSSQL server database.

Through the designed scenario, the DBFI model is followed in this study is clarified. In this study, MSSQL Server 2019 is installed, and a proposed database is designed, implemented, and prepared for the DBFI model phases to be implemented to analyze and determine any internal unauthorized modification that occurred in the database.

In the simulation process, the used DBFI model consists of four stages: identification, artifacts collection, artifacts analysis, and documentation and presentation as shown in Fig. 3 [11]. All stages were taken to obtain valid and admissible evidence.



**Figure 3.** Database forensic investigation model

At the identification stage, the incident type and nature of the target databases are understood. The techniques and means needed in DBFI are identified, the forensic environment is prepared. The database server is isolated from the production environment and networks [11]. In the process of artifacts collection, all relevant data in the compromised database are collected from the database server. The collected data will be analyzed, and then the evidence will be extracted and determined. All the conducted processes during the three stages are documented including who, where, and when conducted. All the findings and data related to the evidence are documented in a timely manner [11].

## 4 Experiment

The experiment was conducted by installing MSSQL Server 2019 standard version on a workstation with a windows 10 pro operating system. The experiment database was built on the MSSQL server. A temporal table for customer's information is built in the database with its historical table as shown in Fig. 4.

```
USE [test]
GO

--CREATE TABLE dbo.Customers(
    [CustID] int IDENTITY(1,1) NOT NULL PRIMARY KEY,
    [CustName] nvarchar(50) NOT NULL,
    [Address] nvarchar(50) NULL,
    [Tel] nvarchar(50) NULL,
    [ValidFrom] datetime2 GENERATED ALWAYS AS ROW START NOT NULL,
    [ValidTo] datetime2 GENERATED ALWAYS AS ROW END NOT NULL,
    PERIOD FOR SYSTEM_TIME ([ValidFrom], [ValidTo])
)
WITH (
    SYSTEM_VERSIONING = ON ( HISTORY_TABLE = dbo.Temporal_Customers_History )
)
GO
```

**Figure 4.** Create a Customer Temporal Table with its Historical

The extended events session created and the data that need to be collected are identified. The created session is configured to be saved to a file automatically as shown in Fig. 5.

After the extended events session started, a number of rows were inserted into the customer table. SQL queries executed to show the changes in temporal and historical tables as shown in Fig. 6. The results of the SQL query shown in Fig. 7 and Fig. 8. Then using another client computer, many rows were inserted, modified, and deleted. After these transactions on the table, the temporal and historical tables data are viewed to show the impact of the insert, update, and delete transactions on the historical table. The extended events session is viewed and the events reviewed to check the data are collected during the execution of the transaction on the table.

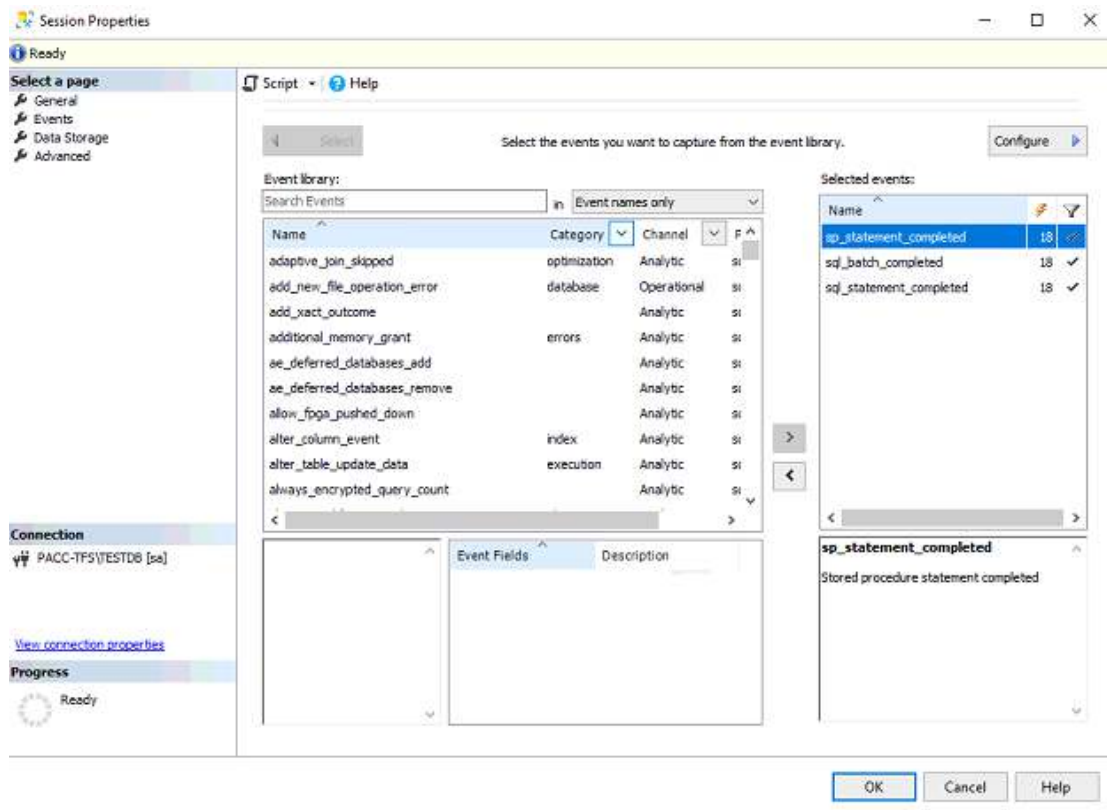


Figure 5. Extended events session properties

```
SELECT CustID
      ,CustName
      ,Address
      ,Tel
      ,ValidFrom
      ,ValidTo
FROM Test.dbo.Customers
SELECT CustID
      ,CustName
      ,Address
      ,Tel
      ,ValidFrom
      ,ValidTo
FROM Test.dbo.Customers
FOR SYSTEM_TIME BETWEEN '2021-06-20 19:02:43.9992811' AND '2021-06-24 19:02:43.9992811'
```

Figure 6. SQL queries to retrieve data from the temporal and historical tables



---

	CustID	CustName	Address	Tel	ValidFrom	ValidTo
1	1	Customer1	France	0101235467	2021-06-23 16:19:55.5971923	9999-12-31 23:59:59.9999999
2	2	Customer2	Germany	0201234568	2021-06-23 16:24:34.1475024	9999-12-31 23:59:59.9999999
3	3	Customer3	Italy	030456231	2021-06-23 16:24:34.1943972	9999-12-31 23:59:59.9999999
4	4	Customer4	Sweden	0405632145	2021-06-23 16:24:34.2256511	9999-12-31 23:59:59.9999999
5	5	Customer5	Spain	0705633345	2021-06-23 16:24:34.2568903	9999-12-31 23:59:59.9999999

Figure 7. Retrieved Data from Temporal Table

	CustID	CustName	Address	Tel	ValidFrom	ValidTo
1	1	Customer1	France	0101235467	2021-06-23 16:19:55.5971923	9999-12-31 23:59:59.9999999
2	2	Customer2	Germany	0201234568	2021-06-23 16:24:34.1475024	9999-12-31 23:59:59.9999999
3	3	Customer3	Italy	030456231	2021-06-23 16:24:34.1943972	9999-12-31 23:59:59.9999999
4	4	Customer4	Sweden	0405632145	2021-06-23 16:24:34.2256511	9999-12-31 23:59:59.9999999
5	5	Customer5	Spain	0705633345	2021-06-23 16:24:34.2568903	9999-12-31 23:59:59.9999999

Figure 8. Retrieved data from Historical Table

According to a suspected unauthorized modification on the database, a comparison between the current data in the customer temporal table and its historical table is conducted. By comparison, the historical data and current data are viewed and rows dates, and times are collected. The extended events collected data are reviewed due to the collected date and time from the historical table. From the extended events collected data, the executed transaction is determined with its date and time, the number of affected rows, the user who has performed the modification, the client machine, and executed the SQL statement text, etc.

## 5 Results and discussion

The results of the study that was conducted successfully in collecting the temporal and historical table's data and extended events logs artifacts to determine the unauthorized modification evidence.

According to a suspected unauthorized modification on the database, the DBFI model was used to collect the artifacts and determine the evidence. At the identification stage, the MSSQL server version and the tampered database is determined, the accident information is identified, and the Database server is isolated. The tampered database and

the extended events files were collected and transferred to the Database forensic workstation in the artifacts collection stage.

At the artifacts analysis stage, the database is attached to the MSSQL server in the database forensic workstation. The current data from the customer temporal table are viewed using a SQL select statement, and the historical table data are viewed using a SQL select statement with a system time period condition to return the historical data as shown in Figs. 9 - 11.

```

SELECT CustID
      ,CustName
      ,Address
      ,Tel
      ,ValidFrom
      ,ValidTo
FROM Test.dbo.Customers
SELECT CustID
      ,CustName
      ,Address
      ,Tel
      ,ValidFrom
      ,ValidTo
FROM Test.dbo.Customers
FOR SYSTEM_TIME BETWEEN '2021-06-20 19:02:43.9992811' AND '2021-06-24 19:02:43.9992811'
Order BY CustID ASC
    
```

**Figure 9.** SQL queries to retrieve data from the temporal and historical tables

	CustID	CustName	Address	Tel	ValidFrom	ValidTo
1	1	Customer 1	France	0101235467	2021-06-23 16:19:55.5971923	9999-12-31 23:59:59.9999999
2	2	Customer2	Germany	0201234568	2021-06-23 16:24:34.1475024	9999-12-31 23:59:59.9999999
3	3	Customer 100	Italy	030456231	2021-06-23 16:40:53.8654999	9999-12-31 23:59:59.9999999
4	5	Customer5	Spain	0705633345	2021-06-23 16:24:34.2568903	9999-12-31 23:59:59.9999999
5	6	Customer99	UK	0101235467	2021-06-23 16:39:41.7544971	9999-12-31 23:59:59.9999999

**Figure 10.** Retrieved Data from Temporal Table

	CustID	CustName	Address	Tel	ValidFrom	ValidTo
1	1	Customer 1	France	0101235467	2021-06-23 16:19:55.5971923	9999-12-31 23:59:59.9999999
2	2	Customer2	Germany	0201234568	2021-06-23 16:24:34.1475024	9999-12-31 23:59:59.9999999
3	3	Customer 100	Italy	030456231	2021-06-23 16:40:53.8654999	9999-12-31 23:59:59.9999999
4	3	Customer 3	Italy	030456231	2021-06-23 16:24:34.1943972	2021-06-23 16:40:53.8654999
5	4	Customer 4	Sweden	0405632145	2021-06-23 16:24:34.2256511	2021-06-23 16:41:30.4440715
6	5	Customer5	Spain	0705633345	2021-06-23 16:24:34.2568903	9999-12-31 23:59:59.9999999
7	6	Customer99	UK	0101235467	2021-06-23 16:39:41.7544971	9999-12-31 23:59:59.9999999

**Figure 11.** Retrieved data from Historical Table

By comparing the temporal table with the historical table, the investigator found the differences between the data in the two tables. The first difference was due to the CustID field with the value 3 repeated in the historical table with different CustName field Values and different ValidFrom and ValidTo fields Values, which means there is a modification executed on this row. In addition, the second difference was the CustID field value 4 Found in the historical table and not presented in the temporal table which means the row was deleted.

According to the determined modifications and deletion that were presented by viewing the temporal and historical data, the extended events session file was analyzed due to the system dates from the historical table. In the analysis stage, the SQL statement completed events determined and viewed. The collected events details include the client application name, the client hostname, the affected database name, number of affected rows, the database server instance name, the user name who modified the data, the used database user name, and the executed SQL statement text as shown in Fig. 12.

As shown in Fig. 12, the modification happened from client host named “SHADI-PC”, the user name that do the modification was “PACC\shzakarneh”, and the affected database name was “test”.

While the temporal table store the current data, the historical table store the historical data includes the current rows, deleted rows, and the old and modified rows in addition to the two system times columns that are indicated to the created date and time of the rows. By comparing the two tables, any suspected modification will be determined.

Table

In addition, by linkage the date and time column from the historical data with a timestamp in the extended events session, the evidence will be extracted and determined from the details of the event.

name	timestamp	timestamp (UTC)
sql_statement_completed	2021-06-23 19:40:53.8698538	2021-06-23 16:40:53.8698538

Event:sql\_statement\_completed (2021-06-23 19:40:53.8698538)

Field	Value
attach_activity_id.g...	FFD07CB8-61BA-4C61-AB67-DB081329F6B7
attach_activity_id.s...	1
attach_activity_id_...	A2A43A7B-962C-4472-B0C4-03851A773F88
attach_activity_id_...	0
client_app_name	Microsoft SQL Server Management Studio - Query
client_connection_id	25823E7B-9E08-44E0-AD2E-A19E64C32C8C
client_hostname	SHADI-PC
collect_system_time	2021-06-23 19:40:53.8654999
cpu_time	0
database_id	10
database_name	test
duration	8245
last_row_count	1
line_number	1
logical_reads	24
nt_username	
num_response_rows	0
offset	0
offset_end	124
page_server_reads	0
parameterized_plan...	0x
physical_reads	0
query_hash	7250716924140157896
row_count	1
server_instance_na...	PACC-TFS\TESTDB
server_principal_na...	sa
session_id	78
session_nt_username	PACC\shzakameh
session_server_prin...	sa
spills	0
sql_text	Update Customers Set Custname = 'Customer100' Where CustID= 3
statement	Update Customers Set Custname = 'Customer100' Where CustID= 3
task_time	137244654
transaction_sequen...	0
username	sa
writes	2

Figure 12. Extended Events Session Details

## 6 Conclusion

The database is used to store data for businesses and individuals. MSSQL server one of the most popular DBMSs in the world used for small and large data. With the increased use of the database, the DBFI becoming more important to determine the evidence and data recovery. Different techniques and models were used in the DBFI using

transaction log files and data file recovery. This study focused on DBFI using temporal tables and extended events features in MSSQL server new version as new artifacts. The study experiment was conducted using a DBFI model in MSSQL server 2019 with the four stages, identification, artifacts collection, artifacts analysis, and documentation and presentation. In the study results, the evidence was extracted and determined using the temporal tables and extended events artifacts.

## References

- [1] P. A. Carter, *Pro SQL Server 2019 Administration*, (2019).
- [2] D. Korotkevitch, *Pro SQL Server Internals*, (2016).
- [3] L. Davidson, *Pro SQL Server Relational Database Design and Implementation*, (2021).
- [4] B. Ward, *SQL Server 2019 on Linux*, (2019).
- [5] B. Nevarez, *Performance SQL Server*, (2021).
- [6] A. P. Jamdar, M. B. Bhangire, S. G. Shahari, and K. G. Matere, an Efficient Framework for Database Forensic Analysis., *Int. J. Adv. Eng. Res. Dev.*, 4 (5) (2017) 12634–12637
- [7] M. Kamaruzzaman, “Top 10 Databases to Use in 2021,” *Towards Data Science*, <https://towardsdatascience.com/top-10-databases-to-use-in-2021-d7e6a85402ba> (accessed Jun. 11, 2021), (2021).
- [8] Ghanayem, Mark, W. Rohm, and J. Parente, *Temporal Tables*, Microsoft. <https://docs.microsoft.com/en-us/sql/relational-databases/tables/temporal-tables?view=sql-server-ver15> (accessed Jun. 17, 2021). (2016).
- [9] P. Jayaram, *Temporal Tables in SQL Server*, SQL Shake, <https://www.sqlshack.com/temporal-tables-in-sql-server/>, (2019).
- [10] S. Johnson, *Introducing SQL Server*, (2015).
- [11] A. Al-Dhaqm et al., Database forensic investigation process models: A review, *IEEE Access*, 8 (2020) 48477–48490.
- [12] R. Bria, A. Retnowardhani, and D. N. Utama, Five Stages of Database Forensic Analysis: A Systematic Literature Review, *Proc. 2018 Int. Conf. Inf. Manag.*

- Technol. ICIMTech 2018, no. September, (2018) 246–250,
- [13] B. Narwal, A Walkthrough of Digital Forensics and its Tools, March (2020) 13757–13764, 2020.
- [14] J. Wagner, A. Rasin, K. Heart, T. Malik, J. Furst, and J. Grier, Detecting database file tampering through page carving, *Adv. Database Technol. - EDBT*, 2018-March, (2018) 121–132.
- [15] H. Choi, S. Lee, and D. Jeong, “Forensic Recovery of SQL Server Database: Practical Approach,” *IEEE Access*, 9 (2021) 14564–14575.
- [16] R. Jason, A. Wolter, and M. MSFT, Extended events overview, Microsoft, <https://docs.microsoft.com/en-us/sql/relational-databases/extended-events/extended-events?view=sql-server-ver15>, (2019).
- [17] A. Al-Dhaqm, S. Razak, S. H. Othman, A. Ngadi, M. N. Ahmed, and A. A. Mohammed, Development and validation of a database forensic metamodel (DBFM), 12(2) (2017).
- [18] V. K. Gupta, J. Bonde, A. Gorad, and P. Joshi, Duel Security-Detection of Database Modification Attack and Restore Facility from Unauthorized Access, 7(6) (2020) 983–987.

# Rfid Application For Designing Lowcost Learning Device For Play And Learning To Read Early Braille For Blind Children

Bertha Bintari W<sup>1,\*</sup>

<sup>1</sup>Department of Mechanics Design Tecnology, Vocational Faculty,  
Universitas Sanata Dharma

\*Corresponding Author: berthabw@usd.ac.id

(Received 15-12-2022; Revised 21-12-2022; Accepted 24-12-2022)

## Abstract

It is very important for children who have low vision or visual impairment to be able to recognize braille letters and recognize words. This ability will help them to be able to read and write Braille. Braille recognition learning methods currently use technology as a learning aid or assistive device. However, assistive devices with this technology are still rare and unaffordable for some schools and students in Indonesia. The design of this braille learning aid applies RFID as a low-cost solution for learning braille reading aids. This tool integrates several braille learning methods that have been carried out by teachers when teaching braille recognition in schools. The integrated methods are the Mangold method, the Fernald method, the Flashcards method and the scrabble method. This tool helps children recognize braille letters, arrange them as words and is confirmed directly by the tool through sound if the letters arranged as a word are right or wrong. With this integration method, children are expected to be able to learn to read braille while playing, and learn independently.

**Keywords:** learning aids, learning and playing tools, RFID applications, reading braille, low-cost braille

## 1 Introduction

Braille learning aids for children are needed to help children learn to read beginning braille. This reading learning aid [1] is intended for children who are learning to recognize letters and arrange them as words. In addition to learning, this tool is an interactive play facility that is expected to motivate children to learn to read in a fun way. A fun way to learn is to learn to use games or playing media [2]. Learning with the learning while





playing method is proven to improve children's ability to learn to read braille, scramble method as one example used for this process.

The learning method using this tool is conceptualized using a random letter and letter arrangement method which is known as the scrabble method. Research by Adhitya, [3] which concludes that the scrabble method can improve abilities, namely increasing the score obtained by students until they reach a predetermined success indicator of 70. However, this method can only be successful if it is given to children who are already able to read Braille. Braille letters will be pasted on the letter cards. This letter card method is referred to as the flash card method. Apsari [4] states that Braille flashcard media can facilitate children's memory in understanding letters and can improve children's tactile or sense of touch. This designed braille card still requires the interaction of the child to feel it using their fingers to recognize letters. The method used in this touch uses the mangold method or fingering with both hands [5] in addition, according to Khairani [6] the fingering method using two hands can improve the ability to recognize and read braille letters [7].

**Braille** The Indonesian Braille System for the Indonesian Language Section states that "Braille letters are letters that are arranged based on a combination of a six-dot pattern arranged as follows with the rules for the distance between points and the height of the peak of the braille code:

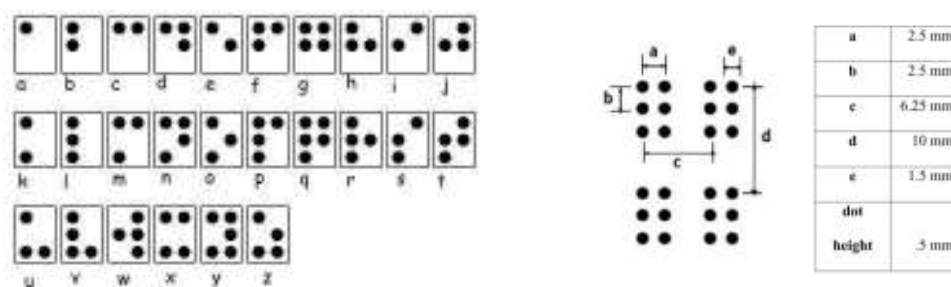


**Figure 1.** Braille letters and standard sizes

Braille letters have standard rules related to the distance between dots and the height of embossed letters for braille letters printed using a braille typewriter [8].



**Learning Method Application** The scramble method [3] is a form of game to form vocabulary from the letters available and have been scrambled to find answers accompanied by available alternative answers that can increase students' concentration and speed of thinking.

Ritawati (1996: 51) in [9] states that there are 5 steps in initial reading, namely recognizing sentence elements, recognizing word elements, recognizing letter elements, arranging letters into syllables and assembling syllables into words. Early reading teaching is more emphasized on the development of basic reading skills. Meanwhile, in reading Braille, the initial steps are: mastery of direction, tactile sensitivity, letter identification techniques and line tracing abilities. This ability cannot be easily mastered, [6] for that we need learning media to help teachers generate enthusiasm for students in recognizing letters and words needed to provoke a good response in reading by increasing vocabulary. Learning with interactive methods is able to make students have a better interest in learning to read [10].

While in the Fernald Method; using reading material from the words spoken by the child and each word being taught in its entirety. This method relies on reading braille and speaking aloud. When students say the word, then students will remember words that have similarities to the words they have learned [11].

The Manggold method is a way of reading braille by touching it with both hands. Touching using both hands reduces errors in crossing braille letters that are close together, reducing rubbing and back and forth [5]. Reading using the mangold method is an effective method in learning the beginning of reading braille [12].

The flashcard method refers to the use of cards that have pictures and words as a medium for learning words for children. Then the child will memorize based on the pictures and words in the flashcard [4], [6].

In the design of learning aids to read Braille, it is necessary to pay attention to matters related to the use of electrical, mechanical and control. These three things are elements of robotics, so the rules regarding the design of tools for children have special guidelines related to the safety of electricity and the use of resources and the wiring network [13].

The category of reading learning aids needed by blind students is easy access, portable which includes battery life, light weight, and not thick. In addition, the tool is durable, technically non-malfunctioning, sturdy, easy to use, is an effective learning tool, attracts interest, can be used for various functions and provides direct feedback in the form of audio [14],[15].

## 2 RFID Application Methods in Designing Braille Reading Learning Aids

Braille learning reading aid products that already exist are still unaffordable tools due to the high technology used in these aids. The means that can be used to improve the experience of knowledge in visually impaired children are assistive technology. Assistive technology is a tool that leads to items, products, items that are modified to be able to provide accommodation for children with special needs, including visual impairments according to Bryant, (2012) in Handoyo [16] Therefore, the design of this tool applies RFID technology which is relatively affordable in terms of cost (low cost) as an assistive technology for the blind. The application of an RFID reader is used as a concept for a braille card reader that has an RFID tag that has been inputted as data in the microcontroller program library.

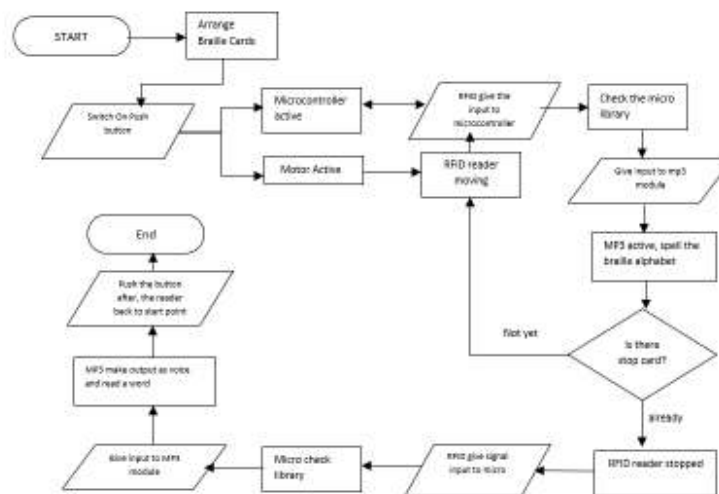
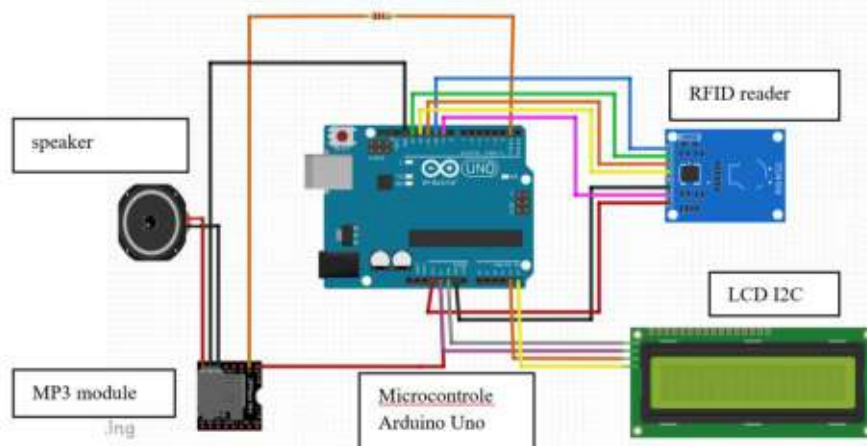


Figure 2. Braille reading aids schematic

The RFID tag used is a Mifare type card that is used as a flash card by attaching a braille symbol to the back of the casing. Semi-conductor system Mifare cards, cards and readers for this card use a frequency of 13.56 MHz This card is suitable to be applied to this braille card because the system is capable of recording data [17].

**Circuit System** The card case is designed to cover the RFID card with braille. The tool case is designed to protect the equipment circuit and controls. These RFID cards are then treated as letter cards that are scrambled and then touched and then arranged as a word. The arrangement of the RFID card is then read by the RFID reader. The microcontroller used is Arduino Uno R3 microcontroller. Circuit uses an Arduino Uno R3 component as a microcontroller, an RFID reader Mifare to read RFID tag cards, an I2C LCD to display words composed of braille letters, an MP3 module which contains a voice recording to confirm the arrangement of letters and speakers to amplify the sound from the MP3 module. Programming using Arduino IDEE software.



**Figure 3.** The main electrical circuit of the prototype

The RFID tag reader is driven by a DC motor which is controlled by an RFID input that is read by programming settings. The actuator to activate the function of the tool uses 2 (two) rechargeable 18650 Lithium batteries.

**Prototype Design Concept.** The design concept integrates the Fernald method, the mangold method, and the flashcard method with a playing system and learning to read

braille using the scramble method. The Fernald method applied is the teacher writes a word using Braille and students feel it to read. Then students say the word they read. Direct word confirmation is done when students say the words they read. Word recognition by voice and confirmation of truth and error by voice. The mangold method here uses the tactile method of braille letters found on braille cards. The application of an RFID card as a braille flashcard equipped with a casing with a braille symbol is a flashcard method. This flashcard method does not use one card as one word, but one card as one braille letter. The cards are then shuffled, and students arrange the cards as a word, as a way of playing braille reading. This method is a scramble method.

The application of RFID is in the use of rfid cards and RFID readers. Cards with braille letters are arranged on a card tray totaling 6 places. In the design of this prototype, the arrangement of letters is limited to 5 letters. The 6th placeholder is where the card stops, as a marker for the rfid reader to finish reading the card. The RFID reader will provide input information to the microcontroller which will confirm the word read is true or false. The confirmation is voiced through the MP3 module which is activated by the microcontroller.

Determination of matters related to security and success of the function is carried out by several series and program trials. Once the circuit is working, then design a case for both the card with braille and the case for the whole device. The RFID reader is driven by a control on the motor driver which is located separately from the casing and protected by the motor casing. Cables that stick out are wrapped in a safety cover. The push button is placed in the place closest to the front of the tool and has a diameter of 1.5 cm so that it is easily palpable by the child's hand.

Braille reading aids as a starting Braille reading aid, there are 6 card slots. The card slot for letter card placement is limited to 5 letters and the last slot is as a stop card to command the MP3 module to confirm by voice.

### **3 Results and Analysis**

The reading function by the RFID reader is already functioning properly. The reading distance with the card position can still be read at a distance of 15 cm. The use of

acrylic as a prototype material is still not optimal because it still feels heavy, and the cutting angle is still a bit sharp. Acrylic material is less flexible.

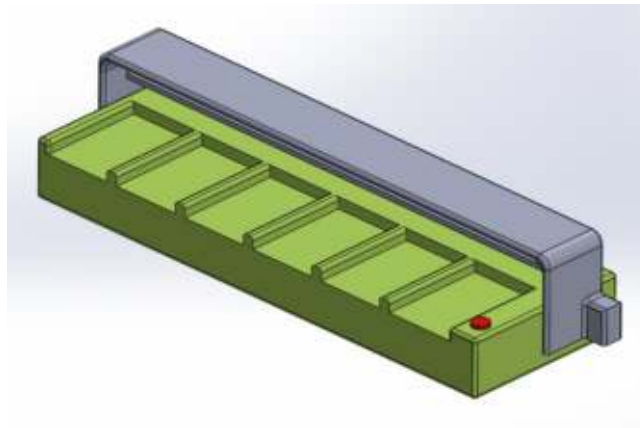


**Figure 4.** Drawing of braille reading aid design



**Figure 5.** The RFID cards of braille for Braille learning reading aid

The results of the new prototype voiced confirmation of true false, not yet voiced the reading by letter. In the next prototype improvement, it is planned to confirm by voice by letter. Card design will be modified so that the companion or teacher can also visually see the card directly even though it has been visualized through the LCD screen. The trials are conducted internally, to test the functionality of the tool.

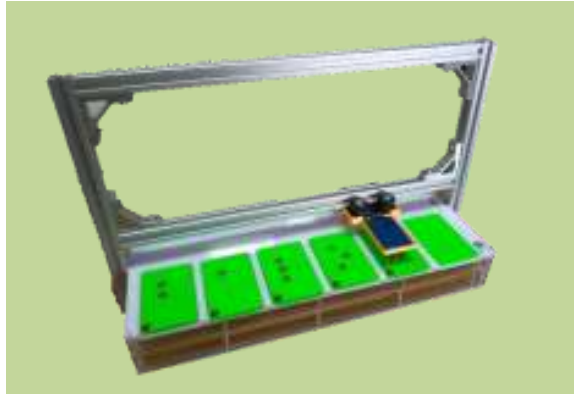


**Figure 6.** The RFID Braille learning reading aid prototype

## 4 Conclusion

Prototype This braille reading aid is functionally able to accommodate children learning to understand braille. The RFID card which is equipped with embossed braille is easy to feel well, equipped with a marker so that the card is not placed upside down. The RFID reader runs smoothly in the direction of reading from left to right at a program-controlled speed. Confirmation of letters and words by voice will add value to the success of this tool. With the improvement of the program, this tool is ready to be tested on students who have low vision or are blind.

## References

- [1] I. P. A. Padma Diana, I. G. A. Putu Raka Agung, and P. Rahardjo, Perancangan Modul Pembelajaran Huruf Braille Berbasis Mikrokontroler Untuk Membantu Proses Belajar Disabilitas Netra, *J. SPEKTRUM*, 5 (1) (2018) 5.
- [2] C. N. Aulina, Pengaruh Permainan Dan Penguasaan Kosakata Terhadap Kemampuan Membaca Permulaan Anak Usia 5-6 Tahun, *Pedagog. J. Pendidik.*, 1(2) (2012) 131.
- [3] G. Adhitya, Peningkatan Kemampuan Membaca Permulaan Huruf Braille Melalui Metode Scramble Pada Siswa Tunanetra Kelas I Di SLB A YPTN Mataram, *Widia Ortodidaktika*, 6 (2) (2017) 139–148.
- [4] Adinda Apsari Anindita, Pembelajaran Braille Bermedia Flashcard Di Tklb

- Tunanetra, (2020) 1–8.
- [5] T. Maryatun, Pengelolaan Pembelajaran Membaca Permulaan Tulisan Braille Melalui Sistem Mangold Pada Siswa Tunanetra, *Manajer Pendidik.*, 10 (5) (2016) 502–506.
- [6] M. Khairani, Media Flashcaed Braille terhadap Kemampuan Membaca Permulaan Anak Tunanetra, *J. Pendidik. Khusus Unesa*, (2016) 1–5 [Online]. Available: <https://jurnalmahasiswa.unesa.ac.id/index.php/jurnal-pendidikan-khusus/article/download/17862/16152>
- [7] Jumaidi, Atmazaki, and H. E. Thahar, Peningkatan Kecepatan Efektif Membaca Tulisan Braille Dengan Teknik Dua Tangan Bagi Tunanetra Kelas V Slb Negeri 2 Padang, *Bahasa, Sastra dan Pembelajaran*, 1 (3) (2013) 60–70, [Online]. Available: <http://ejournal.unp.ac.id/index.php/bsp/article/view/5016/3968>
- [8] L. J. Lieberman, Teaching students with visual impairments, *Case Study. Adapt. Phys. Educ. Empower. Crit. Think.*, April, (2019) 140–142,
- [9] S. Anna, M. Angelina, and A. Budiman, Penggunaan Metode Scramble Dalam Meningkatkan Kemampuan Membaca Braille Bagi Siswa Tunanetra Kelas Iii Di Slbn Weri Larantuka.
- [10] D. Nusyirwan et al, TEPIKAN (Tebak Pilihan Ikan) Menggunakan Card Tag RFID Berbasis Arduino Uno Sebagai Media Belajar Anak Sekolah,”*Simetris J. Tek. Mesin, Elektro dan Ilmu Komput.*, 10 (2) (2019) 589–602.
- [11] Sudartiningtyas, Penggunaan Metode Fernald Untuk Meningkatkan Prestasi Membaca Braille Bagi Siswa Tunanetra Kelas II Di SLB-A TPA Jember Semester II Tahun Ajaran 2016/2017, *SPEED J. J. Spec. Educ.*, 4 (1) (2020) 12–16.
- [12] Lusiana Kilen dan Ehan, Teknik MANGOLD untuk Meningkatkan Kemampuan Membaca Permulaan Braille Pada Peserta Didik Tunanetra, 19 (1) (2018) 25–31, [Online]. Available: [https://www.mendeley.com/catalogue/cf23404b-8e35-3086-8f6468890c7c70ab/?utm\\_source=desktop&utm\\_medium=1.19.8&utm\\_campaign=open\\_catalog&userDocumentId=%7B417546a2-31d9-4e4e-af0a5c0680c8574c%7D](https://www.mendeley.com/catalogue/cf23404b-8e35-3086-8f6468890c7c70ab/?utm_source=desktop&utm_medium=1.19.8&utm_campaign=open_catalog&userDocumentId=%7B417546a2-31d9-4e4e-af0a5c0680c8574c%7D)
- [13] S. Chiasson and C. Gutwin, *Design Principles for Children ’ s Technology*, (2005).
- [14] E. R. Hoskin, *Development And Design Of Braillebunny : A Device For Braille*

- Literacy Education, Hoskin, Elizab. Robin. Queen's Univ. ProQuest Diss. Publ. (2019) 28389350.
- [15] S. G. Mouroutsos and E. Mitka, A Guide to safety standards of toy-robots, 2012 IEEE/RSJ Int. Conf. Intell. Robot. Syst., no. May, (2012), [Online]. Available: [http://www.researchgate.net/publication/236031868\\_A\\_Guide\\_to\\_safety\\_standards\\_of\\_toy-robots](http://www.researchgate.net/publication/236031868_A_Guide_to_safety_standards_of_toy-robots)
- [16] R. R. Handoyo, Pengembangan bahan ajar kode braille berbasis teori elaborasi bagi guru pendidikan khusus, JPK (Jurnal Pendidik. Khusus), 14 (2) (2019) 46–56.
- [17] H. Djamal, Radio Frequency Identification (RFID) Dan Aplikasinya, TESLA J. Tek. Elektro, 16 (1) (2014) 45–55.



# Smart Technology in Construction Industry: Opportunity during COVID-19 Pandemic

Putri Fatimah<sup>1,\*</sup>, Ahyahudin Sodri<sup>1</sup>, Udi Syahnoedi Hamzah<sup>1</sup>

<sup>1</sup>School of Environmental Science, Universitas Indonesia

\*Corresponding Author: putri.fatimah@ui.ac.id

(Received 20-12-2022; Revised 24-12-2022; Accepted 30-12-2022)

## Abstract

The construction industry is a sector that plays an essential role in economic growth. The COVID-19 pandemic is an uncertain situation that significantly affects humans and industries, including the construction industry. The operational construction projects are complex with various activities and involve a large of workers. Prevention of the spread of COVID-19 that changes lifestyles and improves technology adoption. This study examines the relationship between increased technology adoption and limited workers' social interaction in construction projects during the pandemic. A questionnaire survey was conducted to construction workers in DKI Jakarta, 74 valid responses were collected and correlation analyses were performed with SPSS version 28. The result of this study indicated a significant and positive correlation between increased technology adoption and limited workers' social interaction in a construction project during the pandemic. There are opportunities for the construction industry to implement a digital transformation, Building Information Modelling (BIM), and intelligence visualization technologies to cope with the impact of the COVID-19 pandemic on construction activities. This study provides evidence that smart technologies application has a significant role in supporting the construction industry to mitigate the impact of the COVID-19 pandemic and opportunities for continuous improvement towards post-pandemic.

**Keywords:** COVID-19, construction, industry, smart technology

## 1 Introduction

World Health Organization (WHO) announced coronavirus disease (COVID-19) as the name of a new disease [1]. COVID-19 affected the world's population, put pressure on the global health system, and was declared a pandemic by the World Health Organization (WHO)[2]. Confirmed cases of COVID-19 in Indonesia until December 2022 fluctuate. Based on the WHO dashboard, from 3<sup>rd</sup> January 2020 to 16<sup>th</sup> December 2020, there were 160,362 fatalities and 6,707,504 confirmed cases of COVID-19 in



Indonesia [3]. The COVID-19 pandemic has occurred for over two years and is still ongoing. This crisis has an impact on various sectors, including the construction industry. Table 1 informs the impact of the COVID-19 pandemic on the construction industry from previous study.

**Table 1.** Impact of the COVID-19 pandemic on the construction industry

<b>Locations</b>	<b>Impact of the COVID-19 pandemic</b>
The United Kingdom	Construction companies suffered losses, financial constraints from clients and banks, delayed projects due to material deficiencies, extended project completion targets, and social distancing provisions became a major challenge in construction activities [4].
North America	Delays in material delivery result in material shortages, reduced efficiency and productivity, slowdown of ongoing projects and delays in new projects, additional costs, and workplace safety [5].
China	Management difficulties including stricter workplace supervision, difficulties in collaboration, reduced work efficiency, project delays, supply chain disruptions, longer material delivery times, temporary shutdown of construction sites, increased construction costs for COVID-19 prevention, increased material costs, machinery costs, extended project time, and reduced project profits [6].
Malaysia	Project delays, labor shortages and job losses, time overruns, cost overruns, company financial impacts, planning, and scheduling disruptions, movement restrictions, material price fluctuations, and uncertainty of company continuity [7]. Decreased project productivity, increased compliance costs, and exposure

	of construction workers challenges to safety and occupational health [8].
Indonesia	Impacted to project performance, implementation of health protocols requires additional cost, and project completion time [9]. Significant impact on construction projects' completion time, project budget, and occupational health and safety [10].

---

The emergence of a complex pandemic impact on various aspects encourages companies and individuals to survive in this crisis condition, including optimizing the potential opportunities. The adoption of information technologies and digital transformation has accelerated due to the pandemic. Developing smart technologies significant impacts cost savings, quality improvement, and productivity gains on the project, which also supports the smart construction project approach to management [11]. A smart technologies system is integrated technologies used to monitor and manage environments or external system, improving human life and work, and accelerate the performance of routine or industrial operations [12].

Iqbal et al. [13] state that the construction sector should pursue innovative and digital approaches to improve business operations and leverage opportunities. In the COVID-19 pandemic context, research by Yang et al. [6] related to the impact of the COVID-19 pandemic on the construction industry in China, the result states that the positive impact of the COVID-19 pandemic is the improvement of technology adaptation. On a similar point, Li et al. [14] argue that the COVID-19 pandemic brings several opportunities for developing smart construction technologies and innovations in construction management. In addition, organizations must allocate resources to survive the pandemic, and be prepared for any uncertainties that may occur in the future [13]. The opportunities are applied by improving technology adoption and innovation that can support construction operations during the COVID-19 pandemic. This study examines the relationship between workers' interaction and technology adoption in the construction project. This study also explores the smart technology that can be applied to improve the construction industry's performance to cope with the pandemic.

## **2 Research Methodology**

This study focused on the construction project in DKI Jakarta, based on data COVID-19 task force in Indonesia, that the distribution of confirmed COVID-19 cases in Indonesia is highest in DKI Jakarta [15], thus referred to as the epicenter of COVID-19 cases [16]. This study was conducted at a private construction company (PT X) located in DKI Jakarta, based on the value of the project contracts undertaken, the company is a large category construction service company. The population in this study are workers who work on high-rise building construction projects in DKI Jakarta, where PT X is responsible as the main contractor. In order to examine the relationship between workers interaction and technology adoption, an online questionnaire survey was conducted for construction workers as the main data collection. Data were collected from September to October 2022. The respondent criteria are construction project workers who had work experience in DKI Jakarta during the COVID-19 pandemic. A simple random sampling method was employed with the calculation number of samples using the Isaac and Michael formula with an error degree of 5%. The minimum sample is 71 workers, and the actual survey collected 74 respondents.

A questionnaire survey uses a Likert 5-rating scale, with a rating of 1 expressing strongly disagree, and 5 expressing strongly agree. Attitudes, opinions, and perceptions of social phenomena are measured using the Likert scale [17]. The optimal number of alternative responses is five scales [18]. Correlation analysis was used to evaluate the strength of the relationship between variables. Correlation analyses were performed with IBM SPSS Statistics version 28. Kendall's tau value interpretations include weak correlations ( $>0-0.25$ ); moderate correlations ( $>0.25-0.5$ ); high correlations ( $>0.5-0.75$ ); very high correlation ( $>0.75-0.99$ ); and value of 1 for perfect correlation [19].

## **3 Results and Discussions**

### **3.1 Demographic characteristics of the respondents**

All respondents confirmed working on construction projects in DKI Jakarta during the COVID-19 pandemic. According to Table 2, almost 73% of respondents experienced

more than 10 years, and other 27% have experienced more than 3 to 10 years. Based on this result, it can be deduced that all respondents have experience in the construction project. Various positions in the construction project were involved in this study, including project manager, site manager, HSE, engineers, and other positions representing the perspective of general construction workers. Detail of characteristics of respondents, such as work experience in the construction industry and job positions, are shown in Table 2.

**Table 2.** Demographic characteristics of respondents (N=74)

Characteristics		Frequency (F)	Percentage
Work experience in the construction industry	>3 – 7 years	7	9.4%
	>7 – 10 years	13	17.6%
	>10 – 19 years	25	33.8%
	20 years or more	29	39.2%
Job position	Project Manager	4	5.4%
	Site Manager	14	18.9%
	Engineer	11	14.9%
	Commercial	8	10.8%
	HSE	11	14.9%
	General Affair	3	4%
	Quality Supervisor	11	14.9%
	Quantity Surveyor	4	5.4%
	Drafter	8	10.8%

Source: Primary data analysis, 2022

### 3.2 Questionnaire data analysis

Correlation analysis of questionnaire data performed with software IBM SPSS. The output of the correlation analysis between increased technology adoption and limited workers' social interaction during the pandemic shows in Table 3.

**Table 3.** Kendall's tau correlation coefficient

Variables	Kendall's tau correlation coefficient	Significance level
Increased technology adoption during the pandemic Limited workers' social interaction during the pandemic	0.375**	<0.001

\*\* Correlation is significant at the 0.01 level (2-tailed)

Source: Primary data analysis, 2022

Correlation analysis between increased technology adoption and limited workers' social interaction during the pandemic, based on Table 3 Kendall's tau correlation value is 0.375, this value means a positive relationship with moderate strength and significance at the 0.01 level (2-tailed). During the COVID-19 pandemic, social distancing is included in the COVID-19 spread prevention protocol. Increased technology adoption can reduce face-to-face interaction and communication between workers to avoid the spread of COVID-19, but also it can increase the efficiency of construction work and implement COVID-19 prevention protocols [14]. Several innovative technologies have been applied to enhance construction site performance and support the health and well-being of construction workers [6].

### 3.3 Smart technologies in the construction industry

This section discusses some of the smart technologies opportunities that can be applied in the construction industry. Moreover, supporting the survey result described in the previous section. Digital transformation is recognized as a new paradigm of digital innovation, and information technology plays a vital role in the company, especially during the pandemic. Leontie, Maha, and Stoian [20] argue that digitalization is the most helpful to cope with the pandemic situation. The construction sector had to prioritize digital transformation for sustainability, and despite initiatives to implement digital transformation to enhance productivity, the COVID-19 pandemic has significantly increased digital transformation [21]. The digitalization of the construction sector is

linked directly to the use of various information technologies known as construction technology 4.0 [20]. Ben-Zvi and J. Luftman [22] argue that digital transformation brings great changes to human life, and the COVID-19 pandemic drives these changes. Another study has the same point, Kamal [23] states that the adoption of digital technology is an opportunity during the COVID-19 pandemic; digital technology has been proven to support productivity. Digital transformation technologies help improve productivity, enhance safety and risk mitigation, high-quality buildings, and improve collaboration by collecting, analyzing, and using data from the entire supply chain in the construction industry [21].

One of the impacts of the pandemic that mainly occurs in construction projects is delays construction work, and delays in material supply, thus the efficient method is important to mitigate this impact. The Building Information Modelling (BIM) concept as a combination of methods and technology that organize the operational and support the management of the 3D models and other construction information in digital format during the period of the entire building's life cycle [24]. BIM is generally used by engineering positions to build design for each stage. BIM provides visual tools and information on the operations and materials, improving the quality and consistency of project life cycle costs [25]. BIM is a process, method, information project design, faster project management, cost-effective, and reduces environmental impact [26]. BIM can help facilitate the construction process more efficiently, and BIM-based design models can contribute to sustainable construction [27]. The application of BIM can prevent design errors and effective use of materials, and reduce the potential for construction waste generation [28].

The architectural engineering and construction industries have the popularity of visualization technologies such as virtual reality, augmented reality, and automation technology using robots and intelligent algorithms [11]. Artificial intelligence (AI) can address a productivity issue in the construction sector; throughout the building lifecycle AI utilize the data and leverages other technological capabilities to improve the construction process [29]. In context of the COVID-19 pandemic, using technology will have benefits for improving the quality of learning [30]. Visual technology can be adopted to promote health protocols and increase construction workers' awareness of complying

with COVID-19 protocols, and audio-visual training can make it easier for workers to understand the training content.

In other applications, biometric identity methods such as facial recognition can be used by attendance systems to prevent the spread COVID-19 caused by physical touch [31]. Smart recognition gates enable effective and efficient workforce management by recording attendance and preventing unauthorized visitors [11]. According to Rafiq, Alimudin, and Rani [31], a face recognition attendance system has been implemented with the main concept when people face or objects appear then the camera will activate and show up on the monitor, and the temperature sensor will detect the object, the implementation has successfully achieved a high accuracy level of 80%. The application of smart recognition gates can develop with the application of the COVID-19 protocol, for example measuring body temperature, and COVID-19 vaccination status as screening when workers enter the project area.

## 4 Conclusions

Construction workers' interactions have been restricted due to the COVID-19 pandemic. Based on the result and discussion, it was shown that there is a significant and positive correlation between increased technology adoption and limited workers' social interaction during the COVID-19 pandemic. In short, the COVID-19 pandemic accelerates technology adaptation in the construction industry. There are prospects for the construction industry to adapt smart technology such as digital transformation, Building Information Modelling (BIM), and intelligence construction technologies. The limitation of this study is that the survey was conducted to workers regarding technology adoption in general. Therefore, the suggestion for further study is to conduct specific survey on the technology adoption based on each position, and cost-benefit analysis of smart technology. Besides the limitation, this study provides evidence that applying smart technology support improvement in the performance of the construction industry to cope impact of the COVID-19 pandemic and opportunities for post-pandemic.



## **Acknowledgments**

The authors would like to thank the private construction company in DKI Jakarta (PT X) for permitting this study and appreciate the participation of construction workers willing to be respondents and other parties involved in this study.

## **References**

- [1] World Health Organization, Novel Coronavirus(2019-nCoV) Situation Report – 22, (2020), [Online]. Available: [https://www.who.int/docs/default-source/coronaviruse/situation-reports/20200211-sitrep-22-ncov.pdf?sfvrsn=fb6d49b1\\_2](https://www.who.int/docs/default-source/coronaviruse/situation-reports/20200211-sitrep-22-ncov.pdf?sfvrsn=fb6d49b1_2).
- [2] M. Usman, Y. Ali, A. Riaz, A. Riaz, and A. Zubair, Economic perspective of coronavirus (COVID-19), *J. Public Aff.*, 20 (4) (2020) 1–5,
- [3] World Health Organization, WHO Health Emergency Dashboard - Indonesia Situation, (2022), <https://covid19.who.int/region/searo/country/id> (accessed Dec. 17, 2022).
- [4] A. Shibani, D. Hassan, and N. Shak, The Effects of Pandemic on Construction Industry in the UK, *Mediterr. J. Soc. Sci.*, 2117 (2020) 48–60.
- [5] M. Raoufi and A. R. Fayek, Identifying Actions to Control and Mitigate the Effects of the COVID-19 Pandemic on Construction Organizations: Preliminary Findings, *Public Work. Manag. Policy*, 26 (1) (2021) 47–55,
- [6] Y. Yang et al., Opportunities and Challenges for Construction Health and Safety Technologies under the COVID-19 Pandemic in Chinese Construction Projects,” *Int. J. Environ. Res. Public Heal. Artic.*, 18 (13038) (2021).
- [7] D. Y. Gamil and A. Alhagar, The Impact of Pandemic Crisis on the Survival of Construction Industry : A Case of COVID-19, *Mediterr. J. Soc. Sci.*, 11 (4) (2020) 122–128.
- [8] A. Olanrewaju, A. AbdulAziz, C. N. Preece, and K. Shobowale, Evaluation of measures to prevent the spread of COVID-19 on the construction sites, *Clean. Eng. Technol.*, 5 (100277) (2021).
- [9] D. Larasati, N. Ekawati, S. Triyadi, A. F. Muchlis, and A. Wardhani, Impact of the

- Pandemic COVID-19 on the Implementation of Construction Contracts, IOP Conf. Ser. Earth Environ. Sci., 738(1) (2021) 1–12,
- [10] R. Susanti, S. Fauziyah, and P. U. Pramesti, Lesson from pandemic Covid-19 for sustainability construction in Indonesia, AIP Conf. Proc., 2447 (1) (2021) 30013.
- [11] M. Xu, X. Nie, H. Li, J. C. P. Cheng, and Z. Mei, Smart construction sites: A promising approach to improving on-site HSE management performance, J. Build. Eng., 49 (2021).
- [12] M. Ion and G. Căruțașu, Smart Technology, Overview, and Regulatory Framework, Rom. Cyber Secur. J., 2 (1) (2020), [Online]. Available: <https://rocys.ici.ro/spring-2020-no-1-vol-2/smart-technology-overview-and-regulatory-framework/>.
- [13] M. Iqbal, N. Ahmad, M. Waqas, and M. Abrar, COVID-19 pandemic and construction industry: Impacts, emerging construction safety practices, and proposed crisis management framework, Brazilian J. Oper. Prod. Manag., 18 (2) (2021) 1–17.
- [14] Z. Li, Y. Jin, W. Li, Q. Meng, and X. Hu, Impacts of COVID-19 on construction project management: a life cycle perspective, Eng. Constr. Archit. Manag., (2022),
- [15] COVID-19 Handling Task Force, Peta Sebaran Perkembangan Kasus Covid-19 di Indonesia, (2022). <https://covid19.go.id/en/peta-sebaran> (accessed Mar. 22, 2022).
- [16] R. E. Caraka et al., Impact of COVID-19 large scale restriction on environment and economy in Indonesia, Glob. J. Environ. Sci. Manag., 6 (2020) 65–84.
- [17] Sugiyono, Metode Penelitian Kuantitatif, Kualitatif, dan R&D, 19th ed. Bandung: Alfabeta, (2013).
- [18] X. Chen, H. Yu, and F. Yu, What is the optimal number of response alternatives for rating scales? From an information processing perspective, J. Mark. Anal., 3 (2) (2015) 69–78.
- [19] J. Sarwono, Path Analysis dengan SPSS. Jakarta: Elex Media Komputindo, (2012).
- [20] V. Leontie, L. G. Maha, and I. C. Stoian, COVID-19 Pandemic and its Effects on the Usage of Information Technologies in the Construction Industry: The Case of Romania, Buildings, 12 (2) (2022).
- [21] S. Kim, M. Lee, I. Yu, and J. W. Son, Key Initiatives for Digital Transformation, Green New Deal and Recovery after COVID-19 within the Construction Industry

- in Korea, *Sustain.*, 14 (14) (2022).
- [22] T. Ben-Zvi and J. Luftman, Post-Pandemic IT: Digital Transformation and Sustainability, *Sustain.*, 14, (22) (2022) 1–11.
- [23] M. M. Kamal, The triple-edged sword of COVID-19: understanding the use of digital technologies and the impact of productive, disruptive, and destructive nature of the pandemic, *Inf. Syst. Manag.*, 37 (4) (2020) 310–317.
- [24] J. P. Carvalho, L. Bragança, and R. Mateus, Optimising building sustainability assessment using BIM, *Autom. Constr.*, 102 (2019) 170–182.
- [25] M. Zoghi and S. Kim, Dynamic modeling for life cycle cost analysis of BIM-based construction waste management, *Sustain.*, 12 (12) (2020) 2483.
- [26] J. Čabala, M. Kozlovská, Z. Struková, and A. Tažíková, Benefits of BIM models and mixed reality in the implementation phase of construction projects, *IOP Conf. Ser. Mater. Sci. Eng.*, 1252 (1) (2022) 012079.
- [27] S. Soltani, The Contributions of Building Information Modelling to Sustainable Construction, *World J. Eng. Technol.*, 4 (2) (2016) 193–199.
- [28] A. Turkyilmaz, M. Guney, F. Karaca, Z. Bagdatkyzy, A. Sandybayeva, and G. Sirenova, A comprehensive construction and demolition waste management model using PESTEL and 3R for construction companies operating in central Asia, *Sustain.*, 11 (6) (2019).
- [29] S. O. Abioye et al., Artificial intelligence in the construction industry : A review of present status , opportunities and future challenges, *J. Build. Eng.*, 44 (2021).
- [30] H. Suparwito, Information Technology and Learning Methodology amid the COVID-19 Pandemic, *Int. J. Appl. Sci. Smart Technol.* 2 (2) (2020) 107–118.
- [31] A. A. Rafiq, E. Alimudin, and D. P. Rani, Employee Presence Using Body Temperature Detection and Face Recognition, *Int. J. Appl. Sci. Smart Technol.*, 4 (2) (2022) 173–184.

This page intentionally left blank

# **Performance of Low Power Electric Energy Clothes Dryers for Households**

Doddy Purwadianto<sup>1\*</sup>, Budi Sugiharto<sup>1</sup>

Department of Mechanical Engineering, Faculty of Science and Technology,  
Sanata Dharma University, Yogyakarta, Indonesia

\*Corresponding Author: purwadodi@gmail.com

(Received 24-04-2023; Revised 27-04-2023; Accepted 01-05-2023)

## **Abstract**

One of the problems faced by middle to lower economic class people in big cities is drying clothes, both in the dry season and in the rainy season. Artificial clothes drying equipment is needed that can replace the role of solar energy. The purpose of this study was to determine the performance of electric energy clothes dryers and the length of time needed to dry clothes on a household scale. The clothes dryer works by using a heat-pump based on the vapor-compression cycle. The total power of the heat pump is 200 watt. The working fluid of the heat-pump is R134a. The working fluid used to dry clothes is air, using a closed airflow system. The research was carried out experimentally by varying the amount of clothes in the drying chamber. The clothes dryer performance (COP) of the heat pump is 7.94. Drying time for 15, 25 and 40 clothes respectively for 210 minutes, 330 minutes and 450 minutes.

**Keywords:** Dryer, Performance, Clothes, Heat Pump, Vapor Compression Cycle

## **1. Introduction**

The process of drying clothes is the process of eliminating water in clothes. The process of drying clothes is done after the clothes are washed and the water is squeezed out. Squeezing clothes can be done by hand or by using a washing machine, then clothes can be dried by the evaporation process. The process of evaporation of water on clothes can be done in various ways, such as: aerating, drying in the sun, passing hot air, passing hot and dry air. After the clothes are dry, the clothes are ironed, in addition to smoothing the clothes, it is also to kill the germs that are on the clothes.



Once tidied up, the clothes are stored in the wardrobe. When the clothes will be worn, the clothes are taken and put on.

The main process in drying clothes is the evaporation of water contained in clothes. The evaporation process is the process of changing the water phase from the liquid phase to the water vapor phase. During the evaporation process, water is transferred from the clothes to the air. The evaporation process requires heat. The heat of vaporization is taken from the air. The air temperature will decrease and the water content in the air will increase. The specific humidity of the air increases. This process is known as the cooling and humidifying process. The drying process is influenced by several air conditions, such as: air temperature, air humidity and air flow [1]

Drying by drying is natural drying. Drying with the help of drying equipment, called artificial drying. Combined drying is drying with solar-energy and other-energy drying equipment. Energy sources for drying equipment can come from waste fuel energy or biomass (husk, straw, corn cobs, sawdust, and coconut-fiber), LPG, CNG, or electricity. Research with the help of drying equipment has been carried out by several researchers. Saptariana, et al dry the traditional rengginang food made from sticky rice using an LPG drying oven [2]. Doddy Purwadianto and Petrus Kanisius Purwadi dried corn chips using an electric energy drying oven [3]. Petrus Kanisius Purwadi drying clothes using an electric energy drying oven <sup>[4]</sup>. Wibowo Kusbandono, Petrus Kanisius Purwadi and A. Prasetyadi drying wooden planks in an electric energy drying oven [5,6]. Adhi Prasnowo dries potato chips using an electric energy oven [7]. Tri Mulyanto and Supriyono dry the chili using an electric oven and solar energy [8]. Dian Morfi Nasution et al, Sari Farah Dina, et al, dry cocoa beans using solar energy and electrical energy [9,10]. Efriwandy Simbolon et al dried cloves in an oven burning coconut waste [11].

Disadvantages of the process of drying clothes by drying in the sun are: long and depending on the weather. Drying with an LPG-fired oven can be done at any time (morning, afternoon and evening) and does not depend on the weather (can be done during the dry season, or during the rainy season). Drying with LPG ovens can be done indoors and can dry quickly. Disadvantages of drying with an oven: impractical or complicated, less safe because it has the potential for fires, wastes energy, is not

environmentally friendly because it creates exhaust gas pollution, and the environment is not clean.

In big cities, many middle-class people find it difficult to dry clothes naturally, because they do not have a large outdoor yard in their house. The solution that can be given is to make artificial clothes drying equipment using a heat pump that has low electric power. The heat pump works on the basis of the vapor-compression cycle. With a heat pump, you can get the dry and hot air needed to dry clothes. No electric heating elements are used in the drying process. Electricity is only used to drive the compressor and fan. Air drying is carried out by the evaporator while air heating is carried out by the condenser. The evaporator and condenser are the main components of the heat pump, apart from the compressor and capillary tube. The drying time is not a problem if the dryer is only for household use (not for doing business). With the use of a heat pump, the process of drying clothes can be abandoned. Safe, because the potential for the heat pump to pose a minor hazard. Clothes drying can be done indoors, and can be done at any time, regardless of the weather, safe and comfortable.

Research on drying clothes involving heat pumps has been carried out by: Pradeep Bansal, Amar Mohabir, William Miller [12], Ward TeGrotenhuis, Andrew Butterfield, Dustin Caldwell, Alexander Crook, Austin Winkelman [13]. In addition to being able to be used at any time, the use of a heat pump produces high performance, is practical and environmentally friendly. Another study using heat pumps to dry clothes was carried out by Purwadi, PK using 800 watts of electric power, as well as that carried out by Cakra, et al, using 1 PK of electric power [14]. Research conducted by Gordon, et al, uses a lower electric power of 0.5 PK [15]. For people of middle economic class, a clothes dryer that is suitable for household use is a dryer that uses a heat-pump with low electric power. In this study, the energy needed to drive the heat pump is 200 watt.

#### **a. Heat pump**

The clothes dryer used in this study uses a heat pump based on a vapor compression cycle. The working fluid in the heat pump is called refrigerant or freon. Requirements for the use of refrigerants must be safe and environmentally friendly so

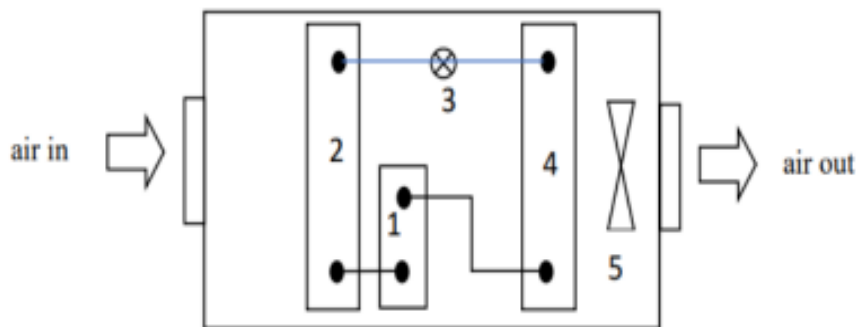
as not to damage the ozone layer. The vapor compression cycle is usually used in refrigeration engines [16]. The ideal vapor compression cycle is composed of several main processes: the compression process, the desuperheating process, the condensation process, the pressure reduction process and the evaporation process. To improve engine performance, additional processes can be added to the standard vapor compression cycle, namely superheating and subcooling processes. The heat pump has main components: compressor, condenser, capillary and evaporator. The compressor functions for the compression process, the condenser for desuperheating and refrigerant condensation processes, the pipe-capillary functions to reduce pressure and the evaporator functions for the evaporation process. Fig. 1 presents a series of main components of a heat pump.

Fig. 2 presents the vapor-compression cycle on the P-h diagram. In the condenser, a process of releasing heat occurs when the refrigerant undergoes a process of desuperheating and condensation, and in the evaporator, absorption of heat from the environment occurs when the refrigerant undergoes a boiling process. In the heat pump there is an energy balance. The energy entered into the heat-pump (which is absorbed by the evaporator) plus the energy used to drive the heat-pump (which is used to drive the compressor) equals the energy released by the heat-pump (energy released by the condenser to the environment).

When the vapor compression cycle machine is running, refrigerant successively flows from the compressor, condenser, capillary-pipe, evaporator, and then flows to the compressor again. As long as there is electricity, the vapor-compression cycle in the heat-pump continues continuously. The function of the compressor is to increase the refrigerant pressure at a fixed entropy value (isentropic), from low pressure  $P_1$  to high pressure  $P_2$ . The work done by the compressor per unit mass of refrigerant is expressed by  $W_{in}$ . In addition to experiencing an increase in pressure, the refrigerant temperature increases so that the gas condition changes from saturated gas to superheated gas. Exiting the compressor, refrigerant enters the condenser. The condenser's job is to dissipate heat into the surrounding air. There are two processes that refrigerants undergo, the desuperheating process and the condensation process. When removing heat in the desuperheating process, the refrigerant temperature



decreases. The condition of the refrigerant gas changes from superheated gas to saturated gas at high pressure  $P_2$ . The process continues with the condensation process. The condensation process in the condenser takes place at constant pressure and constant temperature. The refrigerant phase changes from a saturated gas phase to a saturated liquid. If desired, the refrigerant phase can be made in the superfluid state. In this case, a sub-cooling process is required. The amount of heat that is discharged by the condenser into the ambient air is expressed by  $Q_{out}$ . Exiting the condenser, the refrigerant flows into the capillary-pipe. Before flowing into the capillary-pipe, the refrigerant flows through the filter, to undergo a process of filtering impurities. When the refrigerant flows into the capillary tube, the refrigerant pressure drops until it reaches low pressure  $P_1$ , and the refrigerant temperature also drops. This process takes place at a constant refrigerant enthalpy. The pressure drop in the refrigerant is caused by friction between the inner surface of the capillary-pipe and the flowing refrigerant. Because the diameter of the capillary tube is quite small, the pressure drop that occurs is quite large. Some of the refrigerant changes phase to vapor. The refrigerant then enters the evaporator, and the refrigerant absorbs heat from the surrounding air to be used to change the refrigerant phase from a liquid and gas mixture to a saturated gas.



**Figure 1.** Series of main components in a heat pump

Description in Fig. 1:

- |   |            |   |                |
|---|------------|---|----------------|
| 1 | compressor | 3 | capillary pipe |
| 2 | evaporator | 4 | condenser      |
| 5 | fan        |   |                |

Fig. 1 besides presenting a series of main components in a heat pump, also presents the direction of air flow when passing through the heat pump. The air entering the heat pump is first passed through the evaporator and lastly through the condenser. After passing through the condenser, the air is removed from the heat pump. The air released by the heat pump is then fed into the clothes drying room. The air entering the evaporator is air that has dried the clothes in the drying chamber.

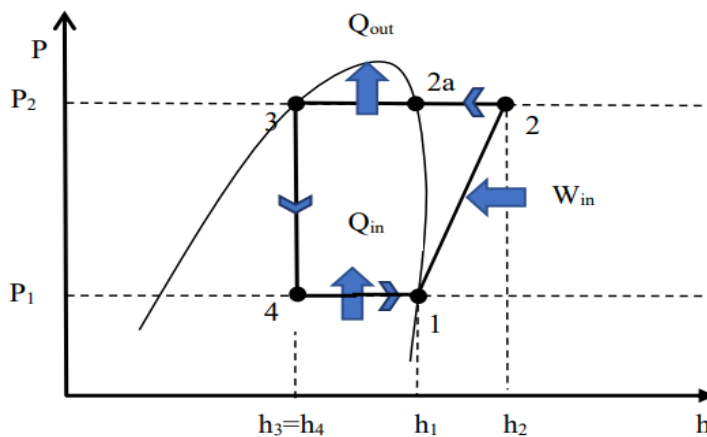


**Figure 2.** Vapor compression cycle on a Mollier diagram, without superheating and subcooling

The ratio of useful energy to the energy required to drive a vapor-compression cycle engine is called performance. In this case, the useful energies are  $Q_{in}$  and  $Q_{out}$ . The performance or coefficient of performance or COP of the clothes drying oven is calculated using Equation (1).

$$COP = \frac{(Q_{in} + Q_{out})}{W_{in}} \quad (1)$$

In Equation (1),

$$Q_{in} = h_1 - h_4 \quad (2)$$

$$Q_{out} = h_2 - h_3 \quad (3)$$

$$W_{in} = h_2 - h_1 \quad (4)$$

In Equations (2), (3) and (4),  $h_1$  represents the enthalpy of refrigerant before it enters the compressor,  $h_2$  represents the enthalpy of refrigerant when it leaves the compressor,

$h_3$  is the enthalpy of refrigerant when it enters the capillary-pipe and  $h_4$  is the enthalpy of refrigerant when it enters the evaporator.

### b. Clothes Dryer

Fig. 3 presents a schematic of a clothes dryer using a heat-pump. The refrigerant used in the heat pump is R-134a. The fluid used to dry clothes is dry and hot enough. The air flow used in the drying process is a closed air cycle. No airflow is introduced into the drying chamber or removed from the clothes drying chamber. To obtain dry and hot enough air, air is circulated through a heat-pump by passing air through finned pipes from the evaporator and condenser components. Air can flow, because of the fan inside the heat pump. Dry and hot enough air then flows through the entire surface of the clothes which are hung on hangers in the clothes drying room. After the air has passed through the clothing, the air temperature will drop but the air humidity will increase. The air is then flowed repeatedly to the evaporator again. The air cycle is repeated until dry clothes are obtained with the desired degree of dryness.

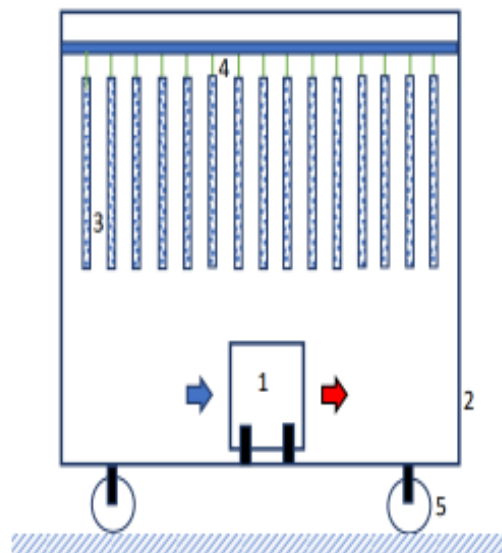


**Figure 3.** Schematic of a clothes dryer using a heat pump

Description in Fig. 3.

- |                  |                         |
|------------------|-------------------------|
| 1 Heat pump      | 4 Hanger                |
| 2 Drying chamber | 5 Drying chamber wheels |
| 3 Clothes        |                         |

## **2. Research Methodology**

The research was conducted experimentally. At the time of the study, the heat pump was placed in the clothes drying chamber. The size of the drying chamber is 1.1 m long, 1.1 m wide and 1.15 m high. The drying chamber is made of wood with a thickness of 8 mm. In the drying chamber there are a number of clothes hanging on hangers. The arrangement of the clothes is shown in Fig. 3. The total electric power used by the heat pump is 200 watts. The evaporator used in the heat pump is of the finned-pipe type, with the pipe material being made of copper and the fins of aluminum material. The condenser used is also of the finned pipe type, with pipes made of copper and fins made of aluminum. The capillaries are made of copper, having a diameter of 0.026 inches. The research was conducted by varying the number of clothes used in the drying room: (a) 15 clothes, (b) 25 clothes and (c) 40 clothes. During the drying process the clothes drying chamber is tightly closed. There is no inflow of air and no outflow of air. The clothes that are dried are in the form of t-shirts made of cotton, with size XL.

## **3. Results and Discussion**

Fig. 4 presents the vapor compression cycle in the P-h diagram R-134a of a heat pump used in a clothes dryer. The delineation can be obtained using the absolute pressures  $P_1$  and  $P_2$ . The absolute pressure  $P_1$  is the working pressure of the evaporator and the absolute pressure  $P_2$  is the working pressure of the condenser. The  $P_1$  and  $P_2$  values are based on the measuring working pressure plus the outside air pressure. A vapor compression cycle is described assuming no superheating and no subcooling. From the vapor compression cycle, it can be seen that the working temperature of the evaporator ( $T_{\text{evap}}$ ), the working temperature of the condenser ( $T_{\text{kond}}$ ), the enthalpy values  $h_1$ ,  $h_2$ ,  $h_3$ , and  $h_4$  are presented in Table 1. However, the enthalpy values  $h_1$ ,  $h_3$  and  $h_4$  are presented in Table 1, taken from the table of the properties of refrigerant R-134a in order to obtain accurate data. By knowing the enthalpy value, the  $Q_{\text{in}}$ ,  $Q_{\text{out}}$ ,  $W_{\text{in}}$  and COP of the heat pump can be calculated, the results of which are presented in Table 2. The working temperature of the evaporator is the boiling temperature of

the refrigerant in the evaporator at low pressure  $P_1$  and the working temperature of the condenser is the temperature of the refrigerant condensing in the condenser at high pressure  $P_2$ .

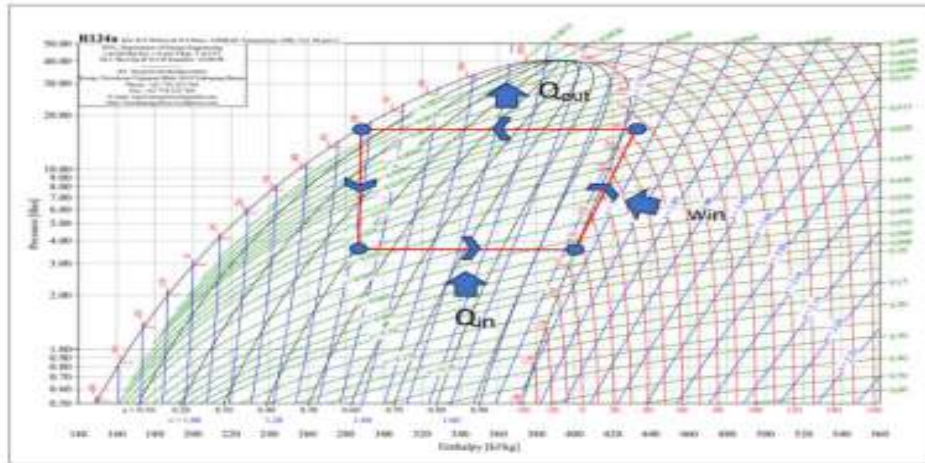


**Figure 4.** Heat pump vapor compression cycle in diagram P-h, R-134a

**Table 1.** Research data for the characteristics of a vapor compression cycle based heat pump used in clothes dryers, with 15, 25 and 40 clothes

Researched machine	$P_1$ (bar)	$P_2$ (bar)	$T_{evap}$ (°C)	$T_{kond}$ (°C)	$h_1$ (kJ/kg)	$h_2$ (kJ/kg)	$h_3$ (kJ/kg)	$h_4$ (kJ/kg)
Heat pump	3,496	16,813	5	60	400,07	432,55	287,39	287,39

**Table 2.** Characteristics of heat pumps for drying 15, 25 and 40 clothes

Researched machine	$P_1$ (bar)	$P_2$ (bar)	$Q_{in}$ (kJ/kg)	$Q_{out}$ (kJ/kg)	$W_{in}$ (kJ/kg)	COP
Heat pump	3,496	16,813	112,68	145,16	32,48	7,94

**Table 3.** Air conditions in the drying process

Amount of clothes	Average air temperature before entering the evaporator, (°C)	Average air temperature out of the condenser (°C)
	$T_{db,A}$	$T_{db,D}$
15 clothes		
25 clothes	38,6	53,87
40 clothes		

**Table 4.** Length of time for drying clothes

No	Amount of clothes	Initial total mass wet clothes (kg)	Final total mass dry clothes (kg)	Mass of wet clothes-mass of dry clothes (kg)	drying time (menit)
1	15	3,94	2,55	3,94-2,55 = 1,39	210
2	25	6,57	3,96	6,57-3,96 = 2,61	330
3	40	10,51	6,51	10,51-6,51= 4,00	450

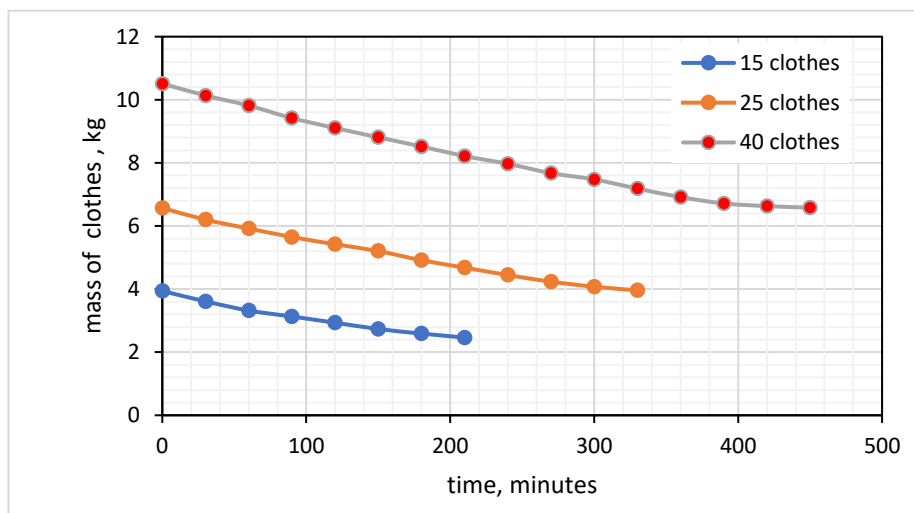


**Figure 5.** The total mass of clothes over time during the drying process.

When drying clothes, air flows by repeated air-cycles in the dryer. The air cycle consists of 4 processes: air cooling (sensible cooling), air cooling process accompanied by condensation of water vapor (cooling and dehumidifying), air heating (sensible heating) and cooling accompanied by an increase in specific humidity (evaporative cooling). The cooling and cooling and dehumidifying processes occur when air passes through the evaporator, the heating process occurs when air passes through the condenser, and the evaporative cooling process occurs when air is drying the clothes.

In the sensible cooling process, the process takes place in the evaporator. Dry-ball air temperature and wet-ball air temperature decrease. The sensible cooling process runs with a fixed humidity-specific value. Before the air undergoes the

sensible cooling process, the air condition is at point A which has a dry bulb air temperature  $T_{db,A}$  and a wet bulb air temperature with  $T_{wb,A}$ . At the end of the process, the air condition is at point B, with dry-ball air temperature expressed by  $T_{db,B}$  which is lower than  $T_{db,A}$  and wet-ball air temperature by  $T_{wb,B}$  which is also lower than  $T_{db,B}$ . The results showed that at the end of the sensible cooling process, the dry-bulb air temperature and wet-ball air temperature had the same values  $T_{db,B} = T_{wb,B}$  and had a relative humidity (RH) value of 100%. Thus the RH of the air has increased until it reaches 100% RH. In the sensible cooling process, heat is released from the air, and the heat released by the air is absorbed by the evaporator to be used to boil some of the refrigerant flowing in the evaporator pipes.

In the process of cooling the air which is accompanied by condensation of water vapor from the air (cooling and dehumidifying), the process takes place at a constant relative humidity of 100%, but the dry bulb air temperature and wet bulb air temperature decrease. This process can occur because the working temperature of the evaporator ( $T_{evap}$ ) is much lower than the temperature of the condensation of water vapor in the air. This causes in this process the condensation of water vapor from the air. The water content in the air decreases. A specific moisture reduction process occurs. When the air temperature leaves the evaporator, the dry bulb air temperature is expressed by  $T_{db,C}$  and the wet bulb air temperature is expressed by  $T_{wb,C}$ . The condition of the air coming out of the evaporator can be said to be dry. Even though it has an RH of 100%, the water content in the air is low. In this process, air releases heat, because in the phase change process from water vapor to the liquid phase (condensation) it always releases heat. The heat released by the air is also used to boil some of the refrigerant flowing in the evaporator pipes or is used to change the phase from a liquid and gaseous refrigerant mixture to a saturated gas.

The total amount of heat absorbed by the evaporator from the air in the sensible cooling process and in the cooling and dehumidifying process, the refrigerant mass unit is expressed in  $Q_{in}$ . The process of heat absorption in the evaporator through the surface of the fins installed on the evaporator pipes and through the outer surface of the evaporator pipes. In order for the heat absorption process through the fins and the pipe surface to run quickly, the fin material is selected from aluminum and the pipe

material is selected from copper. Both of these materials have relatively high thermal conductivity values and affordable selling prices. A fan is installed near the evaporator to increase the speed of the air flow. By increasing the air speed, it will increase the value of the convection heat transfer coefficient. The higher the value of the convection heat transfer coefficient, the greater the rate of heat transfer that occurs from the air fluid to the refrigerant flowing in the evaporator.

Coming out of the evaporator, air is passed through the condenser. When it passes through the condenser, the process of heating the air occurs. In this process, the process runs at a fixed specific humidity. The temperature of the dry bulb air and the wet bulb air temperature rising from the evaporator increases, from  $T_{db,C}$  and  $T_{wb,C}$  to  $T_{db,D}$  and  $T_{wb,D}$ . The air temperature rises because the working temperature of the condenser is higher than the air temperature. There is a flow of heat from the refrigerant flowing in the condenser into the air. Refrigerant can release heat, because the refrigerant in the condenser experiences a decrease in temperature from superheated gas to saturated gas (desuperheating process), and undergoes a phase change from a saturated gas phase to a saturated liquid phase (condensation process). The condenser releases heat into the air through the fins on the pipes and through the outer surface of the condenser pipes. Inside the condenser finned pipes, there is a process of decreasing temperature and the process of refrigerant condensing which releases heat

In the evaporative cooling process the dry bulb air temperature ( $T_{db,D}$ ) decreases, while the wet bulb air temperature remains ( $T_{wb,D}$ ). In an ideal process, the process runs at a fixed enthalpy value. The evaporative cooling process occurs when the air coming out of the condenser passes through clothes that are hung on hangers in the drying chamber. When air passes through the clothes, the water in the wet clothes evaporates, and the water moves from the clothes into the air. Clothes dry. The water phase changes from the liquid phase to the water vapor phase. In the process of changing the phase from the liquid phase to the water vapor phase, it requires heat, and the heat is taken from the air that passes through the clothes. Hence the dry bulb air temperature decreases. The amount of sensible heat provided by air is equal to the amount of latent heat used for the process of evaporating water from clothes. In this



process there is an addition of water content in the air, then the specific humidity of the air increases.

From Table 4, it appears that the length of time for drying clothes depends on the amount of clothes being dried or depending on the mass of clothes to be dried. The more clothes or the larger the mass of clothes to be dried, the longer the drying time will be. This is because the more clothes or the greater the mass of clothes that are dried, the more water has to be evaporated from the clothes. The degree of dryness obtained on clothing is evenly distributed for all clothing and in all clothing positions. Everything dries evenly like solar energy drying does. From Table 4 it can be seen that the average temperature before passing through the evaporator is 38.6°C and the air temperature leaving the condenser is an average of 53.87°C.

Some of the advantages of using a clothes dryer using a vapor compression cycle-based heat pump are: practical, safe and comfortable, environmentally friendly, can be used anytime and anywhere. The potential for fire is small, as there is no fire, oxygen and fuel. Oven work does not make noise and does not cause hot air conditions outside the oven. The environment is kept clean. Because it uses electrical energy, the clothes dryer is easy to operate and doesn't bother the user. The use of dryers does not pollute the environment, because there is no combustion process that produces exhaust gases. The dryer can work regardless of the weather. Can be done during the dry season or rainy season, morning, afternoon, evening or night, indoors or outdoors.

#### **4. Conclusion**

The conclusions of this study are (a) electrical energy clothes dryer using a vapor compression cycle-based heat pump has a performance (COP) of 7.94 (b) the time needed for a clothes dryer using a heat pump to dry 15 clothes, 25 clothes and 40 clothes respectively takes 210 minutes, 330 minutes and 450 minutes.

#### **Acknowledgements**

The author would like to thank the Head of LPPM Sanata Dharma University for the grant support provided, so that this research can be carried out and completed properly and smoothly. To the Head of Mechanical Engineering Study Program,

Deputy Dean I and Dean of FST Sanata Dharma University, we also express our deepest gratitude for the permission and for all the support given.

## **References**

- [1] Syarif Hidayat, Suparman Karnasudirdja, Sifat pengeringan alami dan pengeringan sinar matahari sebelas jenis kayu asal Kalimantan Barat, *Jurnal Penelitian Hasil Hutan Forest Product Research Journal* 2 (2)(1985) 5-9.
- [2] Saptariana, Meddiati Fajri Putri, Titin Agustina, Peningkatan kualitas produksi rengginang ketan menggunakan teknologi pengering buatan, *Rekayasa Jurnal Penerapan Teknologi dan Pembelajaran* 12 (1) (2014) 10-14.
- [3] Doddy Purwadianto, Petrus Kanisius Purwadi, Karakteristik mesin pengering emping jagung energi listrik, *Prosiding Seminar Nasional Universitas Respati Yogyakarta* 1 (2) (2019) 116-123.
- [4] Petrus Kanisius Purwadi, Mesin pengering kapasitas limapuluh baju sistem tertutup, *Jurnal Ilmiah Widya Teknik* 16 (2) (2017) 91-95.
- [5] Wibowo Kusbandono, Petrus Kanisius Purwadi, Effects of the existence of fan in the wood drying room and the performance of the electric energy wood dryer, *International Journal of Applied Sciences and Smart Technologies* 03 (1) (2021), 83–92.
- [6] Petrus Kanisius Purwadi, A. Prasetyadi, Characteristics of Wooden Furniture Drying Machine, *International Journal of Applied Sciences and Smart Technologies* 04 (1) (2022), 75-88.
- [7] M Adhi Prasnowo, Shafiq Nurdin, Analisis kelayakan mesin pengering keripik kentang, *Agrointek Jurnal Teknologi Industri Pertanian* 13 (1) (2019), 10-13.
- [8] Tri Mulyanto, Supriyono, Proses manufaktur mesin rotari tipe hibrida untuk pengering cabai, *Jurnal Asimetrik: Jurnal Ilmiah Rekayasa & Inovasi*. 1 (2) (2019) 125-132.
- [9] Dian Morfi Nasution, Himsar Ambarita, Safri Gunawan, Studi Awal Desain dan Pengujian Sebuah Mesin Pengering Hibrida Pompa Kalor dan Tenaga Surya, *Prosiding Seminar Nasional Rekayasa (SNTR) III*. (2016) 173-177.

- [10] Sari Farah Dina, Harry P. Limbong, Siti Masriani Rambe, Rancangan dan uji performansi alat pengering tenaga surya menggunakan pompa kalor (hibrida) untuk pengeringan biji kakao, *Jurnal Riset Teknologi Industri*, 12 (1) (2018) 22-33.
- [11] Efriwandy Simbolon, Jannifer Alfredo, Briand Steven Kaligis, Moh. Fikri Pomalingo, Ichiro Davidson Piri, Siti Vahira Cantika Kawuwung, Desain dan pabrikasi mesin pengering cengkeh berbahan bakar limbah kelapa untuk mempercepat proses penjemuran cengkeh, *Jurnal Keteknikan Pertanian Tropis dan Biosistem*, 10 (1) (2022) 21-28.
- [12] Pradeep Bansal, Amar Mohabir, William Miller, A novel method to determine air leakage in heat pump clothes dryers, *Elsevier*, 96 (1) (2016) 1-7.
- [13] Ward TeGrotenhuis, Andrew Butterfield, Dustin Caldwell, Alexander Crook, Austin Winkelman. Modeling and design of a high efficiency hybrid heat pump clothes dryer, *Elsevier, Applied Thermal Engineering* 24 (2017) 170-177.
- [14] Cakra M.A., Himsar Ambarita, Taufiq B. N, Alfian Hamsi Terang UHS Ginting, Pramio G. S, Karakteristik laju pengeringan pada mesin pengering pakaian sistem pompa kalor, *Jurnal Dinamis*, 4 (3) (2016) 1-13.
- [15] Gordon Httm, Azridjal Aziz, Rahmat Iman Mainil, Karakteristik pengujian pada mesin pengering pakaian menggunakan air conditioner (AC) ½ PK dengan siklus udara tertutup, *Jurnal Sains dan Teknologi*, 16 (1)(2017), 24-30.
- [16] Wibowo Kusbandono, The Effect of water impact on the refrigerant pipeline between compressor and condensor on COP and efficiency of cooling machine, *International Journal of Applied Sciences and Smart Technologies*, 3 (2) (2021), 203–214.

This page intentionally left blank

# Application of Augmented Reality-Based Solar System Recognition Using Metaverse Studio

Izza Wildan Ridhoni<sup>1</sup>, Muhammad Sholeh<sup>2\*</sup>

<sup>1,2</sup>Department of Informatics

Institut Sains & Teknologi AKPRIND Yogyakarta, Indonesia

\*Corresponding Author: muhash@akprind.ac.id

(Received 30-11-2022; Revised 30-12-2022; Accepted 02-01-2023)

## Abstract

Learning media is currently developing with various innovations, especially in utilizing information technology. One of the technologies used for the learning process is Augmented Reality (AR). The purpose of the research is to provide alternative learning media using information technology, especially focusing on the use of AR. The learning that will be developed in this case is learning aimed at children to introduce learning about the solar system using interactive AR. The content of the learning media developed includes several things, namely learning the solar system and quizzes to test children's knowledge about the solar system. The research method used in developing learning media uses the Research and Development (R&D) method. The application development process can be done by adding features. The results of this study produce an AR-based application that describes learning the solar system in 2D/3D form and is equipped with a quiz to train children's knowledge.

**Keywords:** Planets, Solar System, Augmented Reality.

## 1 Introduction

Learning media is currently developing with various innovations, especially in utilizing information technology. One of the learning media that can be used is Augmented Reality (AR). AR is a technology that combines computer-generated 2D/3D with a real environment [1-2]. AR is different from Virtual Reality (VR). VR is a technology that can describe real technology that is simulated by a computer, while AR only adds or completes applications with 2D/3D [3]. According to Setiawan AR is very supportive as a learning medium, because AR applications can improve understanding of learning materials. Learning media using AR is more effective than using books, videos and other media [4].

Research conducted by Fendi [5] developed an AR application to support learning basic chemistry courses. The use of AR is used to describe atoms, molecules, chemical



bonds, the periodic system and some other materials in 2D/3D form. The benefits of using AR can motivate students in learning basic chemistry. This is because students can interact with the developed application.

Research conducted by Rianto has developed an AR application to introduce traditional musical instruments, especially Lampung traditional musical instruments [6].

The AR research used in addition to the learning model was carried out by Dwi. In his research, he developed an AR application for building recognition. The usefulness of this application can be to introduce students to introducing building information on campus [7].

Research conducted by Alifah developed an AR application about the Tapis Fabric Textile Museum. This application is used to provide information about the collection of tapis cloth which is one of Lampung's cultures [8].

Research conducted by Ilhami Arsyah developed an AR application for a 3D house model. This application is used to help buyers find information on houses to be purchased and make it easier for home sellers as a promotional medium to consumers [9].

AR application research developed by Christian, the results of research conducted to create an AR-based learning media to introduce rare animals in Indonesia (Christian O et al., n.d.). Research conducted by Ramadhan develops AR applications to introduce computer hardware. This application is used to help students study TKJ BLK majors. [10].

Research conducted by Avief Barkah & Agustina designed interactive learning media using AR technology for the introduction of temples in the Malang area [11]. Another research that uses Augmented Reality for learning media is researched by [12-17].

AR applications can be used as an alternative learning media to introduce the planets in the solar system to children. Applications built using AR technology that are simulated in 2D/3D forms can provide information to children about the planets in the solar system. Learning media packaged using AR technology can provide knowledge to children on the material being taught. The use of AR technology makes the material more

interesting because it is packaged in 2D/3D form. Planetary Augmented Reality app developed using Studio.Gometa.io.

The use of the Gometa application in the development of Augmented Reality as a learning medium has been carried out by Lestari [18] and Andika [19]. The research conducted by Lestari discussed the introduction of medicinal plant learning media and Andika's research explored the introduction of animals.

Based on the introduction and the literature that has been described in the introductory section above, in this study developing learning media applications that use information technology, especially focusing on the use of AR. The learning that will be developed in this case is learning aimed at children to introduce an interactive AR-based solar system.

The content of the learning media developed includes several things, namely learning the solar system and quizzes to test children's knowledge about the solar system. The application was developed using the Gometa online application to display objects in 2D/3D form. AR applications developed with Studio.Gometa.io can be seen using the Metaverse Studio application on smartphones.

## **2 Research Methodology**

During the research, researchers must consider and determine which method is appropriate for their research so that the chosen method synergizes with the problem being studied [20]. Researchers can use and choose from various research methods, including qualitative methods, quantitative methods, mixed methods, and research and development methods. In this study, using the Research and Development (R&D) method. R&D is a research method used to make certain products and test the effectiveness of these products [21]. The R&D method is a development method that is suitable for research that aims to find products/find something new/something new and develop products that have been found [22].

The research process is carried out with the R&D stage. The stages of the R&D method are better known as ADDIE. The research stages are shown in Fig. 1. Fig. 1 is a diagram of the development model used in the research process.

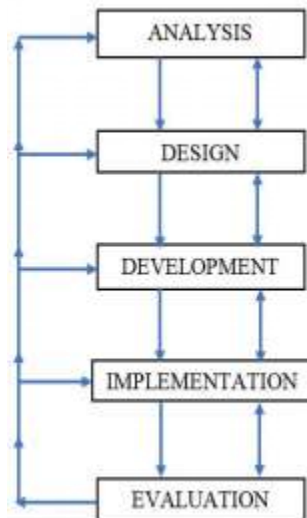


**Figure 1.** ADDIE Stages in the R&D method

This research will produce an AR application that describes the planets in the solar system in 2D/3D form developed using the Gometa application. Fig. 2 display

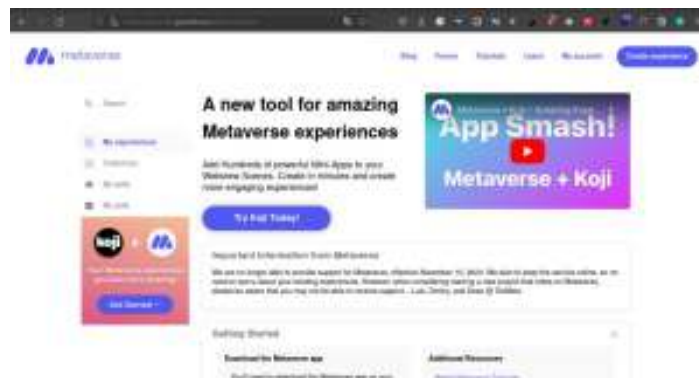


**Figure 2.** The front page of the Metaverse website with the link <https://studio.gometa.io/>



The results of the development of the Augmented Reality application using studio.gometa.io can be seen using the Metaverse application. Metaverse application is an android-based application. Fig. 3 Metaverse application display on android.



**Figure 3.** The front page of the Metaverse application on android

### **3 Results and Discussions**

#### **Linking Scene**

The initial process of making the application begins with making information about the solar system in the form of a scene. Scenes that have been created will be assembled into one interconnected unit. The step to connect a scene with another scene is to select a button that contains a menu and is related or connected to another scene. Fig. 4, an example of a related scene.

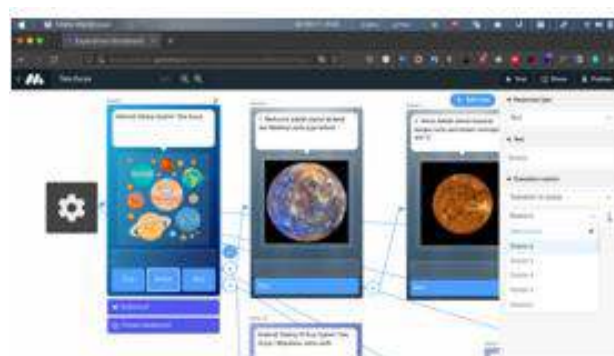


**Figure 4.** Connecting Scenes with other scenes

### **Handling text input from the user**

The developed application is also equipped with a scene containing a list of questions/quizzes. Before answering the question, the user must enter the name data. The process of designing input from the user uses the command / block save text feature. The process of using the save text block feature is shown in Fig. 5.

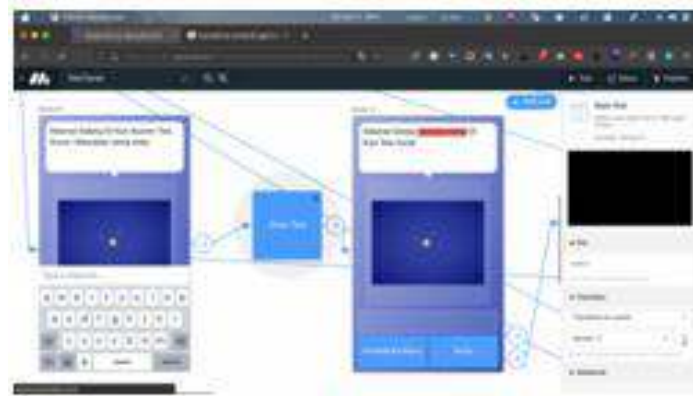


**Figure 5.** Handling text input

Handling text input from the user is by adding a block save text feature by connecting the display scene with the keyboard with the usual scene. In Fig. 5 above, between the 2 scenes, there is a save text block to retrieve the name data in scene 10 then it is stored with the name key in the save text block and the data is retrieved in scene 11 with the `/${props.nama}` command.

### **Creating a Quiz Scene**

The purpose of the quiz scene is for users not only to study the solar system but also to work on questions to determine the extent of the child's ability to understand the material of the solar system. The process of making the scene is in Fig. 6.

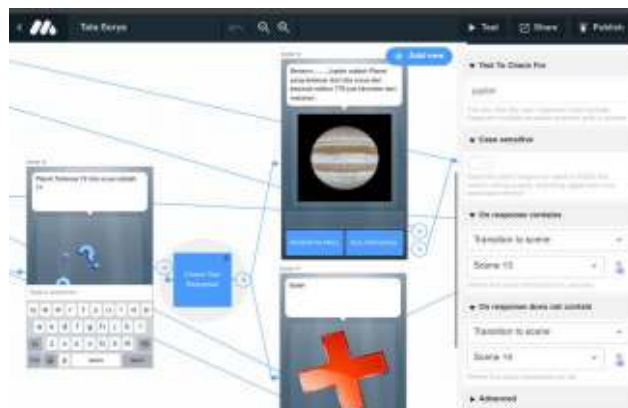


**Figure 6.** Handling the quiz scene

**Augmented Reality Application Results at studio.gometa.id**

The solar system application design is designed and packaged in scenes. Scene contains data about the planets and each scene will be connected to each other to form a unified solar system application. An example of the front page of an application developed in the form of a scene is presented in Fig. 7.



**Figure 7.** The design of one of the scenes of the solar system

There are 16 scenes developed. Each scene is assembled into a single unit so that users can use the application and learn various information about the solar system. The overall design of the planetary AR application in the form of a series of scenes is shown in Fig. 8.

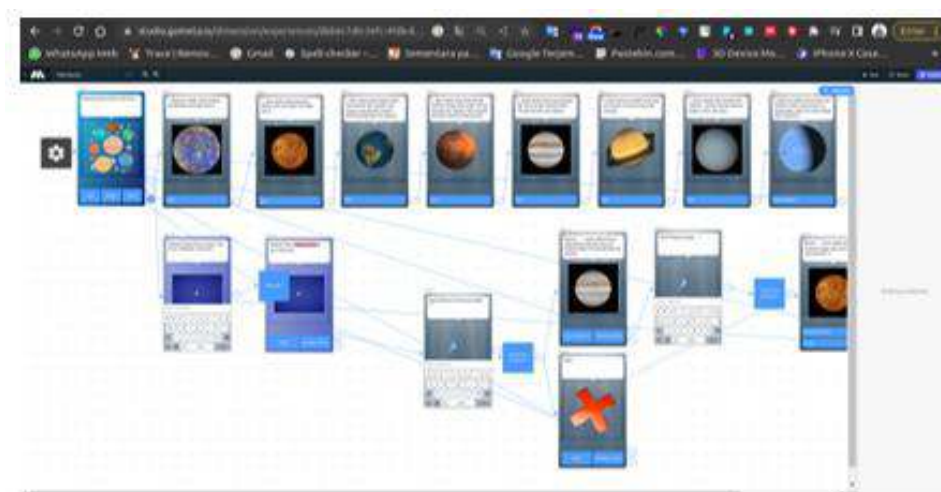


**Figure 8.** Overall Design of Planetary AR Application on Gometa

**Planet App Publication**

The process so that the Augmented Reality application developed can be accessed by users by first doing the publishing process. The results of the publishing process are in Fig. 9.

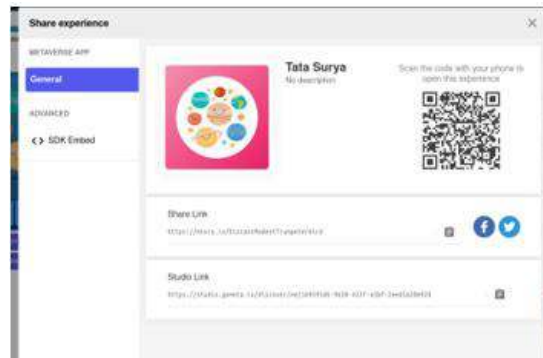


**Figure 9.** Planet Application Publish Page on Gometaverse

Once published, users can run the solar system application by first running the Metaverse application and directing the scanner to the published barcode. Fig. 10, the barcode that users can use to run the application and Fig. 11 the barcode scanning process in the Metaverse application to the Gometaverse website



**Figure 10.** Solar system application barcode



**Figure 11.** The barcode scanning process in the Metaverse application

The results of the scanning process, users can see the appearance of the solar system application in 2D/3D in Fig. 12.

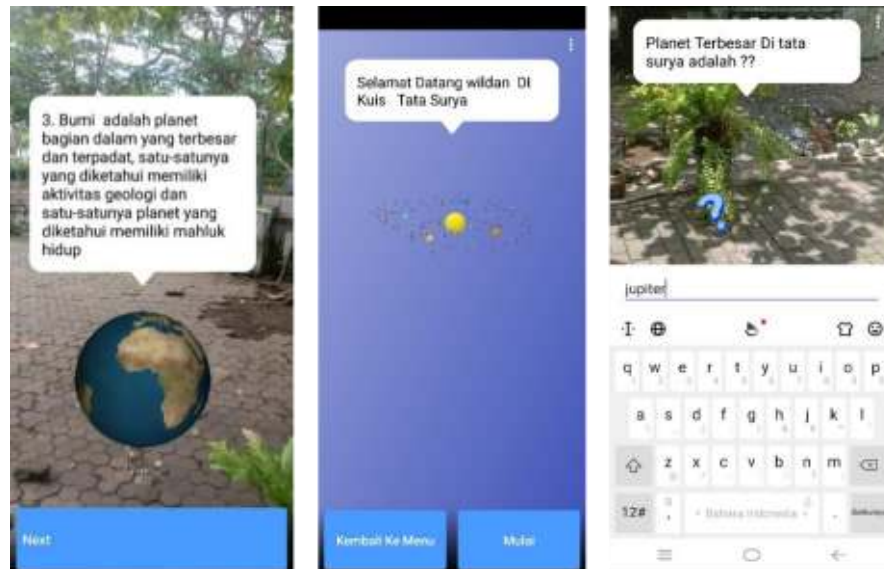


**Figure 12.** Solar system AR results and sample quiz when scanned

## 4 Conclusions

Augmented Reality-based introduction to the solar system can be an alternative learning media. The use of AR is expected to make it easier for children in the learning process, especially the material to recognize and understand the planets in the solar system. The solar system augmented reality application was developed using the Gometa application. The development process is distinguished in the form of interconnected scenes and to see the results of the developed application, it can be seen using the Metaverse application on the smartphone.

## References

- [1] A. Ismayani, *Membuat Sendiri Aplikasi Augmented Reality*. Jakarta: PT Elex Media Komputindo, (2020).
- [2] S. Asmiatun, N. Wakhidah, and A. Novita Putri, *Penerapan Teknologi Augmented Reality Dan GPS Tracking Untuk Deteksi Jalan Rusak*, (2020).
- [3] A. K. Pamudji, M. Setiyowati, and R. Sanjaya, *Mudah Membuat Game Augmented Reality (AR) dan Virtual Reality (VR) dengan Unity 3D*, Jakarta, (2017) 2–5,

- Accessed: Oct. 11, 2022. [Online]. Available: [http://elexmedia.id/users/9786020400389\\_mudah\\_membuat\\_game\\_augmented\\_reality\\_ar\\_dan\\_virtual\\_reality\\_vr\\_dengan\\_unity\\_3d](http://elexmedia.id/users/9786020400389_mudah_membuat_game_augmented_reality_ar_dan_virtual_reality_vr_dengan_unity_3d).
- [4] A. Pramono and M. D. Setiawan, Pemanfaatan Augmented Reality Sebagai Media Pembelajaran Pengenalan Buah-Buahan, (2019).
- [5] K. Fendi, Perkembangan Teknologi Augmented Reality Sebagai Media Pembelajaran Interaktif Pada Mata Kuliah Kimia Dasar, November 2018, 9 (1) (2019) 1,
- [6] N. Rianto, A. Sucipto, and R. Dedi Gunawan, Pengenalan Alat Musik Tradisional Lampung Menggunakan Augmented Reality Berbasis Android ( Studi Kasus : SDN 1 Rangai Tri Tunggal Lampung Selatan ), 2 (1) (2021) 64–72.
- [7] J. Dwi Gotama, Y. Fernando, and D. Pasha, Pengenalan Gedung Universitas Teknokrat Indonesia Berbasis Augmented Reality, J. Inform. dan Rekayasa Perangkat Lunak, 2 (1) (2021) 28–38.
- [8] R. Alifah, D. A. Megawaty, M. Najib, and D. Satria, Pemanfaatan Augmented Reality untuk Koleksi Kain Tapis (Study Kasus: UPTD Museum Negeri Provinsi Lampung),” J. Teknol. dan Sist. Inf., 2 (2) (2021) 1–7.
- [9] U. Ilhami Arsyah, R. Farta Wijaya, R. Budi Utomo, and K. Khairul, Implementasi Augmented Reality Sebagai Media Promosi Penjualan Rumah, Seminar Nasional Royal (SENAR), 1 (1) (2018) 429-434.
- [10] A. F. Ramadhan, A. D. Putra, and A. Surahman, Aplikasi Pengenalan Perangkat Keras Komputer Berbasis Android Menggunakan Augmented Reality (AR), (2021).
- [11] M. Avief Barkah and R. Agustina, Pemanfaatan Augmented Reality (AR) Sebagai Media Pembelajaran Interaktif Pengenalan Candi-Candi Di Malang Raya Berbasis Mobile Android, (2020).
- [12] S. D. Riskiono, T. Susanto, and K. Kristianto, Rancangan Media Pembelajaran Hewan Purbakala Menggunakan Augmented Reality, CESS (Journal Comput. Eng. Syst. Sci., 5 (2) (2020) 199.

- [13] A. Burhanudin, Pengembangan Media Pembelajaran Augmented Reality Pada Mata Pelajaran Dasar Elektronika Di Smk Hamong Putera 2 Pakem, *Pendidik. Tek. Mekatronika*, 7 (3) (2017) 266–274.
- [14] M. R. Mubaraq, H. Kurniawan, and A. Saleh, Implementasi Augmented Reality Pada Media Pembelajaran Buah-buahan Berbasis Android, *It (Informatic Tech. J.*, 6 (1) (2018) 89.
- [15] D. Nurmanto and R. Dedi, Pemanfaatan Augmented Reality dalam Aplikasi Magic Book Pengenalan Profesi untuk Pendidikan Anak Usia Dini, (2020).
- [16] Uliontang, E. Setyati, and F. H. Chandra, Pemanfaatan Augmented Reality pada Media Pembelajaran Sejarah Tentang Benda-Benda Bersejarah Peninggalan Kerajaan Majapahit di Trowulan Mojokerto, *Tek. Eng. Sains J.*, 4 (1) (2020) 19–26.
- [17] Quimillaila, B. H. Susanti, and Zulfiani, Pengembangan Augmented Reality Versi Android Sebagai Media Pembelajaran Sistem Ekskresi Manusia, (2017).
- [18] R. M. Lestari and M. Sholeh, Rancang Bangun Aplikasi Pengenalan Tanaman Obat Tradisional berbasis Augmented Reality dengan Menggunakan Studio.Gometa.io Design and build an Augmented Reality-based Introduction to Traditional Medicinal Plants Application by Using Studio.Gometa.io, *Semin. Nas. Multimed. Artif. Intell. SMAI 2021*, (2021) 55.
- [19] M. Sholeh and M. Andika, Aplikasi Pengenalan Dunia Satwa Berbasis Augmented Reality dengan Menggunakan Metaverse Studio Augmented Reality-Based Application for Introduction to Animal World by Using Metaverse Studio, *Semin. Nas. Multimed. Artif. Intell. SMAI 2020*, (2020) 175–181.
- [20] Wahyu RNS. Metode Penelitian R&D (Research and Development) Kajian Teoretis dan Aplikatif, (2020).
- [21] M. A. Zakariah, V. Alfriani, and K. M. Zakariah, Metodologi Penelitian Kualitatif, Kuantitatif, Action Research, Research And Development (R & D), (2020) 18.
- [22] B. Saputro, Best Practices Penelitian Pengembangan (Research and Development) Bidang Manajemen Pendidikan IPA, *Acad. Publ. Lamongan.*, (2021) 382.

This page intentionally left blank



# Laser Based Vibration Sensor Through Mobile

R. K. Mahapatra<sup>1,\*</sup>, Shalini J. Yadav<sup>2</sup> and Rajan Yadav<sup>2</sup>

<sup>1</sup>Department of Electronics and Telecommunication  
Thakur college of engineering and technology Mumbai, India

<sup>2</sup>Student of Electronics and Telecommunication  
Thakur college of engineering and technology Mumbai, India

\*Corresponding Author: mail2rashmita@gmail.com

(Received 29-05-2022; Revised 22-01-2023; Accepted 19-01-2023)

## Abstract

Machine condition monitoring has gained momentum over the years and becoming an essential component in the today's industrial units. A cost-effective machine condition monitoring system is need of the hour for predictive maintenance. The paper presents the design and implementation using vibration sensor, and also this system operated through smartphones. Vibration analysis plays a major role in detecting machine defects and developing flaws before the equipment fails and potentially damages. The concept of this project was to detect faulty equipment in industry machine so that before damaging the whole machine faulty equipment can be replace and improve the durability of machine.

**Keywords:** Vibration sensor, LDR sensor, Smartphone, Raspberry Pi.

## 1 Introduction

Vibration measurement using different signal processing with suitable set-up data is a powerful tool to identify and predict failure. Conducting different vibration analysis techniques could lead to improve Machine efficiency and availability. Monitoring the vibration characteristics of a machine can provide the information of its health condition, and this piece of information can be used to detect problems that might be incipient or developing. There are two ways for analysis with contact and without contact here this project is based on non-contact analysis. Non-contact analysis based on laser-based vibration sensor. Usually in the contact type vibration sensing, the sensor is

attached to the machines or instruments in order to detect the vibration amplitude and frequency.

Due to accessibility issues or the fact that the contact sensor adds mass to the instrument or machine and might change its vibration characteristics, the addition of a contact sensor is sometimes not practical in situations where precise vibration measurement is needed or in toxic and hazardous environments. nonetheless, non-contact analysis is more affordable, requires less human labour, and produces better findings.

In industry, machine monitoring necessary so that every machine can function properly and do not affect the production of plant. This project gives the solution for this problem by checking vibration level of machine if vibration level increases it will give alert so that faulty equipment can replace on time and production of plant can go on.

## **2 Research Methodology**

Non-contact vibration using a laser for structural cable health monitoring [1]. To measure cable vibration, a non-contact remote sensing laser vibrometer is utilized. It is now necessary for someone to gather vibration data. In the future, it will be upgraded to Bluetooth connectivity so that it may be managed from a secure location. The accuracy of the project can be increased by increasing the frequency. It can be modified in such a way that all parameters such as vibration, force, and damping ratio can be observed in a single device at the same time.

In the development of laser vibrometer [2]. the author has used the optical triangulation principle, with the laser source, target, and detection system forming the three vertices of a triangle. The laser beam strikes the target, and the backscattered light is collected by the detection system. the frequency range between 0-1KHz so it can be increased to 0-1GHz so that reading appear can be accurate.

Next the development of non-contact structural health monitoring system for machine tools[3]. A real time structural health monitoring (SHM) is a paramount for machining processes during machining, vibrations are always brought forth because of mechanical disturbances from various sources such as engine, a sound and noise etc.

The purpose of SHM is to avoid wasteful activities to optimize profitability of products and services to improve the information obtained about the condition of the machine tools being used. Development of non-contact structural health monitoring system for machine tools.

Machine condition monitoring has gained momentum over the years and becoming an essential component in the today's industrial units. Basic block diagram of proposed system is shown in Fig. 1.

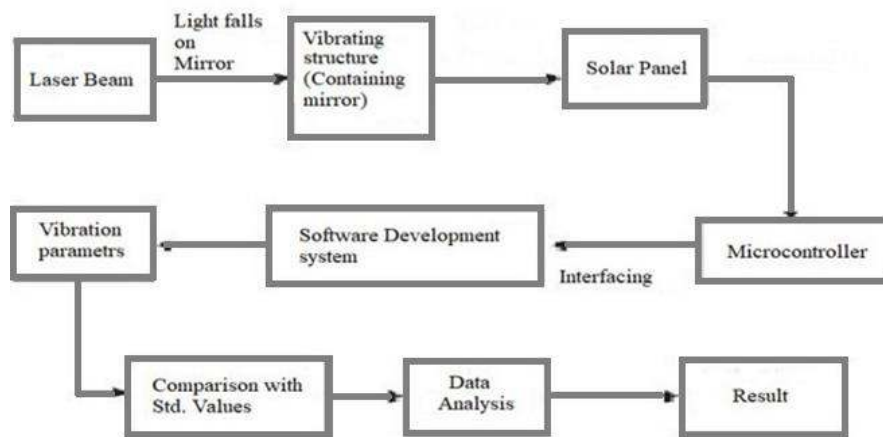


**Figure 1.** Basic circuit connection

Predictive maintenance urgently requires a system for monitoring machine status that is both affordable and effective [4,5]. Vibration that causes no damage is likewise highly helpful [6]. Simultaneous multidimensional measurements are feasible [7]. Additionally, cable-stayed bridges are incredibly efficient [8]. In the modern world, sensors play a significant role [9, 10]. In this paper, we have developed a machine condition monitoring system using smart phone, thanks to the rapidly growing smart-phone market both in scalability and computational power. In spite of certain hardware limitations, this paper proposes a machine condition monitoring system which has the tendency to acquire data, build the fault diagnostic model and determine the type of the fault in the case of unknown fault signatures. Results for the fault detection accuracy are presented which validate the prospects of the proposed framework in future condition monitoring services.

## Results and Discussions

The basic circuit connection is shown in Fig. 2. Vibration sensor is implemented using a laser and LDR sensor in Fig. 3 which are fixed on a wooden board in straight formation. A tube is placed in front of LDR to block noise light.

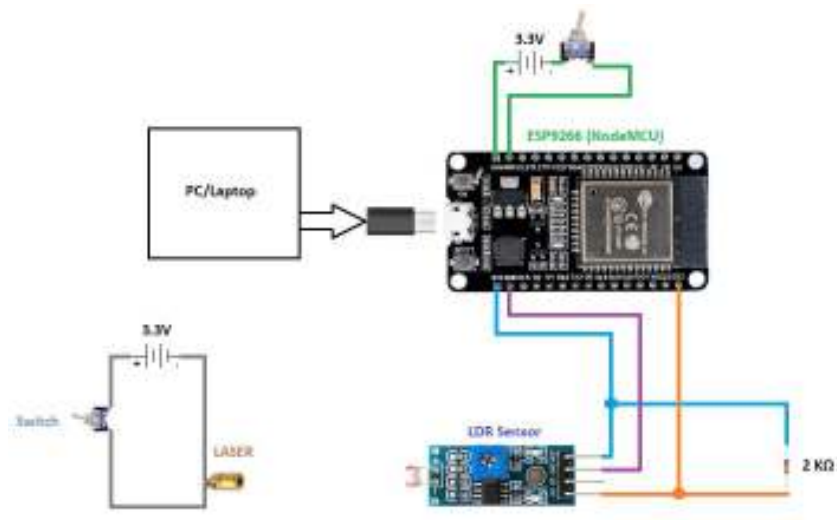


**Figure 2.** Basic circuit connection

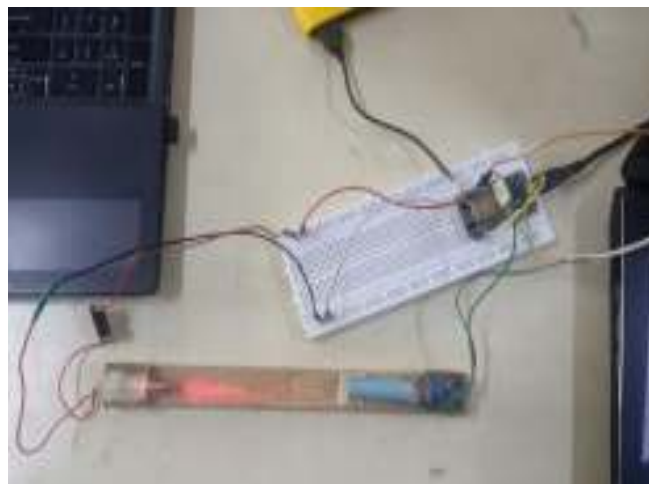


**Figure 3.** Basic physical circuit connection

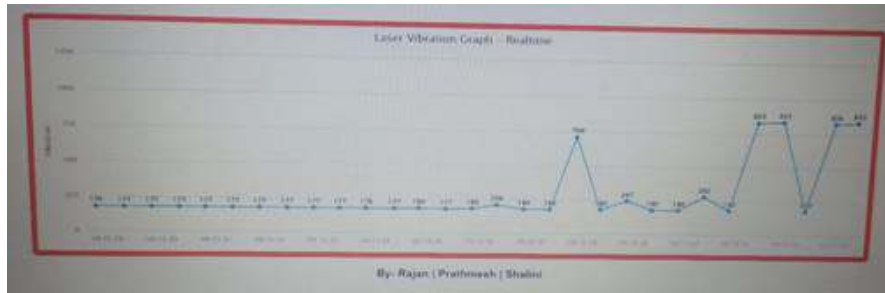


**Figure 4.** Laser based vibration sensor output

The data of Fig. 3 is sent to Raspberry Pi, which is then displayed on default monitor. The Raspberry Pi Code also host a local website which is used to plot value graph and display it.

**Table 1.** Reading Value Obtained on Serial Monitor

<b>IP address</b>	<b>Sensor</b>	<b>Output</b>
<b>14:44:26.567</b>	Vibration sensor	176
<b>14:44:26.567</b>	Vibration sensor	176
<b>14:44:26.567</b>	Vibration sensor	176

The default monitor that shows real-time value which is represented in Table 1 as it shows at very fast speed. The high-speed value recording makes this system accurate and it makes monitoring easier.

### **3 Conclusions**

In this paper, a vibration sensor that is used to detect vibrations in machine parts or structures was deployed using a Laser and LDR sensor. The approach used in this paper was non-contact based because of use of laser which is an upper hand compared to other methods present in market to measure vibrations. With further evolution in light sensing devices and sensors this project can gain many advantages over other methods. With present generation technology and components this system is already accurate and can detect very slight changes in vibrations.

## **Acknowledgements**

We would like to acknowledge TCET for providing us with a platform to instill Research Qualities and providing us with a medium to share and present our ideas. We would also like to thank our Mentor for guiding us throughout the entire journey.

## **Reference**

- [1] Mehrabi, Armin B., and Saman Farhangdoust, A laser-based noncontact vibration technique for health monitoring of structural cables: background, success, and new developments, *Advances in Acoustics and Vibration* (2018).
- [2] Rawat, Aseem Singh, and Nitin Kawade, Development of laser vibrometer, *BARC Newsletter* (2016) 16.
- [3] Goyal, Deepam, and B. S. Pabla, Development of non-contact structural health monitoring system for machine tools, *Journal of Applied Research and Technology*, 14 (4) (2016) 245-258.
- [4] Korkua, Suratsavadee, et al. Wireless health monitoring system for vibration detection of induction motors, 2010 IEEE Industrial and Commercial Power Systems Technical Conference-Conference Record, IEEE, (2010).
- [5] Gondal, Iqbal, Muhammad Farrukh Yaqub, and Xueliang Hua, Smart phone based machine condition monitoring system, *International conference on neural information processing*. Springer, Berlin, Heidelberg, (2012).
- [6] Yen, Wen-Huei P., Armin B. Mehrabi, and Habib Tabatabai. Evaluation of stay cable tension using a non-destructive vibration technique, *Building to Last*, ASCE, (1997).
- [7] Kulkarni, Rishikesh, and Pramod Rastogi, Simultaneous estimation of multiple phases in digital holographic interferometry using state space analysis, *Optics and Lasers in Engineering*, 104 (2018) 109-116.
- [8] Mehrabi, Armin B., In-service evaluation of cable-stayed bridges, overview of available methods and findings, *Journal of Bridge Engineering* 11 (6) (2006) 716-724.

- [9] Mohapatra, Badri Narayan, et al. Easy performance based learning of arduino and sensors through Tinkercad, International Journal of Open Information Technologies, 8 (10) (2020) 73-76.
- [10] Mohapatra, Badri Narayan, et al, Smart performance of virtual simulation experiments through Arduino Tinkercad Circuits. Perspectives in Communication, Embedded-systems and Signal-processing-PiCES 4 (7) (2020) 157-160.

This page intentionally left blank



# Smoothing Module for Optimization Cranium Segmentation Using 3D Slicer

Gilang Argya Dyaksa<sup>1,\*</sup>, Nur Arfian<sup>2</sup>, Herianto<sup>3</sup> and  
Lina Choridah<sup>4</sup>, Yosef Agung Cahyanta<sup>1</sup>

<sup>1</sup>Faculty Science & Technology, Sanata Dharma University, Indonesia

<sup>2</sup>Department of Anatomy, Faculty of Medicine, Public Health and Nursing,  
Universitas Gadjah Mada, Yogyakarta, Indonesia

<sup>3</sup>Department of Mechanical and Industrial Engineering,  
Universitas Gadjah Mada, Yogyakarta, Indonesia

<sup>4</sup>Department of Radiology, Faculty of Medicine,  
Public Health and Nursing, Yogyakarta, Indonesia

Corresponding Author : gilangad@usd.ac.id

(Received 28-04-2023; Revised 03-05-2023; Accepted 04-05-2023)

## Abstract

Anatomy is the most essential course in health and medical education to study parts of human body and also the function of it. Cadaver is a media used by medical student to study anatomical subject. Because of limited access to cadaver and also due to high prices, this situation makes it necessary to develop an alternative anatomical education media, one of them is the use 3D printing to produce anatomical models. Before 3D Print the cranium, it is necessary to do the segmentation process and often the segmentation result is not good enough and appear a lot of noises. The purpose of this research is to optimize a 3D cranium based on DICOM (digital imaging and communications in medicine) data processing using the smoothing modules on 3D Slicer. The method of this research is to process the Cranium DICOM data using 3D Slicer software by varying the 5 types of smoothing modules. The results with default parameter fill holes and median have better results compared to others. Kernel size variations are performed for smoothing module fill holes and medians. The result is fill holes get optimal segmentation results using a kernel size of 3 mm and the median is 5 mm

**Keywords:** anatomy, cranium, 3D slicer, smoothing module

## **1 Introduction**

Anatomical education is one of the most important courses to learn in the health and medical field [1]. Anatomy is studied using a body donor called cadavers. Cadavers can be obtained in several ways, such as direct donations from people who have agreed that they will donate their dead bodies to the university or the bodies of patients who died in hospitals but no family claiming their bodies [2].

The cadavers are high in price and the number of cadavers in university is limited [3]. Universitas Gadjah Mada (UGM) hasn't received any cadavers since 2001. These conditions are the reason for the development of anatomical education media, one of them is the use of 3-dimensional (3D) anatomical models.

Pandemic condition was also the reason for the development of anatomical education media using 3D technology due to the limited access to campus and the lab. 3D anatomical models provide an overview of anatomical structures more practically and are very useful for explaining some of the functions and relationships between anatomical structures. Anatomical education media using 3D models can reduce costs at the institution which is the costs for cadaver storage.

Because of this condition the development of medical advancement and 3D of anatomical model is the one of priority in this modern era [4]. One that is often done is multi modality 3D imaging technology and analysis of DICOM data using computer science and bio informatics. The purpose of this advance development is the medical workers can quickly see the visual of the patient body performed using CT or MRI then the results can be viewed in 3D and medical workers can diagnose patients. 3D imaging can also be used as a reference if the patient has defects or various medical disorders, which is important information in the medical field as a way to plan or determine procedures such as surgery that must be performed on patients [5].

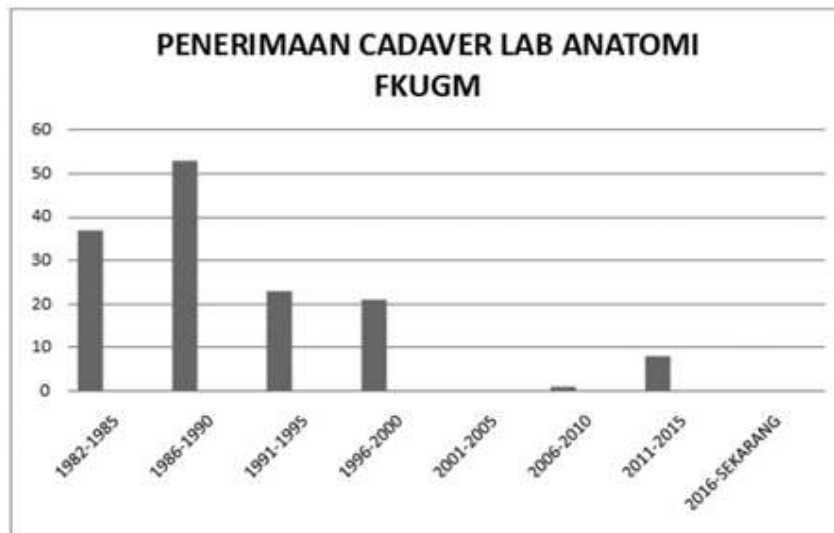


**Figure 1.** Graph of cadaver acceptance in the Department of Anatomy, Faculty of Medicine UGM since 1982 [3].

Analysis of CT results into 3D models can be done using open source software 3D Slicer that can perform medical image processing and visualization from DICOM Data and can be exported to 3D model mesh data such as STL and OBJ format [6]. 3D slicers are often used as a platform for developing and analyzing to produce prototype 3D models that suit clinical needs [7]. The result of prototype can be a 3D model or can be 3D printed to create a physical prototype of anatomical model.

In this reserach, we use 3D Slicer as a software for prototyping and development of cranium image analysis tools for clinical research applications and also provide an optimization using smoothing modules to make an optimal 3D model of anatomical model such as cranium that used in this research.

## **2 Methods**

This research only using cranium as anatomical model and the method to segmentation the cranium data is accordance with research that has been done previously using the threshold technique [8].

- **DICOM Data**

DICOM CT-Scan 3D data of patients were obtained from the radiology department of the Faculty of Medicine, Public Health and Nursing (FKKMK) Universitas Gadjah Mada (UGM) - Central General Hospital (RSUP) dr. Sardjito.

- **DICOM Viewer and segmentation**

The DICOM file was processed using the DICOM Viewer and Segmentation software that is 3D Slicer. The software was used to view the DICOM file and segment it to obtain a region of interest for this research, the cranium. Threshold value that used in this research is 150 for the lower limit and the upper limit using the default value 2976. After the segmentation process, then the next step is to vary the smoothing module with the aim of eliminating some areas that are not included in the region of interest or can also be referred to as noise.

- **Smoothing Modules**

The smoothing module is located in the segment editor which main function is to smooth the area that has been segmented before. There are 5 types of smoothing modules that are median, opening, closing, gaussian, and joint smoothing [9]. Median is to removes small extrusions and fills small gaps while keeps smooth contours mostly unchanged. Applied to selected segment only. Opening is to removes object smaller than the specified kernel size. Closing is fills sharp corner and hole smaller than the specified kernel size. Gaussian has stronger smoothing for all object details, but tend to shrink the object. Joint smoothing is tend to preserving watertight between separate objects.

After vary the 5 types of smoothing modules, 2 modules will be selected for the next step which is vary the kernel size to know the effect on the result of cranium segmentations. Kernel size is diameter of neighborhood that will considered around each voxel. In the 3D Slicer software documentation, it is explained that the greater the kernel size value, will makes the smoothing stronger and more details will be suppressed. In this study will vary 5 values of kernel size, that is 1, 2, 3, 4, and 5 mm with 3 mm is the default kernel size.

### **3 Results and Discussions**

This research used 3D Slicer software for segmentation the cranium from DICOM data. This step used the same threshold value.

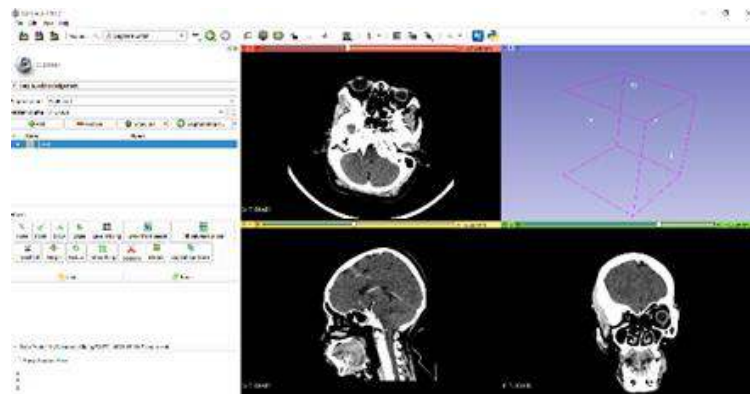


**Figure 2.** User interface of the first software.

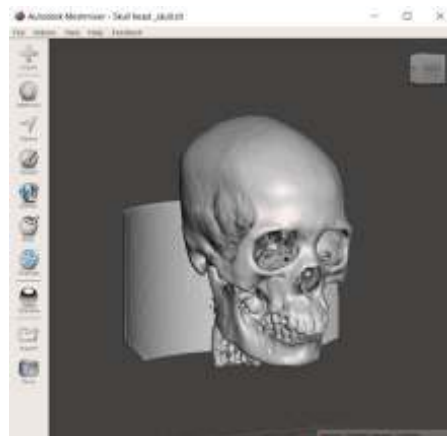


**Figure 3.** Segmentation output

The user interface of the first software is shown in Fig. 2. This software can show three planes commonly used by the medical officer to view CT imaging results,

namely axial, sagittal, and coronal, shown as the red, yellow, and green in window tabs. After opening the DICOM file, segmentation was carried out to determine the region of interest.

The segmentations result showed in Fig. 3 is segmentation without using smoothing module. Next will be discussed the results of segmentation using smoothing modules which will be shown in 2 views that is coronal plane and sagittal plane.

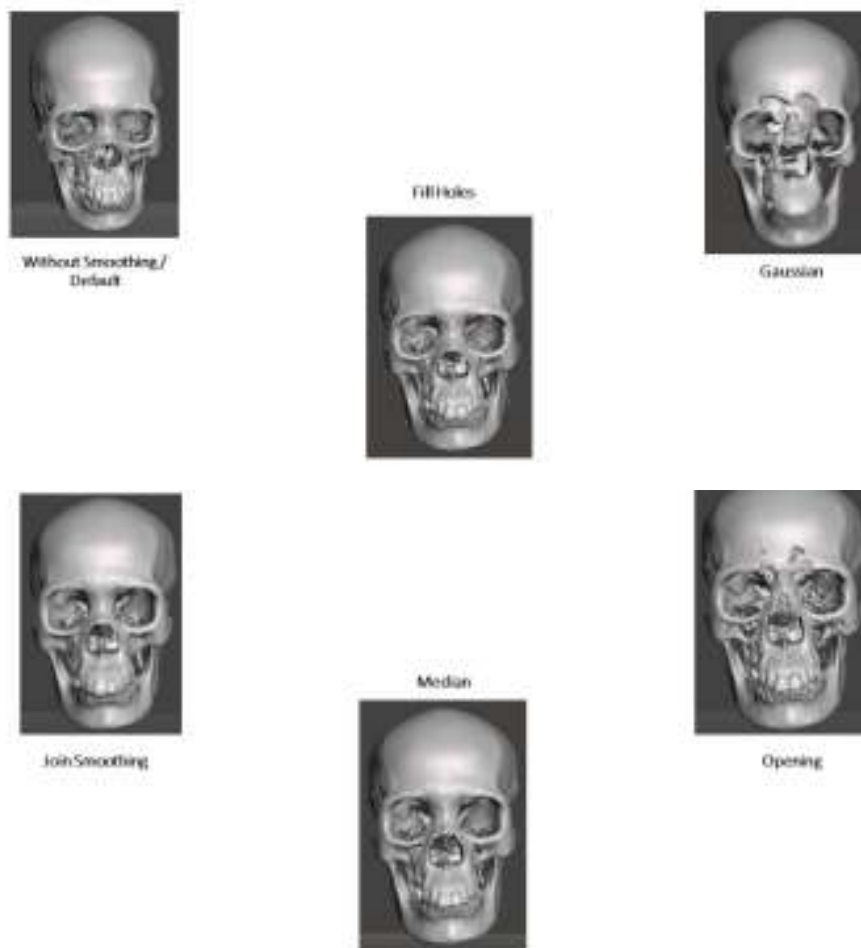


**Figure 4.** Segmentation using smoothing module coronal plane

The results of segmentation using smoothing modules can be seen in Fig. 4 for coronal plane and Fig. 5 for sagittal plane. When viewed from the coronal plane Gaussian has poor results because many details are missing such as in the frontal and maxilla. Opening also has poor results because some parts are perforated and include removing details from the cranium. Join smoothing has quite good results but in the

teeth the details are lost. If from the coronal view, the median and fill holes have the best results among other smoothing modules.

Move to Sagittal View, Gaussian and Opening still have poor results, especially some parts of the cranium that disappear so that the anatomy parts is not very clear. Join smoothing has quite good results as well, but especially in the ethmoid part the cranium loses a lot of parts so it loses a lot of detail.

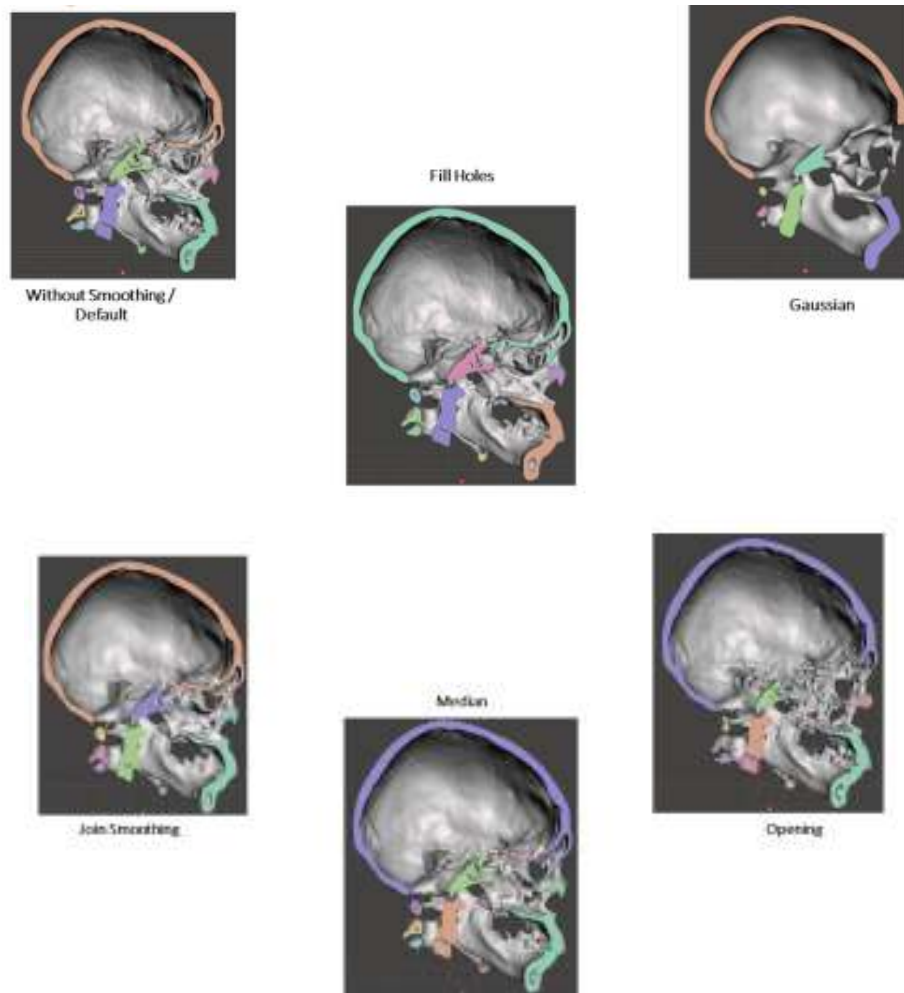


**Figure 5.** Segmentation using smoothing module sagittal plane

Comparison of segmentation results without smoothing module and smoothing module fill holes is shown in Fig. 6. If using fill holes, the result is that many cavities in a bone become more closed. In addition, there are also many parts of the cranium that are connected better using this module and can be seen around the occipital and sphenoid have quite good detailed results.



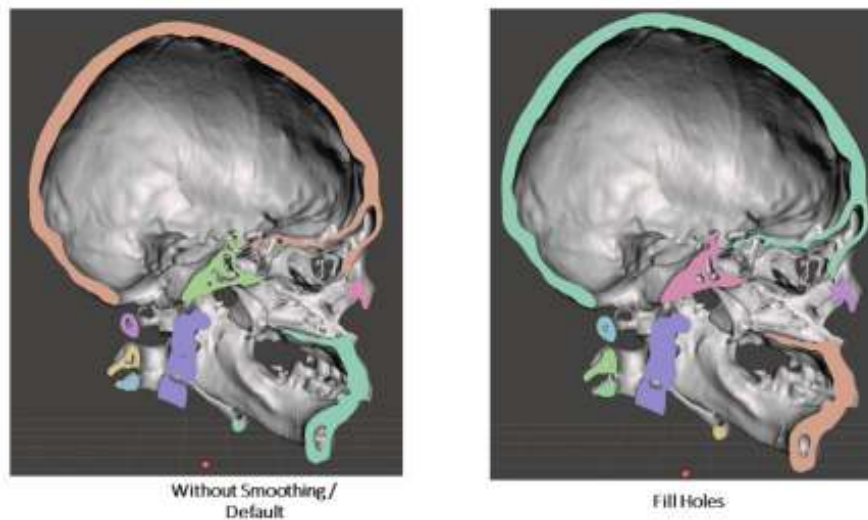


**Figure 6.** Segmentation using smoothing module default (left) and fill holes (right)

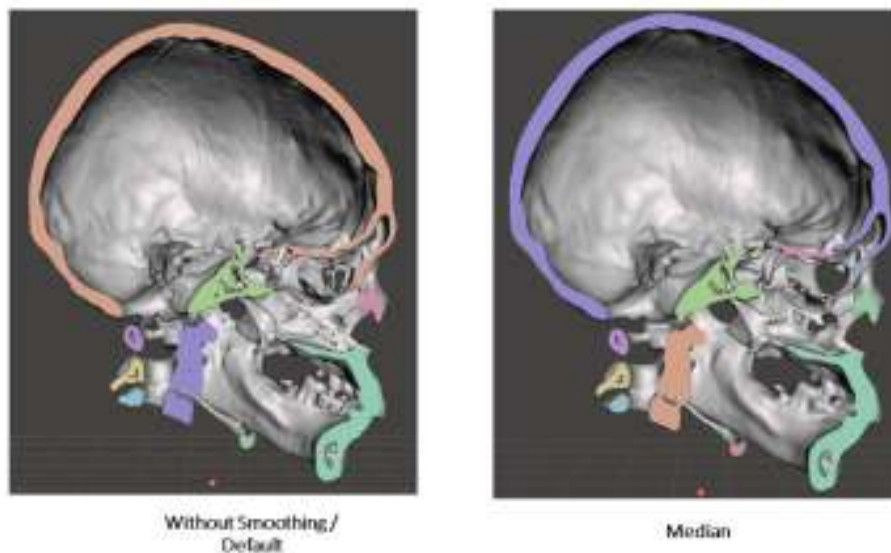


**Figure 7.** Segmentation using smoothing module default (left) and Median (right)

If it use the median smoothing module that can be seen in Fig. 7, the result is almost similar to fill holes, which close several cavities in the bone and can join several separate parts if segmented without using a smoothing module. But in certain parts there are several parts disconnected such as around the frontal and sphenoid.

As a decision in this first step of experiment, smoothing module fill holes and medians will be selected to proceed to the second experimental step, which is to vary



the kernel size of these two smoothing modules to find out the effect to the cranium segmentation.

The results of cranium segmentation using smoothing module fill holes by varying the value of the kernel size can be seen in Fig. 8 for coronal view and Fig. 9 for sagittal view. When viewed from the coronal view for kernel size variations does not provide a significant difference.

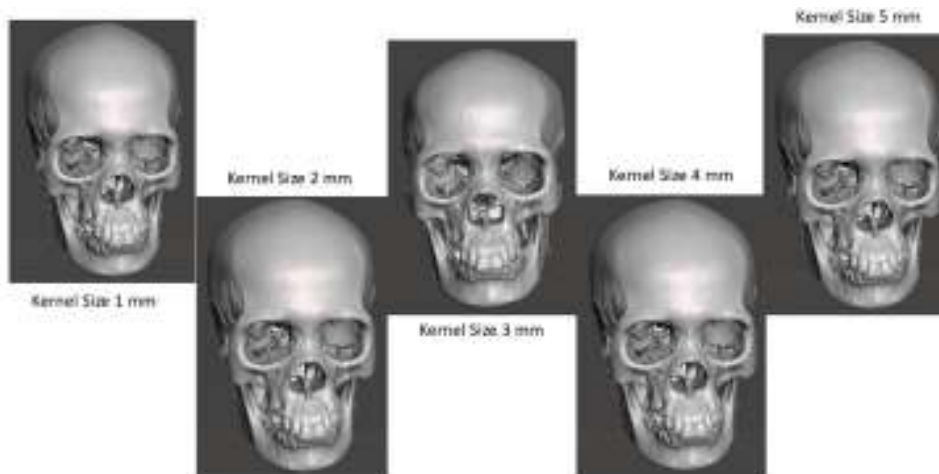


Figure 8. Segmentation using smoothing module fill hole coronal view.

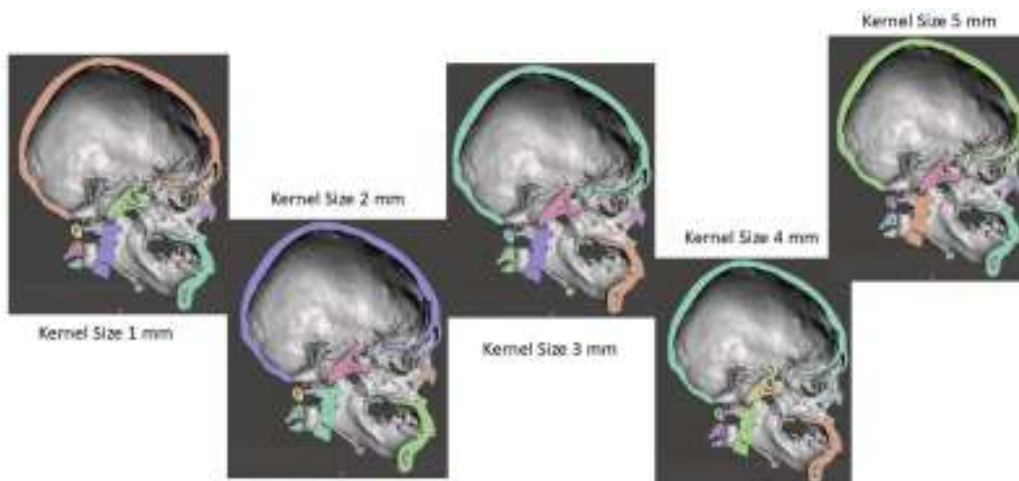
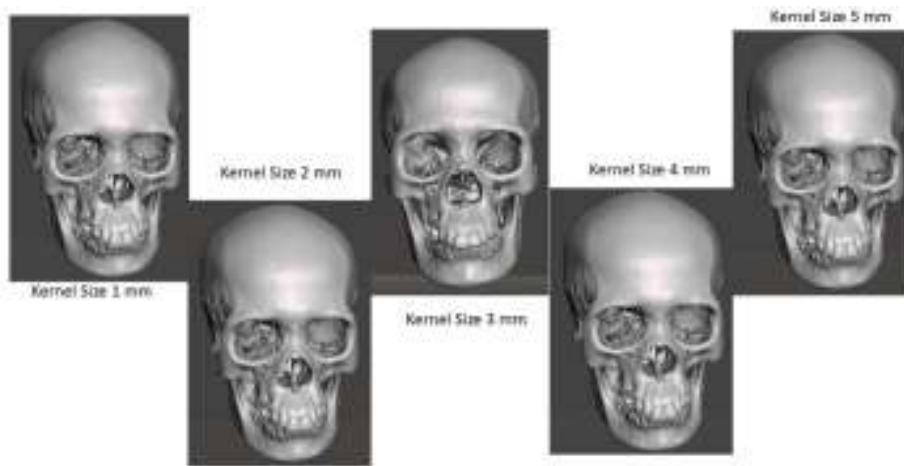


Figure 9. Segmentation using smoothing module fill hole sagittal view.

When viewed from the sagittal view in the kernel size range from 1 mm - 3 mm, in the spine and around the occipital the higher the value of the kernel size value, the cavity will be more closed and also in kernel size 3 (default value) still has a fairly good

anatomical detail around the occipital compared to the kernel size of 1 mm and 2 mm. But in kernel sizes of 4 mm and 5 mm, anatomical details are reduced because the results are almost the same as kernel sizes of 1 mm and 2 mm characterized by cavities that expand back around the mandible, spine, and occipital. The best result of the kernel size variation in smoothing module fill holes is the kernel size of 3 mm.



**Figure 10.** Segmentation using smoothing module median coronal view.

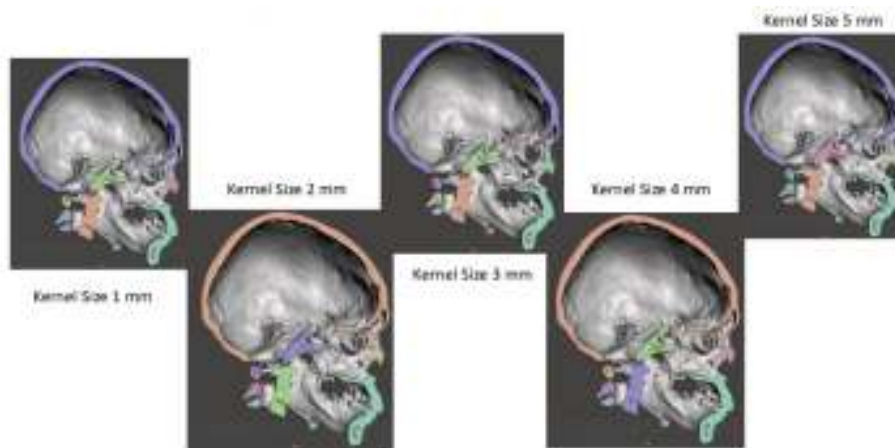


**Figure 11.** Segmentation using smoothing module median sagittal view.

The results of segmentation using the smoothing module median by varying the kernel size can be seen in Fig. 10 for coronal view and Fig. 11 for sagittal view. The coronal view median has a slight difference with fill holes, which is at the kernel size of 3 mm the segmentation results have a slight reduction in detail in the teeth. This reduction is not seen in any other kernel size other than 3 mm. When viewed in sagittal

view, the results are almost similar to fill holes. The results at kernel sizes of 1 mm and 2 mm are similar to the results of kernel sizes of 4 mm and 5 mm. The default kernel size of 3 mm has different characteristics from other kernel sizes which can be seen in comparison with the kernel sizes of 2 mm and 4 mm which will be shown in more detail in Fig. 12.

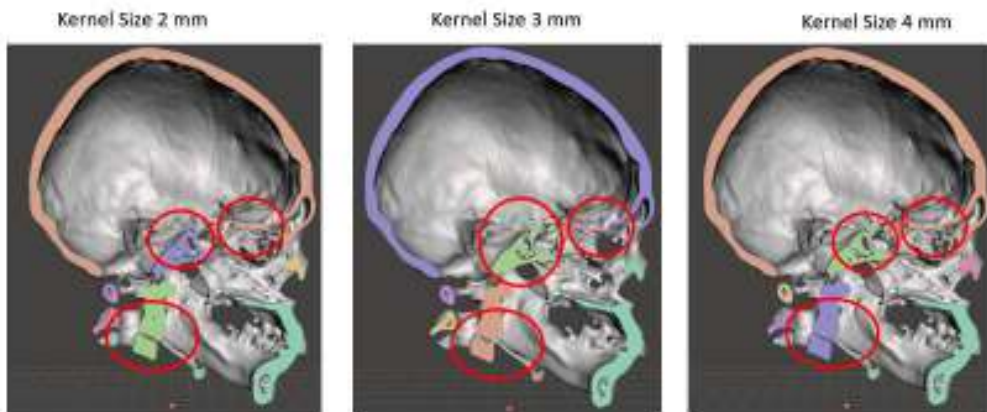


**Figure 12.** Comparison result median sagittal view.

Kernel size 3 mm has quite good segmentation results on the spine and occipital when compared to kernel sizes of 2 mm and 4 mm. But the 3 mm kernel size has disadvantages around the sphenoid parts that do not connect and where the segmentation results in kernel sizes 2 and 4 have better sphenoid results that connect compared to the 3 mm kernel size.

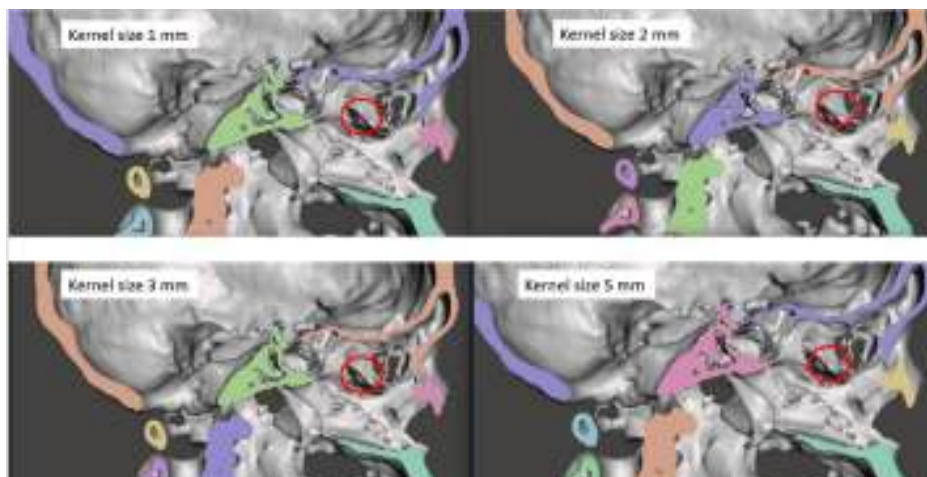


**Figure 13.** Comparison result median kernel size 1, 2, 4, 5 mm.

kernel size other than 3 mm also has other similarities that can be seen in Fig. 13, which both have details around the maxilla that are not found in the kernel size of 3 mm. Therefore, for the most optimal results 5 mm kernel size was chosen even though the results were almost the same as 1 mm, 2 mm, and 4 mm, but the 5 mm kernel size subjectively had more optimal results compared to others.

## **4 Conclusions**

Studies on the effect of smoothing modules and kernel size have been presented on the results of cranium segmentation. The results of this study used 5 types of smoothing modules fill holes, gaussian, join smoothing, median, and opening smoothing. The results with default parameter fill holes and median have better results compared to others. Kernel size variations are performed for smoothing module fill holes and medians. The result is fill holes get optimal segmentation results using a kernel size of 3 mm and the median is 5 mm. This research is limited to its application to cranium segmentation only. The direction of future research is to conduct a study of the optimal smoothing module for each anatomy part such as the brain, heart, liver, and abdomen.

## **Acknowledgements**

I would like to acknowledge and give my thanks to my supervisor Professor. Herianto and Dr. Nur Arfian who made this work possible and for the guidance and advice through all of the writing the research. I would like also to give special thanks to Dr. Lina Choridah from Department of Radiology, Faculty of Medicine, Public Health and Nursing for the continuous support for the data dan also understanding when undertaking my research and writing project.

## **References**

- [1] K. Sugand, P. Abrahams, and A. Khurana, The anatomy of anatomy: A review for its modernization, *Anat Sci Ed*, (2010).

- [2] Biasutto SN et al., Human bodies to teach anatomy: importance and procurement—experience with cadaver donation, (2014).
- [3] M. M. Romi, N. Arfian, and D. C. R. Sari, Is Cadaver Still Needed in Medical Education?, *JPKI*, 8 (3) (2019) 105.
- [4] X. Zhang, K. Zhang, Q. Pan, and J. Chang, Three-dimensional reconstruction of medical images based on 3D slicer, *J., complex., health sci.*, 2 (1) (2019) 1–12.
- [5] A. AlHadidi, L. H. Cevidanes, B. Paniagua, R. Cook, F. Festy, and D. Tyndall, 3D quantification of mandibular asymmetry using the SPHARM-PDM tool box, *Int J CARS*, 7 (2) (2012) 265–271.
- [6] Djoko Kuswanto and A. Tontowi, Development of Additive Manufacturing Methods for Reconstruction and Redesign Cranial Bone Defects in Indonesia, (2014).
- [7] A. Fedorov et al., 3D Slicer as an image computing platform for the Quantitative Imaging Network, *Magnetic Resonance Imaging*, 30 (9) (2012) 1323–1341.
- [8] G. A. Dyaksa, N. Arfian, and L. Choridah, Development of Cranium 3dimension-Puzzle Products Using 3D Printing, (2020).
- [9] C. Pinter, A. Lasso, and G. Fichtinger, Polymorph segmentation representation for medical image computing, *Computer Methods and Programs in Biomedicine*, 171 (2019) 19–26.

This page intentionally left blank

# **Educational Media Introduction To Human Internal And External Organs For High School Students Based On Augmented Reality By Using The Assemblr Application**

I Dewa Ayu Sri Murdhani<sup>1</sup>, Yunika Putri Oktavia<sup>2</sup> and  
Muhammad Sholeh<sup>2,\*</sup>

<sup>1</sup> Data & Information Management Study Program - Faculty of Technology and Informatics, Indonesian Institute of Business and Technology (INSTIKI), Denpasar, Bali, Indonesia

<sup>2</sup> Informatics Study Program - Faculty of Information Technology and Business, AKPRIND Institute of Science & Technology, Yogyakarta, Indonesia

Corresponding Author: muhash@akprind.ac.id

(Received 28-04-2023; Revised 03-05-2023; Accepted 04-05-2023)

## **Abstract**

The development of information technology from year to year always experiences very rapid development, and one of the positive impacts of this development is the existence of innovation in the field of education. Education today already uses information technology, especially augmented reality (AR). The purpose of this study is to help high school students in getting to know human internal and external organs through 2D or 3D virtual objects projected against the real world. The features in the educational media for the introduction of human internal and external organs are learning materials, quizzes, and games to hone students' knowledge. The research method used is research and development (R&D). This research will produce AR applications that discuss human internal and external organs, in addition to the features that will be produced, namely learning materials, quizzes, and games. With these 3 features, it is hoped that high school students will understand the material about human internal and external organs. AR-based learning media is developed using the Assemblr application.

**Keywords:** anatomy, cranium, 3D slicer, smoothing module



## **1 Introduction**

The world today has entered the era of the 4.0 generation industrial revolution which is characterized by increasing connectivity, interaction, and development of digital systems, artificial intelligence, and virtual [1]. This development also has an impact on various sectors of life, such as the economy, culture, politics, health, and education is no exception. In the field of education in the era of society 4.0 students in the learning process can directly face or interact with the visualization of 2D and 3D objects. AR is a technology that combines 2-dimensional and 3-dimensional computer-made objects into the real environment around the user in real-time [2] so that users feel virtual objects are around their environment. AR is a new way, where humans can interact with computers because it can bring virtual objects to the user's environment, then provide a real visualization experience [3]. AR accessibility in students is very open, this is evidenced by research that shows that 98% of smartphone owners are among the millennial generation, namely 18-24 years old [4].

With the accessibility of AR that is open among students, the development of AR-based learning media can be carried out. The research has been carried out by several researchers, including research on organ system learning media that uses AR has been developed with various software in the development process. Lestari's research develops android-based AR learning media in a simulation of human respiratory organ recognition which aims to help students in studying respiratory organs in detail [5]. Similar research was also conducted by [6], and Fuad using the marker base tracking method [7]. Saputra's research, in this study, developed AR learning media in introducing the human digestive system using the single marker system method whose purpose of this study is to increase and deepen students' knowledge of human digestive system material [8]. A similar study was also conducted by [9]. Aripin's research develops biology learning media, namely about the nervous system using AR



technology which aims to deepen students' understanding of the concept of biology learning which has abstract properties [10]. Syariffudin's research discusses the development of AR applications used as a learning medium for human organs in elementary school students, the purpose of this study is to support conventional learning that is applied [11]. The same research was also conducted by Fitriani who discussed the development of AR-based learning media regarding the introduction of organs in the human body [12]. Astiti's research, explores the application of dynamic video AR in android-based circulatory learning, with the hope that it can help teachers in delivering material, especially regarding blood circulation, and attract students to learn and understand the material [13].

From the research that has been carried out, AR is used in the development of learning media for the introduction of human internal and external organs. The process of developing AR-based learning media can be developed with various software, one of which is Assemblr. Assemblr is a software that can work using 2D and 3D visualizations, in addition to existing features including animation, video, music, and text, so it supports student-friendly learning. The use of Assemblr application has been used by Sugiarto in research on the development of learning media regarding the concept of blood circulation [14].

The introduction of human internal and external organs using AR is a means that can provide an overview to high school students about the function of the parts of human internal and external organs so that it can increase student focus and interest in learning, help students understand the material, while also making the learning atmosphere more interactive and fun. The results of the development of AR-based learning media display visualizations of images of human internal and external organs, in addition to that there are also quizzes and games to deepen students' understanding.

## 2 Research Methodology

From the various methods that exist in conducting research, it is selectively selected by researchers according to the theme of the title raised. One of the successes of researchers in conducting research is determined by the selection of the right research method [15]. The Research and Development (R&D) research method is a method used to produce a particular product, and test the effectiveness of that product. To be able to produce certain products, research that an analyst is used [16]. There are several models of R&D research methods, namely the define, design, develop and disseminate (4-D) model, analysis model, design, development, implementation, and evaluation (ADDIE), the Plomp model, the Borg and Gall models [17]. In this study, researchers used the R&D method with the ADDIE model. The stages of the ADDIE model can be seen in Fig. 1.

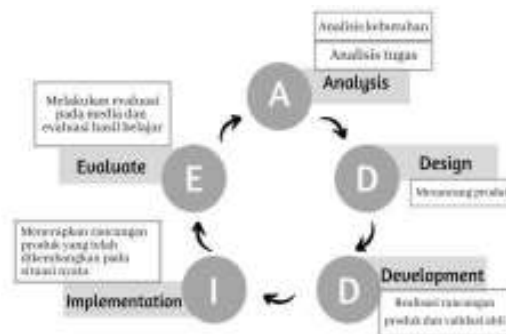


Figure 1. ADDIE Model Stages

This research will produce AR-based human internal and external organ learning media using Assemblr as a development medium. Assemblr is a website-based application with a [www.assemblr.com](http://www.assemblr.com) page. Fig. 2, Assemblr front page view.



Figure 2. Assemblr website appearance

### 3 Results and Discussions

#### Linking a scene

Scenes are used to describe a learning activity packaged in the form of AR. Each learning material is packaged in a different scene and between scenes is connected using the switch scene feature through 3d objects as shown in Fig. 3.



Figure 3. Use of the scene switch feature

#### Annotate

Each 3D object used in the learning process will be added annotated or notes as information of the usefulness in the designated section. Annotation is intended to provide labels in which there is additional information about the 3d object displayed. Annotation can be seen in Fig. 4.



Figure 4. Annotation

#### Change the objects that appear in a single scene

Changing objects that appear in one scene can be done using the move, show, and hide features at the same time. Move function to move objects, the show is used to display objects, and hide is used to hide the previous object to show the next object so that it does not occur buildup. Changing the object that appears using the next button to display the next object and the previous one to display the previous object, can be seen in Fig. 5.

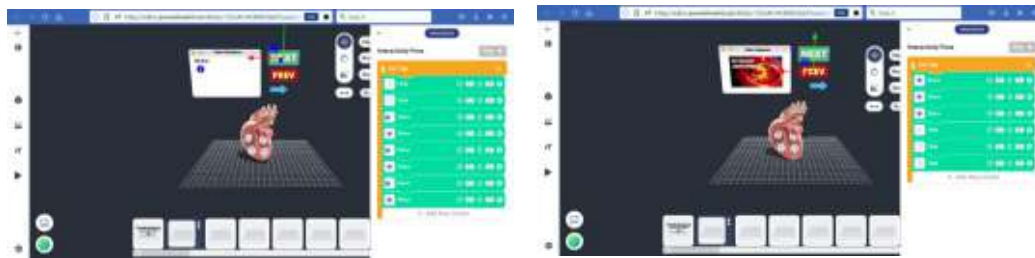


Figure 5. Object display with next button and previous button

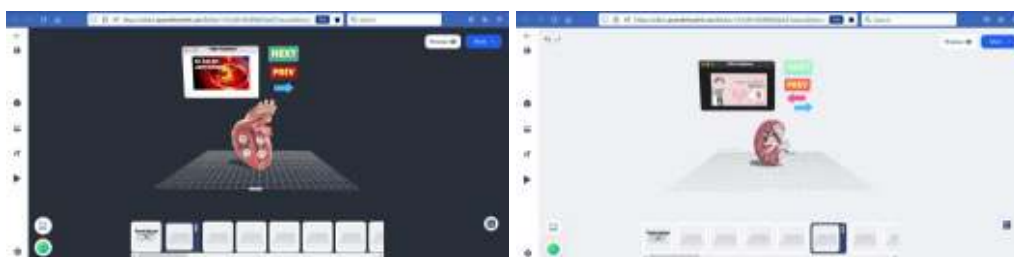
### Create a material scene

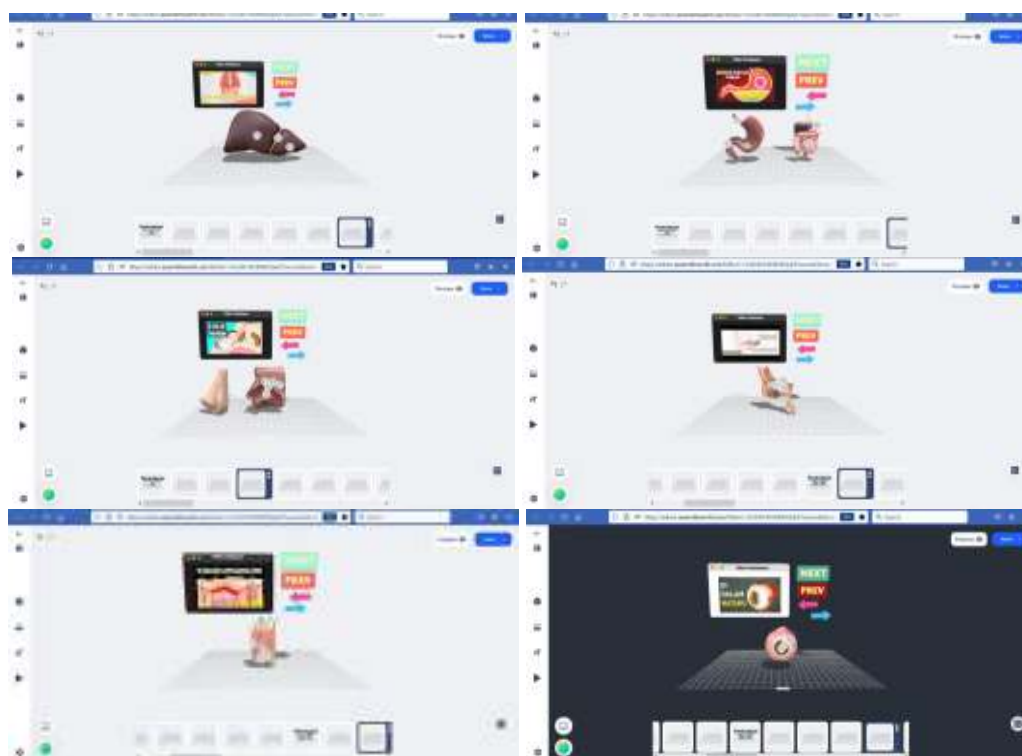
One of the steps in creating a material scene is to add videos and learning materials. The addition of this learning video is carried out aimed at complementing the material learned by the students. Some additional material uses links from existing material on YouTube, such as <https://youtu.be/F2hqR2iqhF8>, <https://youtu.be/QiEIDzKuDzo>. Fig. 6, the use of material on YouTube as a supplement to the material.



Figure 6. Addition of learning materials from Youtube

Video learning that lain among others sourced from links including <https://youtu.be/vGRIcRuGgcM>, <https://youtu.be/Znw6CfnsaMI>, <https://youtu.be/9ZOnqAIQSsw>, <https://youtu.be/g9LvUavRMg>, <https://youtu.be/1VaD8rLh5vk>, <https://youtu.be/zyptq2nYjDo>, <https://youtu.be/2MsbUulBpzY>, <https://youtu.be/HIGjKCHV9SY>. Fig. 7 the use of material from Youtube sources.





**Figure 7.** Addition of material from Youtube sources

Learning materials for human organs, in addition to using material taken on Youtube, are also equipped with learning book materials including biology students from high school grade 11 by Nunung Nurhayati and Resty Wijayanti. Fig. 8, learning material information taken from biology book material.



**Figure 8.** Learning materials in the form of text

### **Create a quiz scene**

The developed learning media is complemented by quizzes. This quiz can be used by students to test their comprehension of the material being studied. Creating a scene quiz using the switch scene feature, so when the user answers right or wrong, it

will be directed to a certain scene. An example of the display of this scene can be seen in Fig. 9.



**Figure 9.** Scene quiz display

### **Create scene games**

This scene uses the move, show, and switch scene features, which were previously explained. This game scene works by retrieving many objects according to the command by clicking on one of the objects then the object will move, but if the object is taken it is not accordingly, it will move to the scene that has been determined. The game scene is shown in Fig. 10.



**Figure 10.** Scene games

### **Publish applications of human internal and external organs**

The way to publish is by clicking the publish button and then filling in the title, image and video preview, description, sharing settings, and categories such as Fig. 11





Figure 11. The process of publishing an AR-based application in Assemblr

### Access to published apps

In accessing AR-based applications that have been published, there are 3 ways such as Fig. 12 .



Figure 12. How to access published AR-based applications

### Access using a web player link

The application is carried out using a browser by using the <http://asblr.com/TGb9f> link, Fig. 13 , the front page view of the application, and Fig. 14, the display of the developed application.



Figure 13. Web Player Link: <http://asblr.com/TGb9f>



Figure 14. AR-Based Application Display

**Access by generating QR markers**

Another way to access AR-based applications is to generate QR markers. This process is carried out by scanning the QR marker made through the Asemblr application. Fig. 15 , a QR marker that can be used to run applications, and Fig. 16, a scan process on a smartphone.



**Figure 15.** Generate QR marker

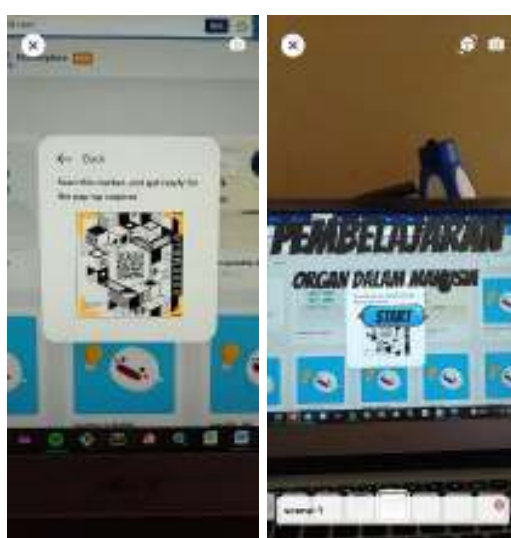


**Figure 16.** QR marker scan process and results after QR scan

## **4 Conclusions**

The development of AR-based learning media is expected to help high school students to deepen their understanding of material regarding human internal and external organs, besides, that it is also expected to change the classroom atmosphere to be more interactive. AR-based learning media is developed using the Asemblr application.



## **References**

- [1] Lase D. Jurnal sundermann. J Sunderman, 1(1) (2019) 28 - 43 Available from: 10.1109/ITHET.2016.7760744
- [2] Ismayani A. Membuat Sendiri Aplikasi Augmented Reality. Elex Media Komputindo, (2020) 224.
- [3] Siti A, Nur W, Novita PA. Penerapan Teknologi Augmented Reality dan GPS Tracking Untuk Deteksi Jalan Rusak [Internet], (2020) 93. Available from: [https://books.google.com.sg/books?id=coHRDwAAQBAJ&printsec=frontcover&dq=Penerapan+Teknologi+Augmented+Reality+dan+GPS+Tracking+Untuk+Deteksi+Jalan+Rusak&hl=id&sa=X&redir\\_esc=y#v=onepage&q=Penerapan+Teknologi+Augmented+Reality+dan+GPS+Tracking+Untuk+Detek](https://books.google.com.sg/books?id=coHRDwAAQBAJ&printsec=frontcover&dq=Penerapan+Teknologi+Augmented+Reality+dan+GPS+Tracking+Untuk+Deteksi+Jalan+Rusak&hl=id&sa=X&redir_esc=y#v=onepage&q=Penerapan+Teknologi+Augmented+Reality+dan+GPS+Tracking+Untuk+Detek)
- [4] Nielsen. Milenial Jadi Pengguna Smartphone Top [Internet]. (2016), Available from: <https://www.nielsen.com/id/insights/2016/millennials-are-top-smartphone-users/>
- [5] Lestari A, Trisnadoli A, Dewi M. Analisis Pengembangan Aplikasi Augmented Reality Untuk Pengenalan Organ Pernapasan Manusia. J Ris Komput. 6 (4) (2019) 42933.
- [6] Amalia EL, Suryani H D. Augmented Reality untuk Sistem Pernafasan pada Manusia. SMARTICS J. 5(2) (2019) 559.
- [7] Nasher F, Aditya D. Pemanfaatan Teknologi Augmented Reality Pada Sistem Pernapasan Manusia Berbasis Android Dengan Menggunakan Metode Marker Based Tracking Sebagai Media Pembelajaran. Media J Inform. 14 (1) (2022) 10.
- [8] Saputra AR, Tolle H, Akbar MA. Pengembangan Media Pembelajaran Untuk Pengenalan Sistem Pencernaan Manusia Menggunakan Teknologi Augmented Reality. J Pengemb Teknol Inf dan Ilmu Komput. 3 (7) (2019) 700613.
- [9] Mauludin R, Sukamto AS, Muhandi H. Penerapan Augmented Reality Sebagai Media Pembelajaran Sistem Pencernaan pada Manusia dalam Mata Pelajaran Biologi. J Edukasi dan Penelit Inform. 3 (2) (2017) 117.
- [10] Aripin I, Suryaningsih Y. Pengembangan Media Pembelajaran Biologi Menggunakan Teknologi Augmented Reality (AR) Berbasis Android pada

- Konsep Sistem Saraf. *Sainsmat J Ilm Ilmu Pengetah Alam*. 8 (2) (2019) 47.
- [11] Syarifuddin F, Purnawansyah, Irawati. Aplikasi Augmented Reality Media Pembelajaran Organ Tubuh Manusia Untuk SD Kelas 5 Berbasis Android. *Bul Sist Inf dan Teknol Islam*. 1 (1) (2020) 238.
- [12] Fitriani L, Rahayu REG, Firmansyah R. Rancang Bangun Media Pembelajaran Pengenalan Organ Dalam Tubuh Manusia dengan Penerapan Metode Augmented Reality. *J Algoritm*. 18 (2) (2022) 57482.
- [13] Wipra Astiti IAP, Arya Sasmita GM, Sukarsa M. Penerapan Augmented Reality Video Dinamis dalam Pembelajaran Peredaran Darah Berbasis Android. *J Ilm Merpati (Menara Penelit Akad Teknol Informasi)*. 6 (3) (2018) 174.
- [14] Sugiarto A. Penggunaan Media Augmented Reality Assemblr Edu untuk Meningkatkan Pemahaman Konsep Peredaran Darah (2022) 1-13
- [15] Budiyo Saputro. Manajemen Penelitian Pengembangan (Research & Development) Bagi Penyusun Tesis Dan Disertasi. *Journal of Chemical Information and Modeling*. (2017).
- [16] Zakariah, M. askari. Afriani, Vivi. Zakariah M. Metodologi Penelitian Kualitatif, Kuantitatif, Action Research, -  
Google Books [Internet]. (2020) 118. Available from:  
[https://www.google.co.id/books/edition/METODOLOGI\\_PENELITIAN\\_KUALITATIF\\_KUANTIT/k8j4DwAAQBAJ?hl=en&gbpv=1&dq=penarikan+kesimpulan+adalah&pg=PA56&printsec=frontcover](https://www.google.co.id/books/edition/METODOLOGI_PENELITIAN_KUALITATIF_KUANTIT/k8j4DwAAQBAJ?hl=en&gbpv=1&dq=penarikan+kesimpulan+adalah&pg=PA56&printsec=frontcover)
- [17] Amali K, Kurniawati Y, Zuhiddah Z. Pengembangan Lembar Kerja Peserta Didik Berbasis Sains Teknologi Masyarakat Pada Mata Pelajaran IPA di Sekolah Dasar. *J Nat Sci Integr*. 2 (2) (2019) 70.

# A Brief on Optical-based Investigation towards The Interfacial Behaviors during High Viscous Liquid/Gas Countercurrent Two-Phase Flow in a Complex Conduit Representing 1/30 Down-Scaled of PWR Hot Leg Geometry

Achilleus Hermawan Astyanto<sup>1, \*</sup>, Indarto<sup>2</sup>, Deendarlianto<sup>2</sup>

<sup>1</sup>Department of Mechanical Engineering, Universitas Sanata Dharma, Kampus III USD Maguwoharjo, Yogyakarta 55282, Indonesia

<sup>2</sup>Department of Mechanical and Industrial Engineering, Universitas Gadjah Mada, Jalan Grafika No 2 Kampus UGM, Yogyakarta 55281, Indonesia

\*Corresponding Author: achil.herma@usd.ac.id

(Received 28-04-2023; Revised 04-05-2023; Accepted 04-05-2023)

## Abstract

The present work briefly investigates liquid/gas countercurrent two-phase flow phenomena which can be specifically found in a mitigation during an accidental scenario in the operation of a nuclear reactor. A comprehensive knowledge on the corresponding phenomena is obviously important to avoid the failure on the cooling mechanism. Here, a pair of fluid containing high viscous liquid/gas flows through a complex conduit representing 1/30 scaled-down of PWR hot leg's typical geometry. Furthermore, the flow structures were visually observed, while the film thicknesses are extracted by an image processing algorithm through the corresponding optical-tabulated data. The obtained results reveal that a rather sharp decrease in liquid film corresponds to the flow regime transition.

**Keywords:** Countercurrent two-phase flow, liquid film thickness, high viscous liquid, complex conduit

## 1 Introduction

A gas/liquid countercurrent two-phase flow can be found in a mitigation of an accident on the operational of nuclear power plants. Here, it is strongly recommended that comprehensive knowledge on the corresponding phenomena is obviously important to avoid the failure on cooling mechanism during the scenario of loss of coolant accident because of a small break (SBLOCA) in the primary circuit of pressurized water reactors



(PWR). Furthermore, the database on the basis of analytical, mathematical, numerical and experimental investigations is able to elaborate the comprehensive behaviors of the corresponding flow phenomena [1].

Various studies have been carried out to investigate the characteristics of the flow structures during countercurrent two-phase flow. Visual observations are widely reported during the investigation on the basis of either large experimental works [2–5] or computational fluid dynamics [6]. Subsequently, measurement methods have also been developed to support the corresponding studies. Here, the studies on the pressure fluctuations were reported by several researches [7, 8]. Furthermore, the development of measurement methods has been conducted through physical measurements and also measurements on the basis of optical data. The concepts of conductance, capacitance and also impedance were largely reported as a particular technique during the measurements on the basis of electronic conceptions [9–13]. However, the characteristics of the flow regimes can be further obtained from the measurement on the basis of both the pressures and mainly interfacial behaviors since they strongly correspond to the fraction either the liquid or the gaseous phase, namely void fraction or liquid holdup, respectively.

On the other hand, the development of the measurements on the basis of optical data were introduced as well as the image processing techniques have been largely reported able to support the algorithm of object detections [14]. Therefore, since the interface between the phases during two-phase flow is defined as particular object, namely edge, the method may be used to support the description of a flooding which is initiated when the stability of the countercurrent flow cannot be maintained. Furthermore, the corresponding technique enables obtaining statistical characteristics of the countercurrent flow structures to be further elaborated as a regime identification method [15]. Here, various studies were conducted in both straight and complex geometries representing PWR hot leg's typical geometry. Moreover, the corresponding development of measurement methods was then applied to investigate the effects of both geometry and fluid properties toward the characteristics of countercurrent flow.

From the aforementioned literature surveys, it is strongly implied that the interfacial behaviors during the visualization may establish practical advantages during the investigation on countercurrent flow. A further challenge to develop measurement

techniques utilizing the optical data provides another opportunity to avoid such intrusive manners of conventional-physical measurements in which the probes should be contacted to the working fluids. Therefore, the present work elaborates the investigation of countercurrent flow phenomena on the basis of visual-optical data through the characteristics of liquid film thickness representing the interfacial behaviors.

## **2 Methods**

Fig. 1 schematically depicts the experimental apparatus. The main components of the constructed facility which mainly represents a small scale of a primary circuit of PWR comprises simulators of a hot leg, a reactor pressure vessel (RPV) and a steam generator (SG). In an accordance with the supply systems of working fluids, a centrifugal water pump and a reciprocating air compressor are utilized to circulate the liquid and gas, respectively.

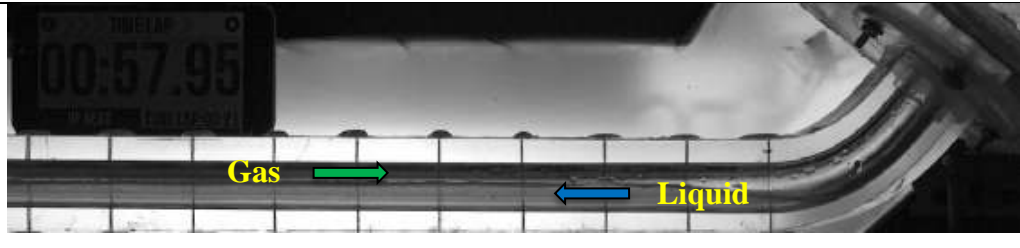
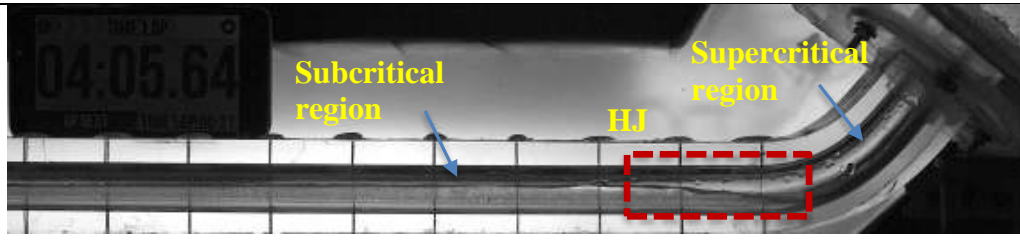
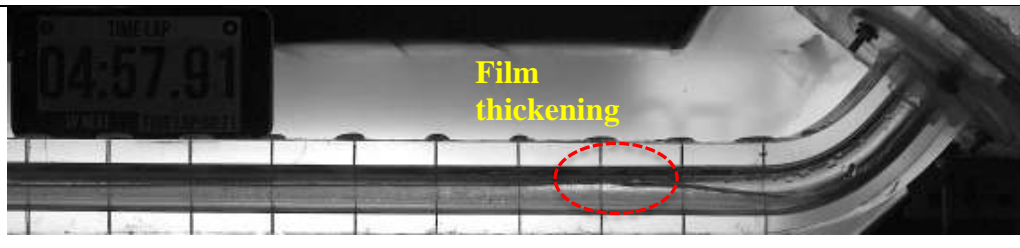
Table 1 provides the information of physical properties of the tested fluids. In order to increase the dynamic viscosity of the liquid, distilled water is mixed with glycerol in a percentage of 40% volume to total volume of the solution. On the other hand, to support the visual observations, a high speed video camera was utilized at 240 frame per second of recording rate.

**Table 1.** Physical properties of the tested fluids

<b>Properties</b>	<b>Gas</b>	<b>Liquid</b>
Density (kg/m <sup>3</sup> )	1.15	1058.13
Dynamic viscosity (kg/m. s)	$1.87 \times 10^{-5}$	$31.67 \times 10^{-4}$
Surface tension (N/m)	-	0.064



In the present work, the flow parameters which comprise the liquid and gas flow rates were varied. For a constant flow rate of the liquid, the gas flow rate was increased stepwise by an increment of 5 liters per minute (lpm). On the other hand, when the gas flow rate is kept constant, the liquid flow rate was increased stepwise by an increment of 2 gallons per hour (gph). In addition, a rather detailed description regarding both the experimental apparatus and procedures can be found in Astyanto et al. [13].

Q <sub>G</sub> (lpm)	Visual
10	
20	
30	

**Figure 2.** A typical set of visualization at the flow condition of  $Q_L = 24$  gph with respect to the change of gas flow rate.

### 3 Results and Discussions

Fig. 2 shows a typical visualization of the countercurrent flow under a constant liquid flow rate,  $Q_L = 24$  gph, with respect to the change of gas flow rate. From the figure it can be clearly seen that under this flow condition, a stratified structure is visually observed with a relatively stable interface on the lower gas flow rate. An inertial



dominated flow, namely supercritical flow, is observed in the inclined section and half of the elbow, while another gravitational dominated flow, i.e. subcritical flow, is observed in almost the entire horizontal section. A hydraulic jump (HJ) is further established as a flow transition from a supercritical to subcritical region. Here the liquid is accelerated by the presence of both riser's elevation and bended geometry. Moreover, as the gas flow rate is increased by a small increment, small waves are formed. They propagate along the direction of gas flow. As a result, a wavier interface followed by thickening film layer around the upper end of the hydraulic jump is further observed as the gas flow rate increases.

Q <sub>L</sub> (gph)	Visual
16	
20	
24	

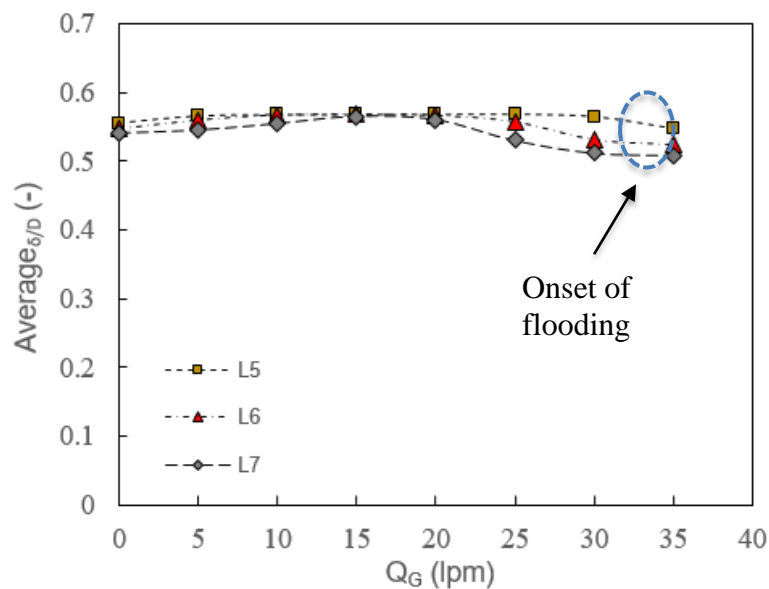
**Figure 3.** Another typical set of flow visualization at the flow condition of  $Q_G= 30$  lpm with respect to the change of liquid flow rate.

On the other hand, Fig. 3 depicts another typical visualization of the countercurrent flow under a constant liquid flow rate,  $Q_G= 30$  lpm, with respect to the change of the liquid flow rate. From the figure it can be seen that under this flow condition, a stratified



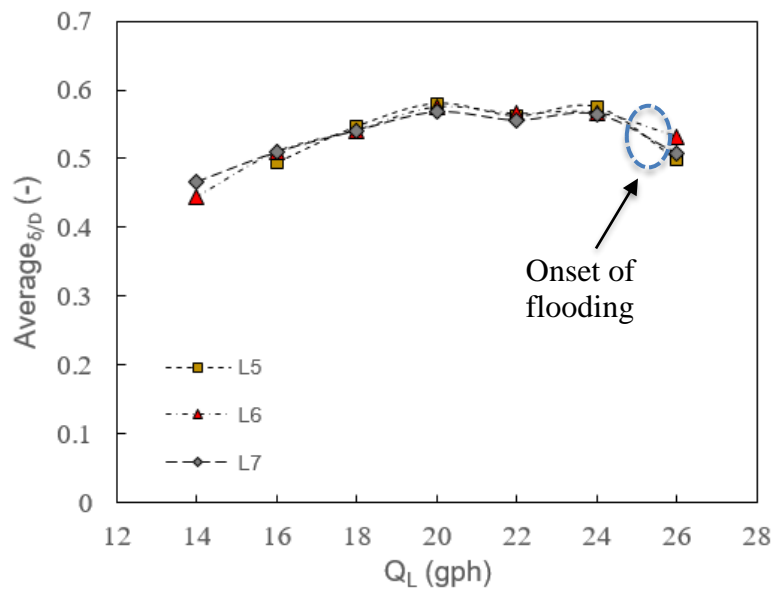
structure is also established with a rather fluctuate interface than the previous on the lower liquid flow rate when the liquid flow rate is kept constant. A supercritical flow is observed in the inclined section and half of the elbow, while a subcritical flow is observed in almost the entire horizontal section. Since in the beginning a lower liquid flow rate is applied here, a hydraulic jump with a shorter length is observed as its transition as the liquid is accelerated. Furthermore, as the liquid flow rate is increased, small waves are formed and propagate along the direction of gas flow. Similarly, a wavier interface with a thickening layer around the upper end of hydraulic jump is further observed as the liquid flow rate increases.

Fig. 4 shows the effect of gas flow rate towards the average of normalized film thickness,  $\delta/D$ , under the flow condition of  $Q_L = 24$  gph at several measurement coordinates (locus; L5, L6 and L7) of the subcritical region. From the figure it can be seen that  $\delta/D$  slightly increases then decreases as the gas flow rate increases. From  $Q_G = 0 - 15$  lpm,  $\delta/D$  slightly increases in which the measurement location nearest the elbow obtains the thickest liquid film. Subsequently, from  $Q_G = 15 - 20$  lpm L5, L6 and L7 exhibit an equal  $\delta/D$ , whereas from  $Q_G = 20 - 35$  lpm,  $\delta/D$  decreases in which the measurement location nearest the elbow exhibits the sharpest slope.



**Figure 4.** The effect of gas flow rate towards the average of normalized film thickness,  $\delta/D$  under the flow condition of  $Q_L = 24$  gph

On the other hand, Fig. 5 describes the effect of liquid flow rate towards  $\delta/D$  under the flow condition of  $Q_G = 30$  gph. From the figure it can be seen that that  $\delta/D$  tends to increase as the gas flow rate increases. Here, from  $Q_G = 14 - 20$  gph,  $\delta/D$  increases in which the measurement location nearest the elbow obtains the thickest liquid film. Subsequently, from  $Q_G = 20 - 24$  lpm,  $\delta/D$  increases then decreases. In addition, from  $Q_G = 16 - 24$  gph, L5, L6 and L7 obtain an almost equal  $\delta/D$ . from  $Q_G = 24 - 26$  lpm,  $\delta/D$  decreases.



**Figure 5.** The effect of gas flow rate towards the average of normalized film thickness,  $\delta/D$  under the flow condition of  $Q_G = 30$  lpm

From Figs. 5-6, it can be inferred that the film thickness tends to fluctuate as the fluid flow rate increases at the subcritical region. In addition, from the visualization at the flow condition of both  $Q_L = 24$  gph,  $Q_G = 35$  lpm and also  $Q_G = 30$  lpm,  $Q_L = 26$  lpm, the limit of stability of the countercurrent flow is reached, and flooding occurs. Here the explanation is that as the fluid flow rate increases, the liquid level around the upper end of hydraulic jump increases. The following phenomena causes a narrow area for gas to pass through. Based on the momentum balance equation of horizontal countercurrent two-phase flow, the relative velocity between the phase increases. As a result, the drag force increases and causes the liquid blocks the entire cross sectional area of the conduit, and

initiates flooding followed by churn. Therefore, a rather sharp decrease of  $\delta/D$  is further reported to correspond to the transition from a stratified to flooding regime [16].

## **4 Conclusions**

The behaviors of interface during gas/liquid countercurrent two-phase flow phenomena was briefly investigated. Here, a pair of fluid containing high viscous liquid/gas flows through a complex conduit representing 1/30 scaled-down of PWR hot leg's typical geometry. The flow structures were visually observed, while the film thicknesses are extracted by an image processing algorithm through the tabulated optical data. The obtained results reveal that a rather sharp decrease on liquid film thickness corresponds to the transition from a stratified to flooding regime.

## **Acknowledgements**

The author thanks to Dr. Apip Badarudin, Dr. IGNB. Catrawedarma, Dr. Setya Wijayanta, Akhlisa Nadiantya Aji Nugroho, M.Eng., and also all members of Multiphase Flow Research Group, Laboratory of Fluid Mechanics and Heat Transfers, Department of Mechanical and Industrial Engineering, Universitas Gadjah Mada for several brief discussions during either the facility installation or particular analyses. Moreover, during a better understanding on the flow phenomenology, a Phantom Miro M310 Lab high speed camera was utilized during the experiments. Therefore, the author also acknowledges PT. Chevron Indonesia for the proper opportunity.

## **References**

- [1] Deendarlianto, T. Höhne, D. Lucas, K. Vierow, Gas-liquid two-phase flow in a PWR hot leg: A comprehensive research review, *Nuclear Engineering and Design* 243 (2) (2012) 214–233.
- [2] Deendarlianto, C. Vallée, D. Lucas, M. Beyer, H. Pietruske, H. Carl, Erratum: Experimental study on the air/water counter-current flow limitation in a model of the hot leg of a pressurized water reactor, *Nuclear Engineering and Design* 241(8) (2011) 3359–3372.

- [3] A. Badarudin, S. T. Pinindriya, Y. V. Yoanita, M. S. Hadipranoto, S. Hartono, R. Ariawan, Indarto, Deendarlianto, The effect of horizontal pipe length to the onset of flooding position on the air-water counter current two-phase flow in a 1/30 scale of pressurized water reactor (PWR), AIP Conference Proceedings 2001 (2018) 03001.
- [4] A. Badarudin, Indarto, Deendarlianto, A. Setyawan, Characteristics of the air-water counter current two-phase flow in a 1/30 scale of pressurized water reactor (PWR): Interfacial behavior and CCFL data, AIP Conference Proceedings 1737 (2016) 040015.
- [5] A. Badarudin, A. Setyawan, O. Dinaryanto, A. Widyatama, Indarto, Deendarlianto, Interfacial behavior of the air-water counter-current two-phase flow in a 1/30 scale-down of pressurized water reactor (PWR) hot leg, Annals of Nuclear Energy 116 (2018) 376–387.
- [6] Deendarlianto, T. Höhne, D. Lucas, C. Vallée, G. A. M. Zabala, CFD studies on the phenomena around counter-current flow limitations of gas/liquid two-phase flow in a model of a PWR hot leg, Nuclear Engineering and Design 241(12) (2011) 5138–5148.
- [7] A. H. Astyanto, Y. Rahman, A. Y. A. Medha, Indarto, Deendarlianto, Time-series differential pressure fluctuations of a flooding regime : A preliminary experimental results investigation on a 1/30 down-scaled PWR hot leg geometry, AIP Conference Proceedings 2403 (2021) 060001.
- [8] A. H. Astyanto, Y. Rahman, A. Y. A. Medha, Deendarlianto, Indarto, Pengaruh Rasio I/D terhadap Permulaan Flooding dan Fluktuasi Voltase Sinyal Tekanan Rezim Flooding pada Geometri Kompleks, Rekayasa Mesin 12 (2021) 447–457.
- [9] Deendarlianto, A. Ousaka, Indarto, A. Kariyasaki, D. Lucas, K. Vierow, C. Vallee, K. Hogan, The effects of surface tension on flooding in counter-current two-phase flow in an inclined tube, Experimental Thermal and Fluid Science 34(7) (2010) 813–826.
- [10] Deendarlianto, A. Ousaka, A. Kariyasaki, T. Fukano, Investigation of liquid film behavior at the onset of flooding during adiabatic counter-current air-water two-phase flow in an inclined pipe, Nuclear Engineering and Design 235(21) (2005) 2281–2294.

- [11] Deendarlianto, A. Ousaka, A. Kariyasaki, T. Fukano, M. Konishi, The Effects of Surface Tension on the Flow Pattern and Counter-Current Flow Limitation (CCFL) in Gas-Liquid Two-Phase Flow in an Inclined Pipe, *Japanese Journal of Multiphase Flow* 18 (4) (2004) 337–350.
- [12] A. Ihsan, A. H. Astyanto, Indarto, Deendarlianto, *Kajian Eksperimental Karakteristik Perilaku Antarmuka Aliran Berlawanan Arah di Geometri 1:30 Hot Leg PWR Menggunakan Sensor Kawat Sejajar*, *Prosiding Seminar Nasional Multidisiplin Ilmu Universitas Respati Yogyakarta*, 3 (1) (2021).
- [13] A. H. Astyanto, J. A. E. Pramono, I. G. N. B. Catrawedarma, Deendarlianto, Indarto, Statistical characterization of liquid film fluctuations during gas-liquid two-phase counter-current flow in a 1/30 scaled-down test facility of a pressurized water reactor (PWR) hot leg, *Annals of Nuclear Energy* 172 (2022) 109065.
- [14] A. Ghoshal, A. Aspat, E. Lemos, *OpenCV Image Processing for AI Pet Robot*, *International Journal of Applied Sciences and Smart Technologies*, Vol 3 Issue 1 (2020) 65 – 82.
- [15] A. H. Astyanto, A. N. A. Nugroho, Indarto, I. G. N. B. Catrawedarma, D. Lucas, Deendarlianto, Statistical characterization of the interfacial behavior captured by a novel image processing algorithm during the gas/liquid counter-current two-phase flow in a 1/3 scaled down of PWR hot leg, *Nuclear Engineering and Design* 404 (2023) 112179.
- [16] A. H. Astyanto, Indarto, K. V. Kirkland, Deendarlianto, An experimental study on the effect of liquid properties on the counter-current flow limitation ( CCFL ) during gas/liquid counter-current two-phase flow in a 1/30 scaled-down of Pressurized Water Reactor ( PWR ) hot leg geometry, *Nuclear Engineering and Design* 399 (2) (2022) 112052.

This page intentionally left blank

# Input Power Measurement System for Driving Motor in Testing Low-Speed Generator

Ignasius Eko Yuliyanto<sup>1</sup>, Tjendro<sup>1</sup>, Bernadeta Wuri Harini<sup>1</sup>,  
Martanto<sup>1,\*</sup>

<sup>1</sup>Department of Electrical Engineering, Sanata Dharma University,  
Yogyakarta, Indonesia

\*Corresponding Author: martanto@usd.ac.id

(Received 28-04-2023; Revised 08-05-2023; Accepted 11-05-2023)

## Abstract

Rapid technological advances are affecting the greater use of electrical energy. One of the devices that can generate electrical energy is a generator. Testing the characteristics of the generator required a drive motor to rotate the generator shaft. This research aims to create a three-phase input power measurement system for driving a motor. The method of measuring input power is by measuring the current and voltage of each phase. The power is obtained from the multiplication between current and voltage. The system consists of current sensors, voltage sensors, a signal conditioning circuit, and an Arduino Mega microcontroller for data processing. The system is equipped with a graphical user interface, data storage, and application. The generator input power measurement system has been created and tested. The measurement system has successfully measured the input power of the generator's driving motor, which in real-time is displayed on the trend graph via the graphical user interface on the laptop. The input power measurement data on the three-phase generator and the time data have been successfully stored inside the micro-SD. The average error of the voltage reading is 2% compared to the measurement of the reference voltmeter. The current reading error was 2% compared to the reference meter ampere measurement.

**Keywords:** driving motor, generator, microcontroller, power measurement

## 1 Introduction

One tool to generate electrical energy is a generator. Electric generators work by converting mechanical energy into electrical energy [1]. One type of generator is a permanent magnet generator which is an electric machine that utilizes mechanical energy to produce electricity. This generator utilizes permanent magnets as the rotor[2]. Low-speed permanent magnet generators are generally used to convert the mechanical power output of water turbines [3] and wind turbines [4][5] into electricity. The rotational speed of the generator needed to produce electricity is a minimum of 1500 rotations per minute



(rpm) [6]. This study used a generator with a rotation of less than 1500 rpm.

Testing the characteristics of the generator can be done by moving the generator shaft using a driving motor. The generator drive motor requires a tool that can provide power with adjustable frequency and voltage to regulate the rotation of the generator shaft. One of the driving motors that can be adjusted rotational speed is a 3-phase induction motor. So, we need a 3-phase speed driver whose voltage and frequency can be adjusted. To find out the efficiency of the generator, it can be done by measuring the electric power output of the generator and the input power of the driving motor. Therefore, it is necessary to measure the three-phase input power with varying voltages and frequencies. The input electric power of the generator driving motor can be obtained by measuring the motor input voltage and current.

Previously, there was research related to measuring power on generators using voltage sensors and current sensors. The power measurement has been done in research entitled “Rancang Bangun Sistem Proteksi Daya Listrik menggunakan Sensor Arus dan Tegangan berbasis Arduino “[7]. Research on the “Rancang Bangun Sistem Monitoring Tegangan, Arus, dan Frekuensi Keluaran Generator 3 Fasa Pada Modul Mini Power Plant Departemen Teknik Instrumentasi”[8] is concerned with monitoring the output voltage, current, and frequency of a 3-phase generator. In this study, ZMPT101B and ACS712 sensors were used to obtain voltage and current values. In this study, there is also monitoring of the output frequency on the generator. From the sensors used to get the values of voltage, current, and output frequency of the generator, the values from these sensors are then displayed on the LCD and loaded in the Openlogger module. In this research, the method used to measure 3-phase voltage and current is only one phase, so it only uses one voltage sensor and one current sensor.

The research entitled “Perancangan Sistem Monitoring dan Proteksi Daya Balik Untuk Generator 1kW 3 Fasa”[9], monitoring measurements using the ZMPT101B voltage sensor and ACS712-20A current sensor. This monitoring is used as an early indication to prevent damage to the generator. In this research, 3 voltage sensors and 3 current sensors are used to sense each phase. From the sensor, the data is processed to produce a power value. The calculation of the power used is active power. The system is equipped with a monitoring display using a TFT LCD. In addition, the system can control



the reverse power protection that occurs. In this system, there is no data storage in memory so the previous data cannot be seen. The measurement system is carried out for power sources with a fixed frequency.

The power measurement system mentioned above is carried out for a power source with a fixed frequency. In testing the low-speed permanent magnet generator, it is necessary to drive a variable rotational speed from a 3-phase power converter with varying frequencies. Therefore this research was made to make a 3-phase electric power meter with an electric power source with varying frequencies originating from the 3-phase converter output used to activate the driving motor. The calculation of the input power to the generator driving motor is obtained by multiplying the voltage and current values for each converter output phase. Therefore a voltage sensor and a current sensor are needed to get the value of the voltage and current. The voltage sensor will sense the voltage by placing the sensors in parallel on each phase. While the current sensor will measure the current by placing the sensor in series on each phase against a given load. The voltage sensor is used to measure the phase voltage. The current sensor is used to measure the phase current. Voltage and current measurements are carried out for the three phases, requiring 3 voltage sensors and 3 current sensors. The processing of the signal from the voltage sensor and current sensor is processed using a microcontroller. The results of voltage, current, and power data are displayed digitally on the LCD and through the GUI in graphical form and can be stored on a micro-SD and can be communicated with other microcontrollers via serial communication.

## **2 Methods**

At this stage, it is designed to measure the electric power originating from the 3-phase converter which is input to the generator drive motor used in testing the low-speed permanent magnet generator. In this study, the generator used was a low-speed permanent magnet generator with a maximum rotational mechanical rotation of 1395 rpm (rotations per minute). The stage starts with designing the appropriate system block. The next step is to design and implement hardware and software according to the system block. The next stage is to test the system for data collection to see the suitability of the results of the tool with the design, which is then analyzed to get conclusions.

The input power measurement system for the generator drive motor is part of a system that has several measurements in testing the low-speed permanent magnet generator. This research is focused on measuring the input electric power of the generator drive motor. Electric power is defined as work per unit of time or electrical energy dissipation per unit of time. The unit of power is the watt or joules per second. Measurement of DC power can be done by measuring current and measuring voltage. There are two measurement configurations as shown in Fig. 1 with the symbol E being the voltage source, A being the measured current, and V being the voltage. The electric power P is the product of the current and voltage values.

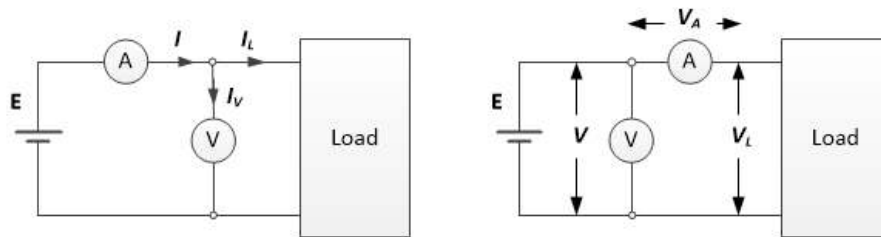


Figure 1. Configuration of power measuring [10]

AC power measurement can be done like DC power measurement, namely through current and voltage measurements. The difference is that for AC voltage, the current and voltage can have different waveforms and different phases. There are several definitions of ac power measurement. Instantaneous power, namely the multiplication of the instantaneous voltage and instantaneous current flowing at the load, is expressed by (1).

$$p(t) = v(t) i(t) \quad (1)$$

In an ac circuit with an ac voltage source that is periodic with a period T, the average power or active power (P) is defined as stated in (2). Active power is the average power consumed by the load[11].

$$P = \frac{1}{T} \int p(t) dt \quad (2)$$

In an ac circuit with a resistive load, the instantaneous power value is expressed in (3), where V is the RMS (root-mean-square) voltage, I is the RMS current, and  $\omega$  is the corner frequency of the power source. Active power is a multiplication between V and I.

$$p(t) = VI(1 - \cos 2\omega t) \quad (3)$$

For a purely reactive load, the instantaneous power value is expressed as in (4). The active power for a reactive load is zero.

$$p(t) = VI \cos 2\omega t \quad (4)$$

For loads with resistive and reactive components, there is a phase difference between the voltage wave and the current wave which is expressed by the angle  $\phi$ . The active power  $P$  is expressed by (5), where  $V_L$  is the rms voltage at the load,  $I_L$  is the rms current of the load, and  $\cos\phi$  is called the power factor. The multiplication between  $V_L$  and  $I_L$  is called the apparent power ( $P_A$ ) or apparent power ( $S$ ), as shown in (6). Reactive power ( $Q$ ) is defined as the multiplication between  $P_A$  and  $\sin\phi$  value as shown in (7).

$$P = V_L I_L \cos\phi \quad (5)$$

$$P_A = V_L I_L \quad (6)$$

$$Q = V_L I_L \sin\phi \quad (7)$$

The mathematical relationship between the types of power that exists, namely active power, reactive power, and apparent power uses the principle of trigonometry, as shown by the power triangle in Fig. 2. The relationship between apparent power  $S$ , active power  $P$ , and with reactive power  $Q$  is shown by (8)

$$S = \sqrt{P^2 + Q^2} \quad (8)$$

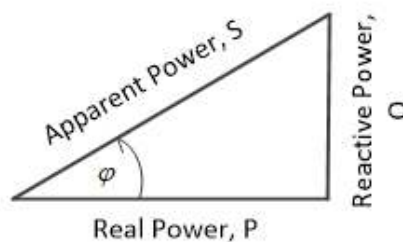
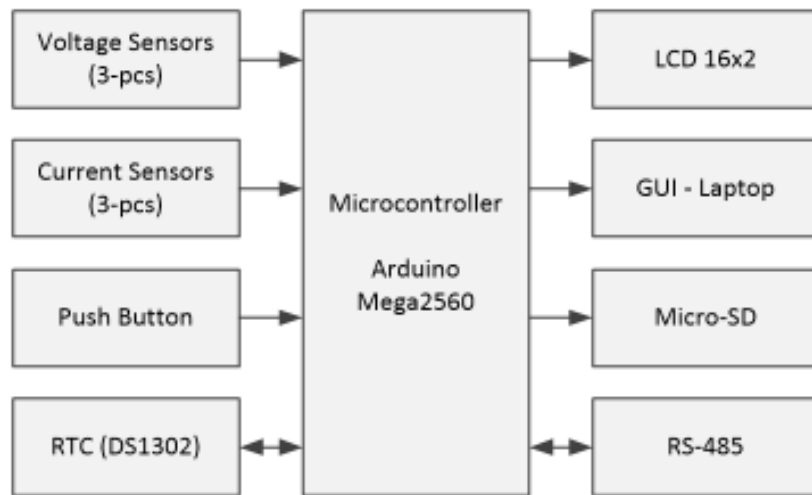


Figure 2. Power triangle.

The input power measurement system in this research is equipped with an LCD viewer and graphic display on a computer, data recording on a micro-SD, and there is an RS485 serial communication facility to communicate with other microcontrollers. Fig. 3 shows a block diagram of the power measurement system design.



**Figure 3.** Block diagram of the system

### A. Hardware Design

This input power meter consists of three voltage sensors, three current sensors, an RTC module, a push button, a microcontroller, an LCD viewer, a micro-SD memory module, GUI on a laptop, and an RS-485 communication module. Voltage and current measurements are carried out at the output of a 1-phase to 3-phase converter with a load in the form of a generator driving motor. The microcontroller used is Arduino Mega 2560. The data obtained from the measurement results will be displayed on a 16x2 LCD, the GUI is in the form of a trend graph, and the measurement data is stored in a micro-SD.

Based on the system box diagram in Fig. 3, then the wiring between the components or modules used is designed. The wiring diagram is shown in Fig. 4. The output of each voltage sensor and the current sensor is connected to the microcontroller's analog input pin. The 16x2 CD module is used to display the results of measuring the power of each phase and the total power. The DS1302 RTC module is used as a real-time reference for recording data stored on the memory module (micro-SD). The RS485 module is used for communication with other microcontrollers for data collection purposes.

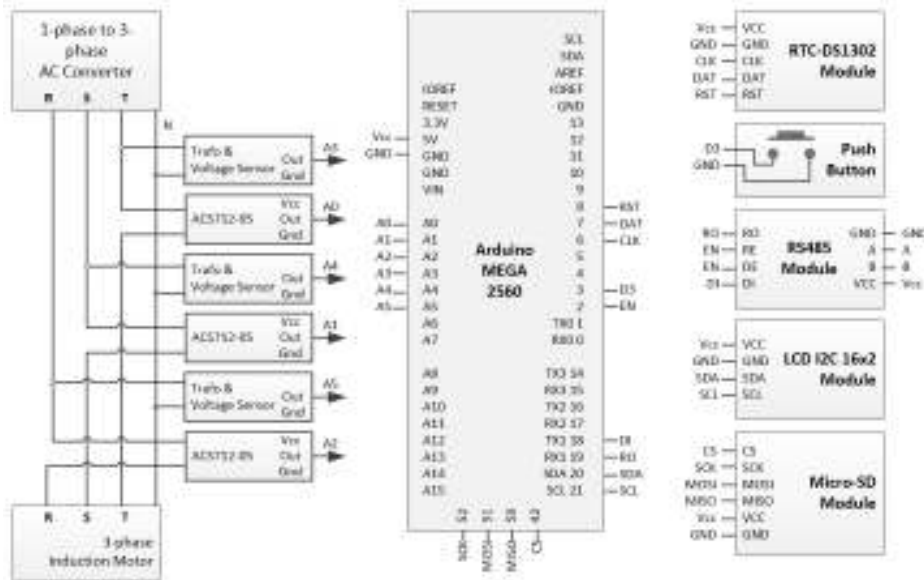


Figure 4. Wiring diagram

The voltage sensor will measure the voltage of each converter output phase, designed to measure voltages up to 250 volts RMS. The voltage sensor used is shown in Fig. 5. The voltage sensor circuit consists of three step-down transformers with a ratio of primary to secondary turns of 220:12. Each transformer's secondary output is connected to a signal conditioning circuit (PS). The signal conditioning circuit consists of a diode bridge, some resistors, and a capacitor. The series of resistors and capacitors function as a filter so that the output voltage of the circuit is even (dc). The characteristics of the sensor are obtained by conducting trials by measuring the converter voltage and the output dc voltage of the sensor, then carrying out the calibration process. Measurements are made for varying converter voltages. The output of each voltage sensor is connected to the microcontroller analog pin.

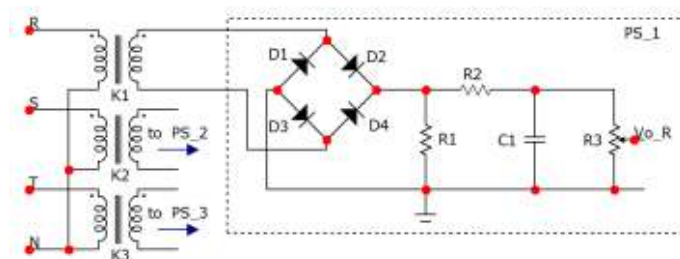
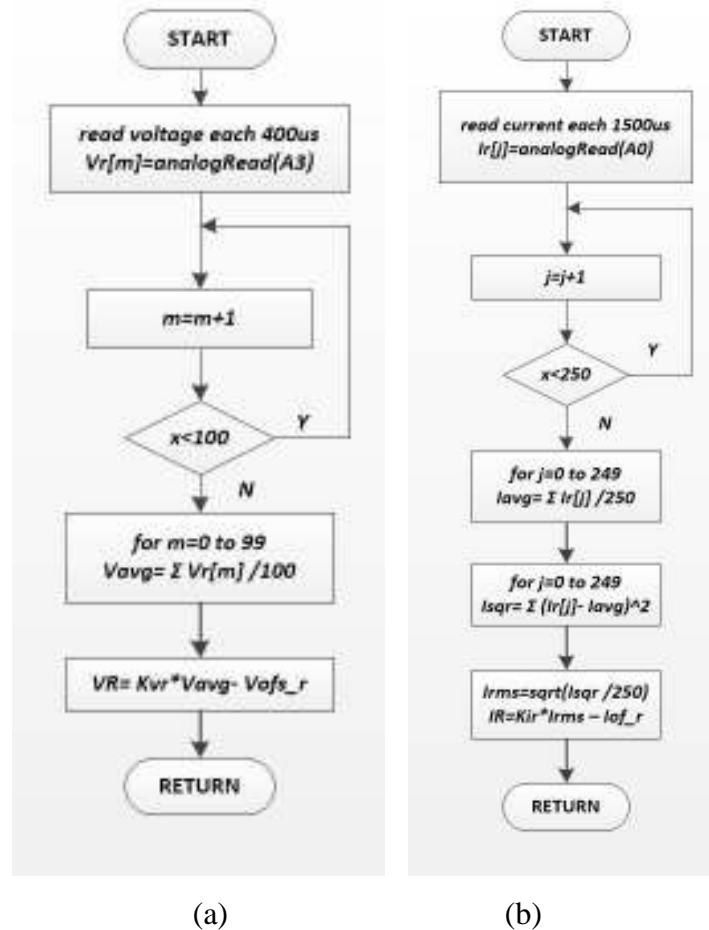


Figure 5. The circuit of the voltage sensor

Three current sensors that use ACS712-05 which are placed on each phase. The current sensor is designed to measure up to 3.5 A (RMS), or a peak current of 4.949 A. When the sensor detects 0 amperes, the current sensor output will be 2.5 volts. According to the sensitivity of the ACS712-05 sensor, for every 1-ampere increase, the current sensor output will increase by 0.185 volts. When the current is positive at 4.949A, the output voltage of the current sensor will be the same as  $V_{OUT}=2.5+(0.185 \times 4.949) = 3.415V$ . Meanwhile, when the current is negative of -4.949A, the sensor output voltage becomes  $V_{OUT} = 2.5 + (0.185 \times -4.949) = 1.554V$ . This value is used as the maximum output voltage value from the current sensor to be processed by the microcontroller.

## **B. Software Design**

The working description of the input power measurement system is using three voltage sensors to get the voltage value of each phase, and three current sensors to get the current value of each phase. The voltage value and current value will be processed by the microcontroller to get the power value of each phase. The program first starts with initializing the port used on the Arduino Mega 2560. The port used in the design consists of modules such as RTC, microSD memory module, LCD, push button, and RS485 module as the communication. In addition, there is an analog port initialization that is used to read voltage sensor data and current sensors. When the push button is pressed, the system will start working. The system works by taking voltage and current data for each phase. Retrieval of voltage and current data on each phase using sampling with a certain period. The current and voltage measured by the current and voltage sensors are averaged using the moving average method to remove noise[12]. The flowchart of the measurement system can be seen in Fig. 6.



**Figure 6.** Flowchart of measurement system (a). Voltage measurement  
(b). Current measurement

The voltage signal is in the form of a DC wave, while the current signal is in the form of a sinusoidal wave. The data is taken gradually starting from the voltage and then the current. For data collection, the voltage will be sampled every 400us with a total of 100 data so it takes about 40ms in one cycle. For data collection, the current will be sampled every 1.5ms with a total of 250 data, so it takes about 375ms in one cycle. The data collection process is carried out alternately, the first is the voltage on the R phase, the second is the voltage on the S phase, and the third is the voltage on the T phase. The voltage data will use the calibration equation using a true-RMS multimeter, so the data obtained is the processing of RMS voltage data. The calibrated voltage of each phase is calculated using (9) – (11).

$$V_{R\_phase} = (81.425 \times V_{avg} - 97.778) \quad (9)$$

$$V_{S\_phase} = (71.653 \times V_{avg} - 67.291) \quad (10)$$

$$V_{T\_phase} = (88.972 \times V_{avg} - 112.96) \quad (11)$$

The calculation of the current value can be seen in (12) -14).

$$i_{R\_phase} = (0.0275 \times i_{rms} - 0.0146) \quad (12)$$

$$i_{S\_phase} = (0.0264 \times i_{rms} + 0.0034) \quad (13)$$

$$i_{T\_phase} = (0.0274 \times i_{rms} - 0.0105) \quad (14)$$

The rms data stored in a variable will be processed into a per-phase power value. After the per-phase power value is obtained, then the data will be processed by the microcontroller to obtain the total power value. All data processed, both per-phase input data and total input power data, will then be stored on the microSD and the data will be displayed on the LCD.

### **3 Results and Discussions**

The results of the design of the tool that has been made are shown in Fig. 7. The system that has been made is shown at the bottom left which is assembled with a 3-phase converter, a 3-phase induction motor as the drive, and the permanent magnet generator being tested. The generator load is not shown in this figure.



**Figure 7.** Result of the design

The procedure for using the tool is as follows: First, when the system is supplied with power, a description of the measuring instrument and a description of the date, month and year will be displayed on the LCD. Then the LCD will display a description of the condition of the SD Card storage. The push button is used to activate and stop the measurement process. As an indicator, a description will appear on the LCD. When the



push button is pressed for the first time it will activate the measurement system. When the push button is pressed a second time it will stop the measurement system. The description of the measurement results will be displayed on the LCD directly. The memory module will automatically store data after the user activates the measurement system.

The measurement data results will be stored in real-time with the timing data obtained via the RTC DS1302. RTC DS1302 is used for recording the time, day, and date of measurement. Data is stored in micro-SD memory with the .csv extension format. This is to make it easier to process data. The stored data will be delimited by commas so that the data obtained is easy to classify. The process of storing data in the SD card begins when the system is ready to start measuring. When the system detects the SD card, the system will be ready to start measuring. Data storage will take place every 1 second starting after the measurement system starts. When the measurement system stops or is inactive, the process of saving data to the SD card will stop.

Power measurement data can be seen on the 16x2 LCD, as shown in Fig. 8. After the push button is pressed, the system will start measuring power. The LCD displays R phase power ( $P_r$ ), S phase power ( $P_s$ ), T phase power ( $P_t$ ), and total power ( $P_T$ ). In addition, voltage measurement data, current measurement data, and power calculation results can be monitored through the 'serial monitor' contained in the Arduino software.



**Figure 8.** LCD of power per phase and total power.

Testing of the measurement system is carried out by connecting the hardware (results of the measuring instrument design) to the converter and the driving motor as the load. As a reference measuring device for current measurement, 3 multimeters are used as shown in Fig. 9, multimeter numbers 1 to 3. Meanwhile, multimeter numbers 4 to 5 are used as a reference measuring instrument for measuring voltage. As a load from the generator, several lamps are used which can be varied. In addition to variations in the load

on the generator, tests were also carried out using a variety of converter indicators. The converter indicator is a description of the numbers printed on the converter LCD. The converter indicator is a sinusoidal frequency setting to adjust the rotational speed of the driving motor. The variation used is from 3 Hz to 13 Hz.



**Figure 9.** Multimeter as a reference for measuring voltage and current

#### **A. Voltage meter testing**

The voltage measurement test uses a generator load of six lamps of 25 watts each and a variation of the converter indicator. The test is carried out alternately the first voltage sensor will measure the voltage on the R phase, the second voltage sensor will measure the voltage on the S phase, and the third voltage sensor will measure the voltage on the T phase. This voltage sensor test is carried out after going through the calibration process. The test results are shown in Table 1 for measuring the R phase voltage, Table 2 for measuring the S phase voltage, and Table 3 for measuring the T phase voltage.

Based on Table 1, Table 2, and Table 3, it can be seen that the value of the voltage measurement on the sensor is not much different from the reference multimeter value. The average error on the first sensor test for phase R is 1.77% with reading ability. The average error on the second sensor test for phase S is 1.08%. The average error in the third sensor test for phase T is 0.61%. The results of the three sensors show that the three voltage sensors can work well, which have an error of less than 2%, for measurements using a reference multimeter.

**Table 1.** Data of R-phase voltage sensor

No	Voltage (V)		Error (%)	Converter Indicator (Hz)
	Voltage Sensor	Voltage Sensor		
1	67,63	68,90	1,84	3
2	72,68	72,40	0,39	4
3	79,15	77,20	2,53	5
4	84,26	81,90	2,88	6
5	89,16	86,50	3,08	7
6	93,27	90,80	2,72	8
7	97,31	94,90	2,54	9
8	101,37	99,00	2,39	10
9	104,45	103,20	1,21	11
10	107,90	106,40	1,41	12
11	111,28	110,40	0,80	13
12	114,10	114,00	0,09	14
13	117,11	117,50	0,33	15
average	95,36	94,08	1,71	-

**Table 2.** Data of S-phase voltage sensor

No	Voltage (V)		Error (%)	Converter Indicator (Hz)
	Voltage Sensor	Multimeter Reference		
1	65,17	66,30	1,70	3
2	70,55	72,00	2,01	4
3	76,35	77,20	1,10	5
4	81,45	81,40	0,06	6
5	86,25	86,00	0,29	7
6	90,27	90,20	0,08	8
7	94,19	94,40	0,22	9
8	97,75	98,40	0,66	10
9	101,32	102,00	0,67	11
10	104,80	105,80	0,95	12
11	108,28	109,90	1,47	13
12	111,04	113,50	2,17	14
13	114,07	117,20	2,67	15
average	92,42	93,41	1,08	-

**Table 3.** Data of T-phase voltage sensor

No	Voltage (V)		Error (%)	Converter Indicator (Hz)
	Voltage Sensor	Voltage Sensor		
1	66,44	67,20	1,13	3
2	71,90	72,50	0,83	4
3	77,65	77,80	0,19	5
4	83,05	82,30	0,91	6
5	87,94	87,10	0,96	7
6	92,33	91,30	1,13	8
7	96,45	95,50	0,99	9
8	100,11	99,40	0,71	10
9	104,03	103,50	0,51	11
10	107,41	107,40	0,01	12
11	111,34	111,20	0,13	13
12	115,15	115,10	0,04	14
13	118,30	118,80	0,42	15
average	94,78	94,55	0,61	-

**B. Current meter testing**

Before being used for testing in a measuring system, the current sensor has gone through a calibration process. The calibration process is carried out by measuring current with a voltage source using a TDGC2-0.5kVA AC variable transformer with a load of several lamps that can be varied, as well as measuring using a reference multimeter. This calibration process is to determine the actual characteristics of the current sensor. Each sensor has different characteristics. Calibration process by taking data with variations in load and voltage. Voltage variations are taken for every 25 V to 125 V increase. Meanwhile, load variations are up to four lamps with 100 Watts for each lamp. This calibration process is carried out on the three sensors used. The data taken is then searched for the linearity equation.

Current meter testing is carried out by applying a lamp load to the generator. The light load used is 6 lamps of 25 watts each and a variation of the converter indicator. The test is carried out by alternating current sensor 1 will measure the current in phase R, current sensor 2 will measure the current in phase S, and current sensor 3 will measure

the current in phase T. The test results of the current sensor are shown in Table 4 for measuring phase current R, Table 5 for the measurement of the S-phase current, and Table 6 for the measurement of the T-phase current.

**Table 4.** Data of R-phase current sensor

No	Current (A)		Error (%)	Converter Indicator (Hz)
	Current Sensor	Multimeter Reference		
1	1,23	1,25	1,60	3
2	1,25	1,26	0,79	4
3	1,31	1,31	0,00	5
4	1,36	1,35	0,74	6
5	1,36	1,36	0,00	7
6	1,37	1,36	0,74	8
7	1,34	1,33	0,75	9
8	1,29	1,31	1,53	10
9	1,29	1,28	0,78	11
10	1,26	1,26	0,00	12
11	1,25	1,24	0,81	13
12	1,22	1,22	0,00	14
13	1,19	1,20	0,83	15
average	1,29	1,29	0,66	-

**Table 5.** Data of S-phase current sensor

No	Current (A)		Error (%)	Converter Indicator (Hz)
	Current Sensor	Multimeter Reference		
1	1,19	1,19	0,00	3
2	1,25	1,25	0,00	4
3	1,33	1,32	0,76	5
4	1,36	1,36	0,00	6
5	1,39	1,39	0,00	7
6	1,37	1,38	0,72	8
7	1,35	1,36	0,74	9
8	1,32	1,33	0,75	10
9	1,31	1,31	0,00	11
10	1,28	1,28	0,00	12
11	1,25	1,26	0,79	13
12	1,24	1,24	0,00	14
13	1,22	1,22	0,00	15
rerata	1,30	1,30	0,29	-

**Table 6.** Data of T-phase current sensor

No	Current (A)		Error (%)	Converter Indicator (Hz)
	Current Sensor	Multimeter Reference		
1	1,25	1,25	0,00	3
2	1,29	1,29	0,00	4
3	1,34	1,34	0,00	5
4	1,38	1,38	0,00	6
5	1,39	1,40	0,71	7
6	1,38	1,38	0,00	8
7	1,36	1,36	0,00	9
8	1,33	1,34	0,75	10
9	1,31	1,32	0,76	11
10	1,30	1,29	0,78	12
11	1,27	1,27	0,00	13
12	1,24	1,25	0,80	14
13	1,23	1,23	0,00	15
average	1,31	1,32	0,29	-

In Tables 3, 4, and 5, it can be seen that the value of the current measurement on the sensor is not much different from the value shown by the multimeter. The average error in testing sensor 1 in phase R is 0.66%. The average error in sensor 2 testing in phase S is 0.29%. The average error on the 3-sensors test in the S phase is 0.29%. The results of the three sensors show that the three current measurements can work properly, with an error of less than 1% compared to the reference multimeter.

**C. Power meter testing**

The power measurement results are obtained when measuring voltage and current. The power measurement data is obtained from recording on the serial monitor from the Arduino software. Tests are carried out using variations when the generator is without load and also when the generator is loaded. The generator when loaded consists of 1 lamp load to 6 lamp loads. In addition, the tests carried out have a variety of indicators from the converter with an indicator range of 3 to 13. The measurement results for a generator load of 6 lamps are shown in Figs 10-12. The 'Measure' curve is the result of a power measurement processed by the microcontroller. While the 'Calculate' curve is the power

value obtained from multiplying the voltage and current by the multimeter measurement results. With each increase in the frequency of the converter, the power will increase, indicating that the generator power will increase with an increase in generator shaft rotation. Based on the test results data used to make the graph, the error value has been calculated between the measurement results and the calculation results. The average error of the R phase power is 2%, the average S phase error is 1.26% and the average T phase error is 0.75%. The average error for all tests is 1.4%. Based on the average error value which is less than 2%, it can be said that the power measurement system (VA) can work properly.

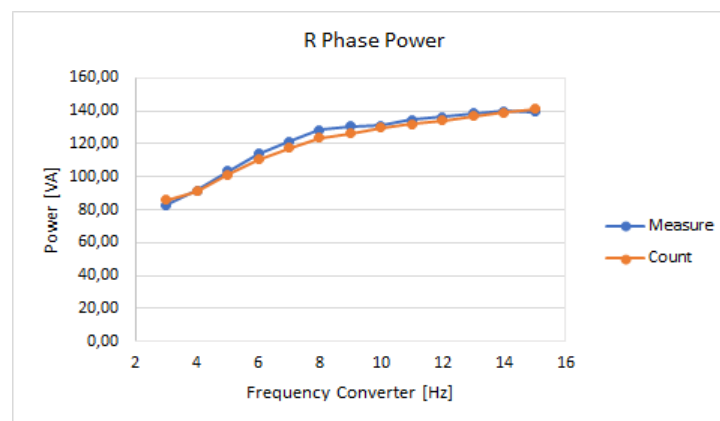


**Figure 10.** Results of measuring the R phase power and calculating the power based on a multimeter with variations in the frequency converter.

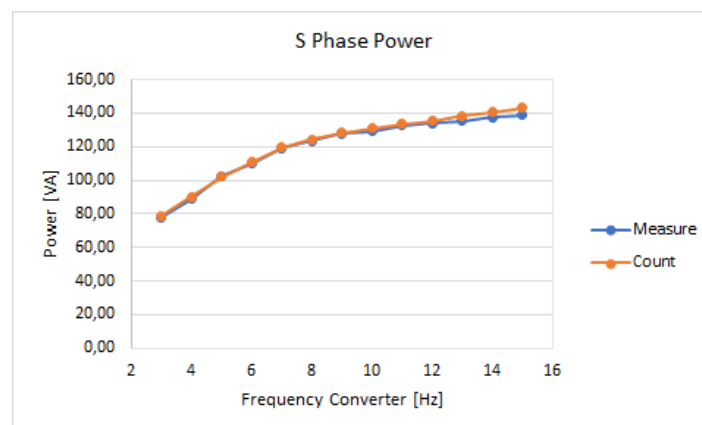


**Figure 11.** Results of S-phase power measurements and power calculations based on a multimeter with frequency converter variations.

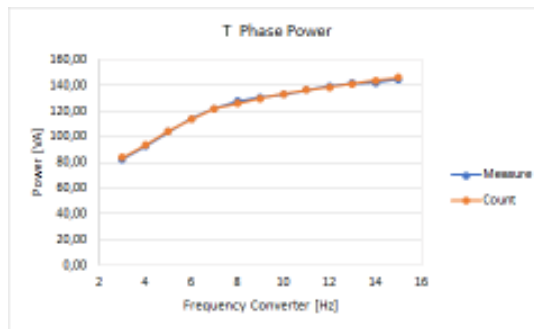


**Figure 12.** Results of measuring phase T power and calculating power based on a multimeter with variations in frequency converters

#### D. Communication with GUI and other Microcontrollers

After the device is connected to a computer/laptop, the user can activate the device by pressing the push button, data will be sent using serial communication. Data from the serial is then read in a GUI application program created using Python which is then plotted as a trend graph in the GUI. The GUI display can be seen in Fig. 13. The power value of each phase and the total power can be displayed numerically and graphically. The horizontal axis shows the measurement time in seconds, and the vertical axis is the power measured in VA units. One window is displayed for every 10 data points, when the curve reaches the right boundary of the graph, then the next time curve will be displayed starting from the left again.

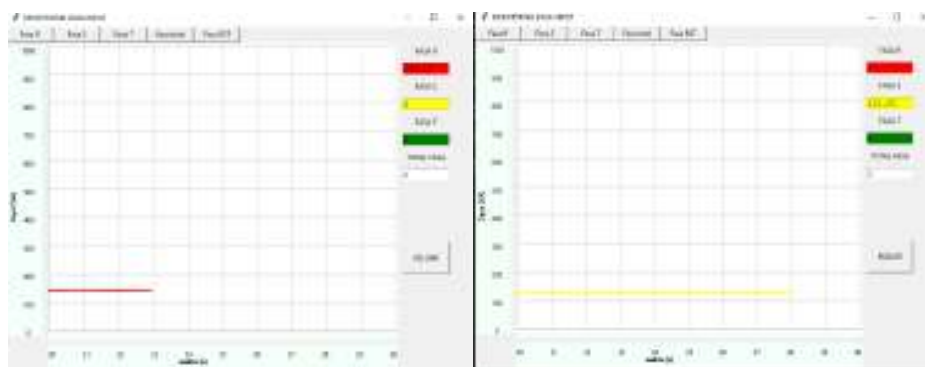


**Figure 13.** The results of displaying graphical trends in the GUI application.

Communication between the system and another microcontroller (master) is designed using the RS-485 serial communication module. The data communication process will take place when the measuring system is active. If the measurement system



is not active there will be no communication. The communication process uses the RS485 module through two lanes A and B. This communication will start when the master sends data in the form of an encoded address desired by the master. Each measurement system on a low-speed permanent magnet generator has its own mutually agreed-upon coding address. For input power measurement coding address is #I\$. When the slave gets data that matches the coding address, the slave will immediately send measurement data. The format of data transmission carried out by the slave is as follows "#i, total power, \$". Fig. x is the result of communication between two slave and master microcontrollers.

## **4 Conclusions**

Based on the design and implementation as well as testing of the input power measurement system for the driving motor, it can be concluded as follows. The measurement system has succeeded in measuring the voltage, current, and apparent power of each phase, as well as the total input power of the generator drive motor. Real-time measurements are monitored and displayed on an LCD viewer and graphs via the GUI on the laptop. Instantaneous measurement data can also be displayed on the LCD. The voltage and current sensors used can be used to measure the input power per phase of the generator with a value close to the multimeter reference. Input power measurement data and time data have been successfully stored in the micro SD. There is an average voltage reading error of 2% against the reference voltmeter. The current reading error is 1% against the reference ammeter. The average power measurement error is 2% against a reference multimeter.

## **Acknowledgements**

Acknowledgments are addressed to LPPM Universitas Sanata Dharma for supporting this research.

## **References**

- [1] M. H. Rashid, *Electric Renewable Energy System*. London: Elsevier Ltd, (2016).
- [2] T. Yee Heng, T. Jian Ding, C. Choe Wei Chang, T. Jian Ping, H. Choon Yian, and M. Dahari, *Permanent Magnet Synchronous Generator design optimization for*

- wind energy conversion system: A review, *Energy Reports*, 8 (2022) 277–282.
- [3] K. I. Liangliang Wei, Taketsune Nakamura, Development and optimization of low-speed and high-efficiency permanent magnet generator for micro hydro-electrical generation system, *Renew. Energy*, 147 (1) (2020) 1653–1662.
- [4] H. Q. and P. J. Wang Fengxiang, Bai Jianlong, Design features of low speed permanent magnet generator direct driven by wind turbine, in *International Conference on Electrical Machines and Systems*, Nanjing, China, (2005) 1017–1020.
- [5] S. D. Zevalukito, Y. Lukiyanto, and F. R. Prayogo, The Experiment of Wind Electric Water Pumping for Salt Farmers in Remote Area of Demak-Indonesia, *Int. J. Appl. Sci. Smart Technol.*, 4 (2) (2022) 185–194.
- [6] P. Ristiano, Generator Ganda Pada Pembangkit Listrik Mikrohidro Dengan Turbin Tunggal, *Avitec*, 1 (1) (2019) 65–70.
- [7] Syafruddin, G. Devira ramady, and R. Ristiadi Hudaya, Rancang Bangun Sistem Proteksi Daya Listrik menggunakan Sensor Arus dan Tegangan berbasis Arduino, *Isu Teknol. Stt Mandala*, 16 (1) (2021) 36–43.
- [8] F. Adi Iskandarianto et al., Rancang Bangun Sistem Monitoring Tegangan, Arus, dan Frekuensi Keluaran Generator 3 Fasa Pada Modul Mini Power Plant Departemen Teknik Instrumentasi, *J. AMORI*, 1 (2020).
- [9] I. M. A. N. and S. M. U. Azmi, Perancangan Sistem Monitoring dan Proteksi Daya Balik untuk Generator 1 kW 3 Fase.
- [10] W. S., *Teknik Ukur dan Peranti Ukur Elektronik*. Jakarta, Gramedia, (1988).
- [11] von M. A., *Electric Power System*. Canada: John Wiley & Sons, Inc., (2006).
- [12] Bernadeta Wuri Harini, Martanto, and Tjendro, Comparison of Two DC Motor Speed Observers on Sensorless Speed Control Systems, *J. Nas. Tek. Elektro dan Teknol. Inf.*, 11 (4) (2022) 267–273.

# Classification of Lung and Colon Cancer Histopathological Images Using Convolutional Neural Network (CNN) Method on a Pre-Trained Models

Brilly Lutfan Qasthari<sup>1</sup>, Erma Susanti<sup>1,\*</sup>, Muhammad Sholeh<sup>1</sup>

<sup>1</sup>Faculty of Information Technology and Business, Institut Sains & Teknologi AKPRIND, Yogyakarta, 55222, Indonesia

\*Corresponding Author: erma@akprind.ac.id

(Received 04-05-2023; Revised 11-05-2023; Accepted 11-05-2023)

## Abstract

Cancer is a severe illness that can affect many young and older people. In Indonesia, lung cancer is the leading cause of cancer-related death, whereas colon cancer, with more than 1.8 million cases worldwide in 2018, is the third most common cancer. This study intends to create a model to categorize histological images of lung and colon cancer into five labels to aid medical professionals' categorization job. This study uses a pre-trained model idea known as VGG19 in its CNN (Convolutional Neural Network) technique. The dataset uses 25,000 histological graphic pictures with a ratio of 80% training data and 20% testing data. The classification system for lung and colon cancer contains five categories: lung benign tissue, lung adenocarcinoma, lung squamous cell carcinoma, colon adenocarcinoma, and colon benign tissue. The training result revealed a 99.96% accuracy rate and a 1.5% loss rate. The model can be rated as excellent based on these results.

**Keywords:** Lung Cancer, Colon Cancer, Convolutional Neural Network, CNN, Pre-Trained

## 1 Introduction

Cancer is a dangerous condition that can affect both young and older people. Cancer has abnormal characteristics that enable it to target cells or other bodily organs without the affected person knowing it. Estimates of cancer incidence and mortality by sex and for the 18 age groups in 2020 for the 185 countries or regions with a population of more than 150,000 in the same year. When the cells lining the lung airways divide improperly



and uncontrolled to generate abnormal tissue, lung cancer results. The most common cancer that causes death is lung cancer [1].

Lung cancer is the leading cause of mortality from cancer in Indonesia [2]. In contrast to colorectal cancer, commonly referred to as colon cancer, this type of cancer develops in the colon, or rectum. The rectum and large intestine are digestive system components of the colon that contribute in the production of energy and the elimination of waste. According to statistics from the American Institute for Cancer Research, colon cancer is the third most prevalent cancer worldwide. There were almost 1.8 million infections in 2018 [3]. In addition to diet, lack of fibre, smoking, and alcohol use, age is the most significant risk factor for colon cancer. Symptoms of colorectal cancer include changes in bowel habits, stomach pain, blood in the stool, anaemia, fatigue, loss of appetite, and weight loss.

Artificial intelligence (AI) technology is used in the medical industry as a decision-support tool for identifying diseases and helps speed up picture analysis. Computer-aided diagnostics can analyze medical photos [3]. The Convolutional Neural Network (CNN) method has been used in several earlier research to demonstrate that cancer may be classified using AI technology, and the resulting model accuracy is good. While compared to manual evaluation by medical experts, AI technology performs computationally more quickly while categorizing lung cancer photos. Modelling the lung cancer categorization system takes two hours of computation [4]. In comparison, a physical examination by medical staff takes 10–14 days to identify lung cancer.

There are several different pre-trained models available on CNN. A few examples of these architectures are Le-Net, Alex-Net, Google-Net, Conv-Net, and Res-Net. In classifying biomedical-based images, the Alex-Net structure is more likely to reach a high accuracy of 90% [5]. In contrast to the ResNet architecture, research utilizing a biomedical-based dataset (Diagnosis of Colonic Adenocarcinoma) was effective in attaining an accuracy of 93% using the ResNet architecture [6].

The pre-trained model is used in this study since it performs well for classification. The average accuracy of the AlexNet and ResNet models is above 90%, based on several prior studies. This work aims to develop a classification system for lung and colon cancer

from histological images using various pre-trained models and to assess which model performs best given the histopathological images used.

## **2 Methods**

Three convolutional layers and two fully connected layers will be combined to create the convolutional neural network (CNN) approach for classification in this study. Additionally, it will take advantage of the VGG pre-trained transfer learning architecture. Transfer learning is an approach that makes use of current network infrastructures. There is no need to start from scratch because the CNN architecture utilized for transfer learning has already been learned from prior data. The use of this design will impact the categorization outcomes.

### **2.1. Convolutional Neural Network**

A pooling layer, a few convolutional layers (+ReLU), more convolutional layers (+ReLU), and another pooling layer are common CNN architectures. The image gets smaller and smaller as it moves through the network, but it also usually gets deeper and deeper (i.e., with more feature maps) because of the convolutional layers. The final layer of the stack-for example, a softmax layer that outputs estimated class probabilities - outputs the prediction after adding a standard feedforward neural network made up of a few fully connected layers and ReLUs at the top [7].

### **2.2. VGGNet**

Reusing the lowest layers of a pre-trained model is frequently helpful to develop an image classifier but need more training data. The VGGNet [8] program, created by K. Simonyan and A. Zisserman, was second in the ILSVRC 2014 challenge. It featured a relatively straightforward and traditional design, consisting of 2 or 3 convolutional layers, a pooling layer, 2 or 3 more convolutional layers, a pooling layer, and so on (for a total of just 16 convolutional layers), plus a final dense network with two hidden layers and the output layer. Despite using multiple filters, it only used 3 filters [7].

According to research [9] the CNN architecture produces good results in case study examples of age estimation. The estimating method with a categorization strategy produces satisfactory results. The researchers' challenge with the CNN architecture is to

develop the optimum loss function with the most Gaussian distribution. Based on the study's review results, the CNN architecture that provides the best prediction is VGG-16.

### 2.3. Research Workflow

The research process is shown in Fig. 1's flowchart, which begins with collecting dataset, preprocessing (gathering lung and colon cancer image datasets, scaling images, and dividing datasets), building CNN models with sequential and pre-trained models, training and testing data, storing models, implementing models into the Flask framework, designing the application GUI, and predicting image.

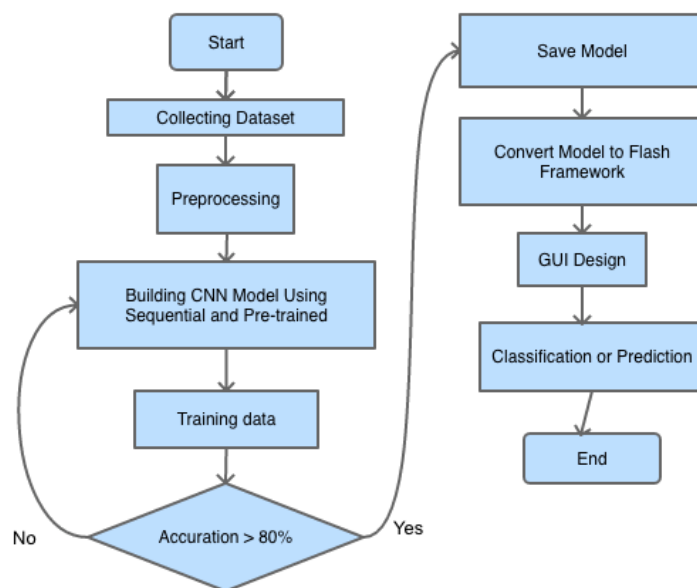


Figure 1. Workflow Research

## 3 Results and Discussions

The initial stages of this research involved gathering datasets (Pictured Data), preparing the data, developing a model, testing it, and deploying it. Pre-trained VGG-19-based model is the one being used.

### 3.1. Collecting Data

The 25,000-image "Lung and Colon Cancer Histopathological Images" dataset from Kaggle served as the source for the image collection. The image collection has five class labels: colon adenocarcinoma, lung squamous cell cancer, benign lung tissue, and colon adenocarcinoma.

### **3.2. Preprocessing**

Data preparation is a step that the user must complete before they edit or add data to a dataset. Because not all incoming data has the same format, the objective is to make understanding easier while reducing confusion during data entry. Preprocessing eliminates the possibility of inaccurate or unnecessary data influencing statistics. 80% of the data are used for training and 20% for testing during the preprocessing stage. The dataset is divided into 20,000 training data for image prediction (training and validation), 4,500 testing data, and 500 dummy data. Afterwards, the information is kept in Google Drive to simplify the image classification process. After that, the picture settings are made, and a data generator is made to produce training and test data.

### **3.3. Building CNN Architecture Model**

Following preprocessing, the next step is the creation of the CNN model. The current study uses pre-trained models. Hence it does not create a model from scratch. The pre-trained principle is to replace the starting layer with the desired layer, often known as fine-tuning. The model can be seen in Table 1.

**Table 1.** The CNN Model Architecture

No.	Layer	Output shape	Paramater
1	Input Layer	224, 224, 3	0
2	Layer Vgg19	0	20.024.384
3	Global average pooling 2d	512	0
4	Flatten	512	0
5	Dense	5120	2.626.560
6	Dropout	5120	0
7	Dense 1	5	25.605

### **3.4. Transfer Learning Process**

Applying the pre-trained model to carry out the transfer learning process comes after choosing the pre-trained model. The frozen layer on the pre-trained model is where the transfer learning process starts. Information on the frozen layer In the context of CNN, using the frozen layer is how to manage the updated weights. A layer's weight cannot be modified once it has frozen. This method can decrease training data computation time while maintaining accuracy.

### **3.5. Results of Training and Testing Data**

Forward and backward propagation are used during the training phase of the CNN algorithm. Fig. 2 displays the outcomes of training testing and data testing. The model performs well, with a loss on training data of 1.5% and an accuracy of 99.96%.

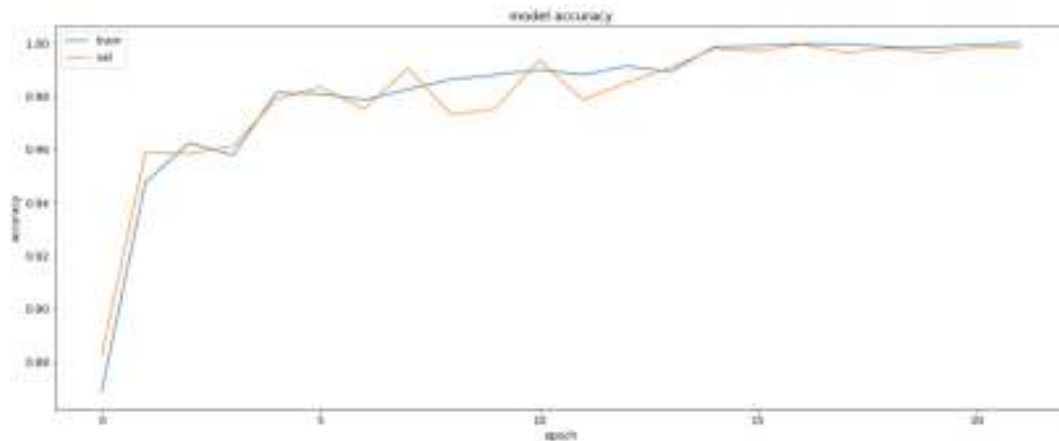


**Figure 2.** The Result of Accuration Training and Testing Data

After performing data training experiments, the matplotlib package is used in the following epoch iteration to show the training data's outcomes. Fig. 2 provides an excellent model in addition to a good graph. Any model that can run or interpret data without being influenced by noise is good. Because it can describe a trend or set of data with a low error rate, the model will not become overly fitted. This results from the model's high accuracy value and minimal loss. The next step is to show a loss graph from the training data used in the previous step. Four thousand five hundred photos were tested. When used with test data, the model achieves an accuracy performance of 99.82% accuracy and 2% loss, which is identical to that of the training data. The loss outcomes are displayed in Fig. 3. Callbacks have shown to be a very efficient way to reduce the amount of time needed for data training. Training data can yield good accuracy on the 17<sup>th</sup> epoch and concludes on the 22<sup>nd</sup> with 30 epochs and 1 hour and 40 minutes of acquisition time.



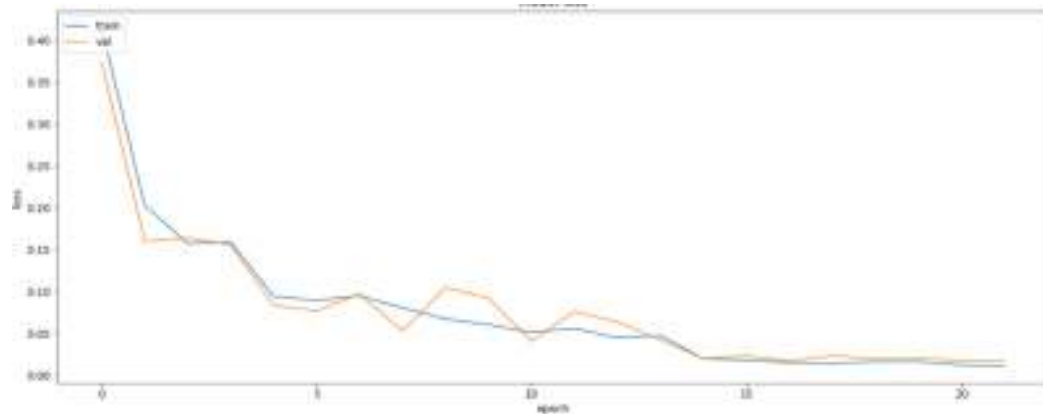


Figure 3. The Result of Loss Training and Testing Data

### 3.6. Classification or Prediction Result

The next step is to test the model by creating image predictions after completing various phases. This prediction test determines whether or not the model can categorize photos. The labels assigned to the prior training data must match the predictions for the images. Fig. 4a illustrates the successful image prediction outcomes using the label for colon adenocarcinoma. Based on the label given, the label prediction in Fig. 4 has a fair chance of coming true. The model correctly predicts the image by the label tested, namely colon adenocarcinoma, with a probability level of 100%. The original image prediction is 768 by 768 in size.

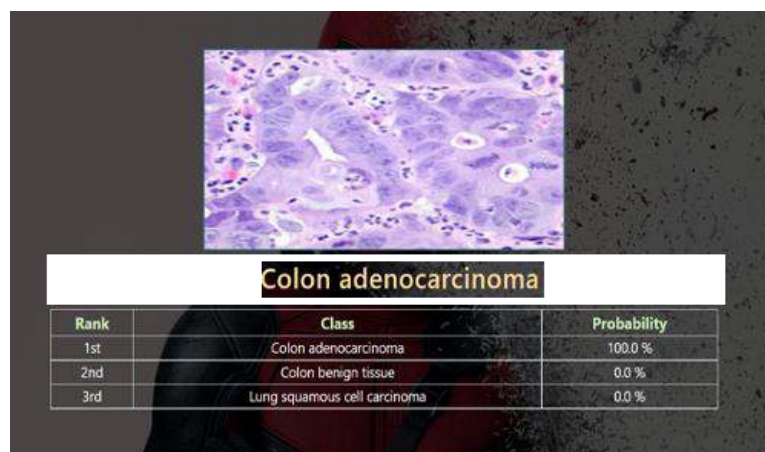
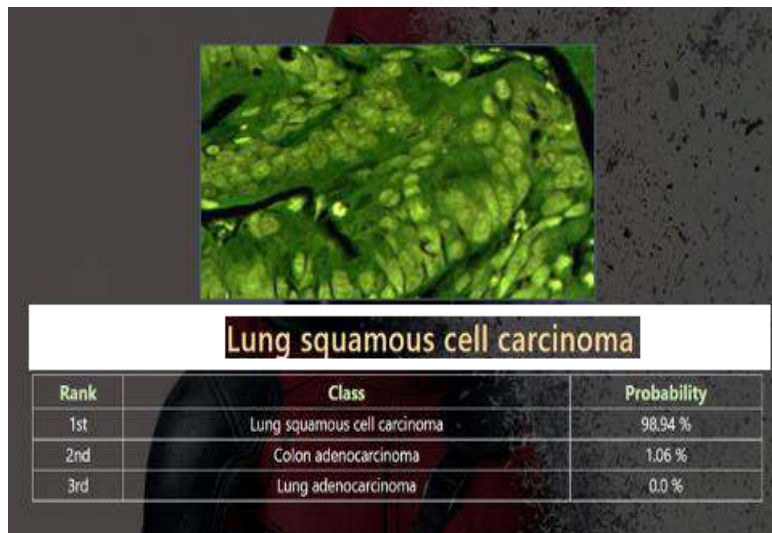


Figure 4. Classification of Colon Adenocarcinoma Label with No Filter



**Figure 5.** Colon Adenocarcinoma Label with Filter

As seen in Fig. 5, the next step is to forecast filtered images using a sample colon adenocarcinoma label with various image forms. The label prediction results could have been better based on the labels given. The filtered image is expected to be  $768 \times 768$  in size before it is resized. The model has not yet forecasted the image per the label examined, namely the colon adenocarcinoma model classifying in the lung squamous cell carcinoma class. Predicting the image that will get the following label is the next stage.

## 4 Conclusions

The development of the CNN model, which began with the data collection phase and ended with the successful model deployment process, produced good classification results, as shown by the model accuracy results, which reached 99.96% with a 1.5% loss in training data. 99.82% of the data were successfully tested using the evaluate function model, with a 2% loss. Because the model used matches the dataset provided, the outcomes at the feature extraction step of data training utilizing images of colon and lung cancer using the VGG19-based pre-trained model can be considered successful. The use of callbacks can also make it easier to train models that include the checkpoint model feature so that the model can quickly assess the weight that came from the training set of data. The accuracy will increase with the number of epochs used, but there is a significant risk of producing a model with an overfit effect if the number of epochs used is high. The

deployment of the model created through the data training procedure on the Flask framework went well. Utilizing the Flask framework, web applications can classify images by the labels provided using models trained on data. The Flask framework can display probability values on the web application interface.

## **Acknowledgements**

The author is grateful for the opportunity to discuss this research with the Study Program and Faculty of Information Technology and Business at IST AKPRIND. We would also like to acknowledge the Python Software, Google Colaboratory, Flask Framework, Keras, Seaborn, and Sklearn packages that were used in this study.

## **References**

- [1] J. Ferlay et al., Cancer statistics for the year 2020: An overview, *Int. J. Cancer*, (2021).
- [2] M. G. Sholih et al., Risk factors of lung cancer in Indonesia: A qualitative study, *J. Adv. Pharm. Educ. Res.*, (2019).
- [3] D. C. Rini Novitasari, A. Lubab, A. Sawiji, and A. H. Asyhar, Application of feature extraction for breast cancer using one order statistic, glcm, glrlm, and gldm, *Adv. Sci. Technol. Eng. Syst.*, (2019).
- [4] R. Apsari, Y. N. Aditya, E. Purwanti, and H. Arof, Development of lung cancer classification system for computed tomography images using artificial neural network, in *AIP Conference Proceedings*, (2021).
- [5] T. Shanthi and R. S. Sabeenian, Modified Alexnet architecture for classification of diabetic retinopathy images, *Comput. Electr. Eng.*, (2019).
- [6] S. U. K. Bukhari, A. Syed, S. K. A. Bokhari, S. S. Hussain, S. U. Armaghan, and S. S. H. Shah, The Histological Diagnosis of Colonic Adenocarcinoma by Applying Partial Self Supervised Learning, *medRxiv*, (2020).
- [7] A. Géron, *Hands-on Machine Learning*. (2017).
- [8] Simonyan Karen and Zisserman Andrew, Very deep convolutional networks for large-scale image recognition, in *3rd International Conference on Learning Representations, ICLR 2015 - Conference Track Proceedings*, (2015).

- [9] P. S. Adi, Development Study of Deep Learning Facial Age Estimation, International Journal of Applied Sciences and Smart Technologies (IJAST), 1 (1) (2019) 45–50, 2019.

## **AUTHOR GUIDELINES**

Author guidelines are available at the journal website:

<http://e-journal.usd.ac.id/index.php/IJASST/about/submissions#authorGuidelines>

This page intentionally left blank